UiA University of Agder

Master

Effect of Rotor Tilt on the Performance of Floating Offshore Wind Turbines

An analysis using engineering wake models.

CAMILLA LEIKVOLL

SUPERVISORS
Professor Sathyajith Mathew
Professor Joao Leal
Knut Sponheim Seim

University of Agder, 2023
Faculty of Engineering and Science
Department of Engineering and Sciences

Obligatorisk gruppeerklæring

Den enkelte student er selv ansvarlig for å sette seg inn i hva som er lovlige hjelpemidler, retningslinjer for bruk av disse og regler om kildebruk. Erklæringen skal bevisstgjøre studentene på deres ansvar og hvilke konsekvenser fusk kan medføre. Manglende erklæring fritar ikke studentene fra sitt ansvar.

1.	Vi erklærer herved at vår besvarelse er vårt eget arbeid, og at vi ikke har brukt andre kilder eller har mottatt annen hjelp enn det som er nevnt i besvarelsen.	Ja
2.	**Vi erklærer videre at denne besvarelsen:** • Ikke har vært brukt til annen eksamen ved annen avdeling/universitet/høgskole innenlands eller utenlands. • Ikke refererer til andres arbeid uten at det er oppgitt. • Ikke refererer til eget tidligere arbeid uten at det er oppgitt. • Har alle referansene oppgitt i litteraturlisten. • Ikke er en kopi, duplikat eller avskrift av andres arbeid eller besvarelse.	Ja
3.	Vi er kjent med at brudd på ovennevnte er å betrakte som fusk og kan medføre annullering av eksamen og utestengelse fra universiteter og høgskoler i Norge, jf. Universitets- og høgskoleloven §§4-7 og 4-8 og Forskrift om eksamen §§ 31.	Ja
4.	Vi er kjent med at alle innleverte oppgaver kan bli plagiatkontrollert.	Ja
5.	Vi er kjent med at Universitetet i Agder vil behandle alle saker hvor det forligger mistanke om fusk etter høgskolens retningslinjer for behandling av saker om fusk.	Ja
6.	Vi har satt oss inn i regler og retningslinjer i bruk av kilder og referanser på biblioteket sine nettsider.	Ja
7.	Vi har i flertall blitt enige om at innsatsen innad i gruppen er merkbart forskjellig og ønsker dermed å vurderes individuelt. Ordinært vurderes alle deltakere i prosjektet samlet.	Nei

Publiseringsavtale

Fullmakt til elektronisk publisering av oppgaven Forfatter(ne) har opphavsrett til oppgaven. Det betyr blant annet enerett til å gjøre verket tilgjengelig for allmennheten (Åndsverkloven. §2).
Oppgaver som er unntatt offentlighet eller taushetsbelagt/konfidensiell vil ikke bli publisert.

Vi gir herved Universitetet i Agder en vederlagsfri rett til å gjøre oppgaven tilgjengelig for elektronisk publisering:	Ja
Er oppgaven båndlagt (konfidensiell)?	Nei
Er oppgaven unntatt offentlighet?	Nei

Acknowledgements

I would like to express my deepest gratitude to all the people who helped me through this thesis and to those who gave me the opportunity to write about something that interests me so greatly.

Firstly I would like to thank my supervisors from the University of Agder for all their knowledge and support. Sathyajith Mathew for his expertise within wind energy, and Joao Leal for his support. I would also like to give a big thanks to my Equinor supervisors Knut Sponheim Seim for technical support, Nils Joseph Gaukroger for both technical support and mental support, as well as Adair Elderberg for giving me the opportunity to investigate this exciting topic. Besides the technical support, I would like to thank my family, friends, roomies, study friends, and boyfriend for their love and support. Their encouragement helped me to stay grounded when I struggled, and their phone calls brightened my days.

Finally, thanks to the University of Agder for this opportunity to study what I am passionate about.

Abstract

This thesis investigated the tilt loss of FOWT in conjunction with power performance. Consisting of three main parts, where the first calculates the power loss of three turbines influenced by tilt, the next part is the AEP of a three-turbine and a 10x10 turbine farm, and at last, is an investigation of the tilt loss of turbines with different spacing. Two engineering wake models are considered and compared, Bastankhah Gaussian (BG) and Jensen (NOJ). Results showed that choosing the wake model is vital due to the deviation of 6.41% from one of the cases. Further, findings show that when three tribunes are placed in an array and downstream turbines are directly influenced by the wake, the BG model gave a total power gain of 2.85%, while a power loss of -3.29% for the NOJ model. For a three-turbine farm, power loss due to tilt showed for both models around -2% loss. The AEP calculations gave a tilt loss for a three-turbine farm of -1.78% (BG) and a 10x10 farm of -0.98% loss. Further, the results obtained in the third part showed that for a three-turbine array, the turbines would gain power with tilted turbines from 3 to 11D, while after 12D, the fixed turbines will produce more. The most significant deviation in tilt loss is a gain of 4.11% at 5D with the BG model and a loss of -3.39% for the NOJ model at 6D. Results obtained seem to indicate a trend of loss due to the tilt, however, some results diverge and this will be discussed in this thesis.

Sammendrag

I denne masteroppgaven undersøkes tilt tap på Floating Offshore Wind Turbines (FOWT) i sammenheng med kraftytelse. Oppgaven er delt inn i tre deler, hvor den første delen ser på kraftproduksjon av tre turbiner i ulike formasjoner med og uten tilt. Del to ser på Annual Energy Production (AEP) av en tre-turbin vindpark og en 100-turbin vindpark. Siste del tester turbinene med ulik avstand for å se hvordan avstand påvirker tilt tapene. Resultatene viser at valg av vake model er viktig for presise resultater. De to ulike vake modellene brukt er Bastankhah Gaussian (BG) and Jensen (NOJ). Videre, med tre turbiner på rekke viste det seg en økning i kraftprodusjon med en tilt på 10°på 2.85% med BG modellen, mens NOJ modellen viste et tap på -3.29% i samme forsøk. Med tre turbiner plasert som en park viste det seg et krafttap på rundt -2%. For neste del med AEP kalkulasjoner viste det seg et tap på -1.78% for tre turbiner i en park, og -0.98% for 100-turbin park. For den tredje delen med ulike distanser viser resultatene at turbinene vil øke produsjonen ved å øke distansen. Videre viste det at med tre turbiner på rad vil turbinene med tilt produsere mer enn turbinene uten tilt opp til 11D distanse, hvor etter 12D turbinene uten tilt vil produsere mer. Største forskjellen mellom de tiltede og utiltede turbinene er ved 5D for BG modellen, med en økning på 4.11%, og et tap for NOJ modellen på -3.39% på 6D. Resultatene viser en trend på tap grunnet tilt av turbine, men noen resultater avviker, og dette vil bli diskutert i denne masteroppgave.

Contents

List of Figures

List of Tables

Nomenclature

ρ	Air density
θ	Tilt angle
A	Area
AEP	Annual Energy Production
BG	BastankhahGaussian
c	Scale
CFD	Computational Fluid Dynamics
Cp	Power Coefficient
Ct	Thrust Coefficient
DOF	Degree of Freedom
DTU	Danish Technical University
f	Probability
F_T	Thrust force
$FOWT$	Floating Offshore Wind Turbine
$HAWT$	Horizontal axis wind turbine
k	Shape
$LCOE$	Levelised Cost of Energy
P	Power
pdf	Probability distribution function
$SOWFA$	Simulator for Wind Farm Applications
T	Thrust force
TI	Turbulence intencity
TLP	Tension-leg platform
U	Wind Speed
v	Velocity
WD	WInd Direction
WFM	Wind Farm Model
WS	Wind speed
WT	Wind Turbine

Chapter 1

Introduction

Wind energy is a form of renewable energy generated by harnessing the power of the wind. It is one of the most rapidly growing forms of renewable energy in the world. According to the International Energy Agency (IEA), global wind power capacity has grown by an average of 17% per year over the past decade and is expected to continue growing in the coming years [1]. This is driven by factors such as declining costs of wind turbines, advancements in wind energy technology, and increasing demand for clean and sustainable energy sources. Many countries have set ambitious targets for increasing their use of wind energy in order to reduce greenhouse gas emissions and mitigate the effects of climate change. The development of wind energy is also a contributor to the UN's Sustainable Development Goals [2], in both goals 7 and 13. Goal 7 is affordable and clean energy, with target 7.2 saying, "By 2030, increase substantially the share of renewable energy in the global energy mix", where wind energy is a necessary form of energy. Goal 13 is Climate Action, where the goal is to slow down the temperature risen and cut CO2 emissions. As the most significant part of the emission is linked to fossil fuels, electricity from wind and other renewable sources is a substitute for this energy and can help reduce fossil fuel usage. Total global wind power capacity is now up to 837 GW (2022), allowing the world to avoid over 1.2 billion tonnes of CO2 annually [3].

However, in Norway, wind energy onshore has met a lot of resistance. Therefore wind energy is forced to find new ways to produce electricity without being in the way of humans. In 2010 a group of people in Equinor sat around a lunch table drawing on a napkin, what now is the largest bet for the renewable part of Equinor, Floating Offshore Wind Turbines (FOWT). As a company, they now have their own offshore wind farms, Hywind Scotland as a pilot project, and Hywind Tampen, which produces power for the oil and gas industry on the Norwegian continental shelf. Besides their projects they are also investing in offshore wind projects worldwide with knowledge, experience and funding. Cost and performance calculations determine if the company should pursue a particular external project. Annual Energy Production (AEP) is used to calculate the Levelised Cost of Energy (LCOE), which determines the feasibility of a FOWT project. These are crucial parameters that are fulfilled repeatedly throughout the project. Onshore wind farms have been working through this for many years, but there is a difference when the turbines are floating. One of the differences is that the support structure is floating and there will be larger excitation in the Degrees of Freedom (DOFs). Since the turbine tower is attached to a floating structure, the wind and waves will influence the position of the turbine.
When the turbine is leaned backward or forward, as seen in Figure 1.1, the turbine is tilted. It is called a static tilt when the structure is inclined from its initial axis. This tilt will influence the power produced by the turbine since when the turbine rotor is tilted away from the incoming wind velocity, the area exposed to the wind is decreased. The turbine will harvest less energy than when fully facing the wind. This will affect the LCOE estimations, and it is crucial to understand how the tilt will influence power production over time. To get a better understanding of the tilt in conjunction with power production this thesis will

investigate the wake effects on power and AEP of turbines with the wake modeling library PyWake.

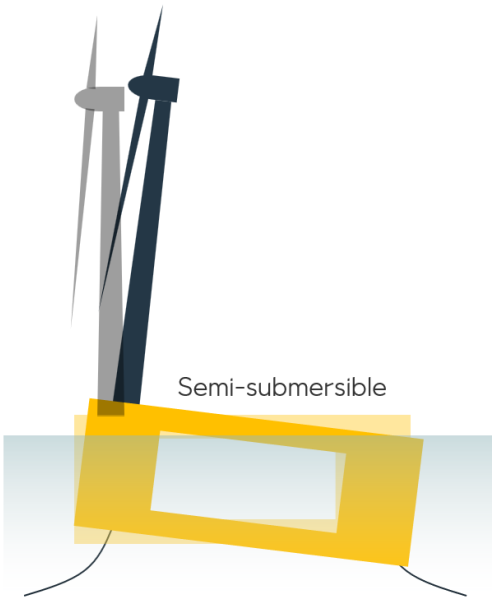

Figure 1.1: Demonstration of a Semi-submersible FOWT, by Nils Joseph Gaukroger.

1.1 Basics of Floating Offshore Wind Turbines

Floating Offshore Wind Turbines (FOWT), unlike bottom fixed turbines, need to have a floating foundation. There are four main types of deep offshore foundations, adapted from the offshore oil and gas industry, seen in Figure 1.2. They vary in type due to different factors and resources.

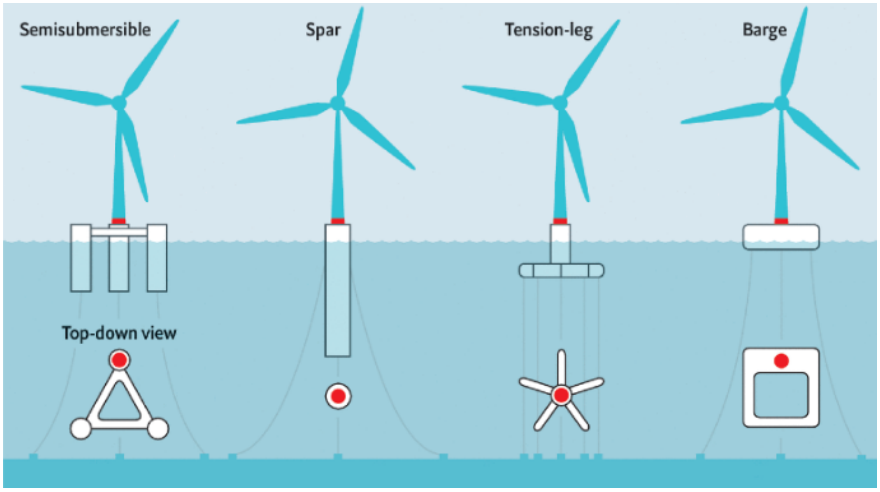

Figure 1.2: FOWT four main types of deep offshore foundations[4].

- **Semi-submersible:** This type of structure consists of a large platform that is partially submerged in the water with a turbine mounted on top.
- **Spar:** This type of structure consists of a long, cylindrical buoy that is anchored to the sea floor. The turbine is mounted on top of the buoy[5].
- **Tension-leg platform (TLP):** A TLP is a type of floating structure that is anchored to the sea floor by a series of cables or chains. The turbine is mounted on a platform

that is suspended from the TLP[6].

- **Barge:** This type of structure is a floating structure that is made up of a lattice structure, the turbine is mounted on top of the lattice structure.

The choice of structure will depend on factors such as water depth, wind conditions, and the size of the turbine being used. The pitching or static-tilt behavior is different for these. The TLP experiences a pitch forward with increasing thrust force, whereas the remaining three experience the opposite, leaning backward. All these factors need to be accounted for when calculating the viability of a FOWT project.

1.1.1 Up to date wind projects

To set the FOWT in context with the development of the world, let's see some of the existing projects, and some planned for the future. Floating wind is still in an early stage, yet there are operating wind farms and demo projects on the sea. This section will present some of the offshore floating wind projects existing today. Some projects with spar are Hywind Scotland [7] and Hywind Tampen [8]. Projects with Semi-submersible are Kincardine Offshore Windfarm [9], WindFloat Atlantic [10], Les Éoliennes Flottantes du Golfe de Lion (EFGL) [11] and Erebus [12]. EolMed is a floating wind farm using a damping pool concrete floater (barge) [13].

Project Name	Location	Launch Year	Capacity
Hywind Scotland	North Sea	2017	30 MW (5 x 6 MW)
Kincardine Offshore WF	Scotland	2020	50 MW (5 x 9.5 MW)
WindFloat Atlantic	Portugal	2020	25 MW (3 x 8.4 MW)
Hywind Tampen	North Sea	2022	88 MW (11 x 8 MW)
EolMed	France	2023	24 MW (3 x 8 MW)
EFGL	French Mediterranean	2024	30 MW
Erebus	Celtic Sea	2027	96 MW

Table 1.1: Floating offshore wind turbine projects and demonstration projects

Hywind Scotland is a floating offshore wind farm project located in the North Sea, around 15 miles off the coast of Scotland. The project is developed by Equinor and it is the world's first floating wind farm. The project consists of five floating wind turbines, each with a capacity of 6 MW, which are connected to the seabed by mooring lines. The turbines are anchored in water depths of around 95-129 meters, providing the turbines with stable and strong winds. The floating wind turbines are connected to the shore by subsea power cables, which transmit the electricity generated by the turbines to the onshore substation. Hywind Scotland has an installed capacity of 30 MW and it can generate enough electricity to power around 20,000 homes. The project is expected to reduce carbon emissions by around 57,000 tons annually. The project is considered a significant milestone in the development of floating offshore wind energy, as it demonstrated the feasibility of using floating wind turbines in deep waters and it's the first to be connected to the grid and supplying electricity to homes and businesses. The project has also provided valuable data and insights for further floating offshore wind projects.
Hywind Tampen is a floating offshore wind farm project that is being developed by Equinor. The project aims to harness the wind energy resources of the North Sea to generate electricity for oil and gas platforms. The Hywind Tampen project will consist of 11 floating offshore wind turbines, each with a capacity of 6 MW. The turbines will be anchored to the seabed in a water depth of around 260-290 meters, which is considered to be too deep for traditional bottom-fixed offshore wind turbines. The floating wind turbines will be connected to the oil and gas platforms by sub-sea power cables, which will transmit the electricity generated

by the turbines to the platforms. The project is expected to generate enough electricity to power about 40,000 homes, and will reduce the carbon emissions from the oil and gas platforms by about 200,000 tons per year.

1.1.2 Future FOWT

In the context of floaters it is interesting to see what type of floater will be used in the future. Spars like those used at Hywind Tampen make sense in Norway because the manufacturing costs are low, and the installation is straightforward because the fjords are deep enough to be installed near shore (i.e., there's enough depth to have the spar upright). In other parts of the world, these installation and manufacturing costs are very different, so often semi-sub are used. The two floating foundation concepts currently in use are the concrete spar used on the Hywind projects and Principle Power's WindFloat semi-sub [14]. They have projects in Portugal, the UK, and France. However, the movement of a spar isn't too dissimilar from a semi-sub. They will both experience tilt loss, unlike a TLP who leans the other way. As mentioned, the spar will have some limitations on a world basis due to being fabricated and assembled in shallower/less deep water. Further, as the semi-submersible already is planned for many projects, the tilt of the turbine has to be understood.

Figure 1.3: Demonstration of the current wind turbine which is investigated for tilt, figure provided by Equinor.

1.2 Tilt

This report will investigate the tilt losses, as mentioned. The tilt losses are the power deviation between the power produced by the fixed turbine and the tilted turbine. When mentioning the tilt in this thesis, it is a static tilt, meaning the tilt of the whole structure, as seen in Figure 1.4. Static tilt is the tilt due to the average loads, while dynamic tilt is also including the variations due to varying loads (changes in wind speed and direction, and waves/current). However, the simulations in this thesis will only tilt the rotor part of the turbine as a simplification.

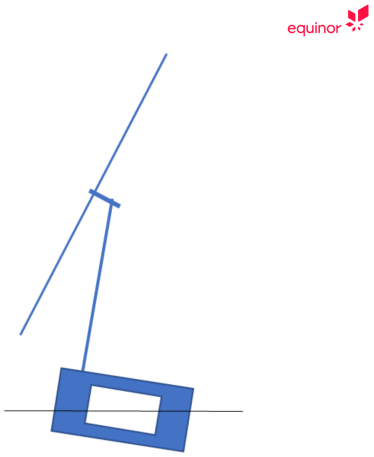

Figure 1.4: Static tilt of a floating turbine, figure provided by Equinor.

The static tilt of the turbine will create a deflection of the wake, as seen in Figure 1.5. When the turbine is leaned backward which occurs when the wind velocity is high from the front of the turbine, the wake is deflected upwards. When we are talking about the tilt it is relative to the rotor vertical axis. If the turbine is tilted as seen in Figure 1.4 it has a positive tilt angle, if the rotor is faced downwards, it has a negative tilt angle. This is however defined differently in different literature but will be used as notation in this thesis. The angle of the floater is called pitching. The pitch angle will have the same notation in the positive and negative direction as the tilt. If the tilt angle is negative, the wake is deflected toward the ground, while for a positive tilt, the wake is deflected upwards.

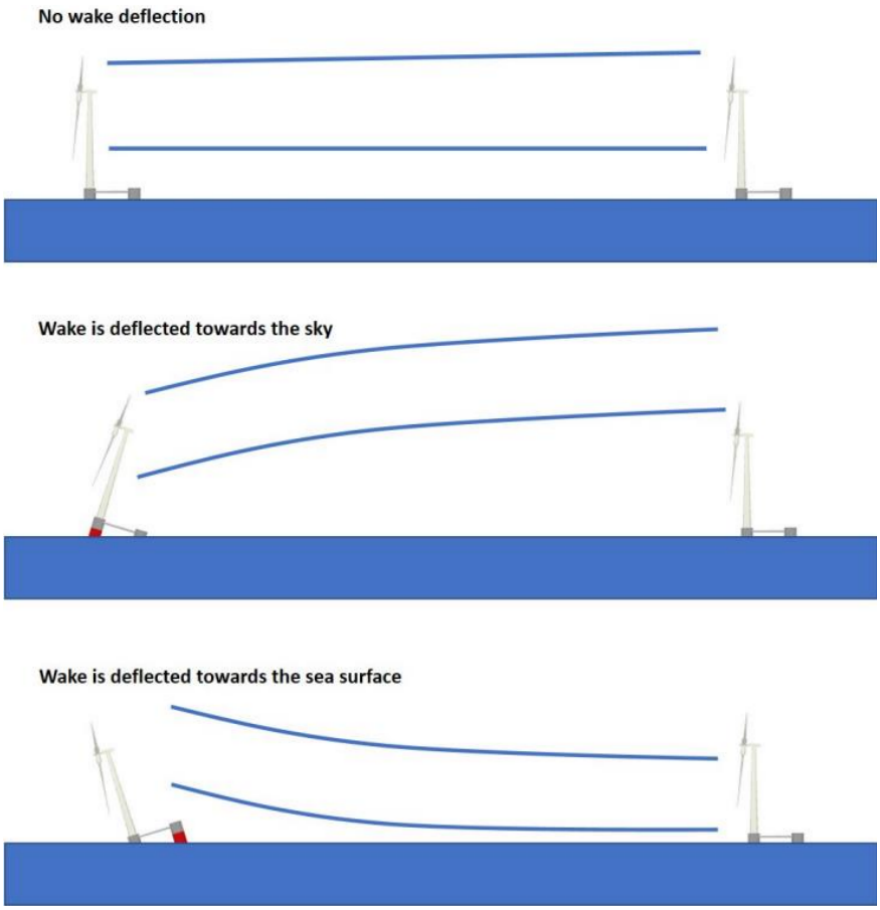

Figure 1.5: Demonstration of wake deflection of a FOWT due to static tilt, figure by Equinor [15] .

1.2.1 Degree of Freedom of a FOWT

The static tilt or pitch of the floater as it is called, is only one of six degrees-of-freedom (DOF) of a floating wind turbine, as seen in Figure 1.6. The conventional rigid body DOF are incorporated: surge X, sway Y, heave Z, roll, pitch, yaw [16]. The tilt is not investigated to a high degree due to FOWT being a new area. The rotational degrees of freedom are different in terms of their effect on production from the traditional degrees of freedom. With floating foundations, wind turbine control faces a dramatic increase of DOF to be controlled, thus resulting in under-actuation reality [17].

Figure 1.6: Demonstration of six DOF for a FOWT, figure modified from Equinor.

1.3 Problem description

Tilt loss is the loss of power production due to the mean inclination of a passive ballast floating wind turbine. When the turbine is tilted backward or forward, it results in a decrease in the projected area facing the wind while generating power. The tilt loss of a passive ballast floating wind turbine is hence not sufficiently understood.
Hence, it is essential to understand how it will affect a single turbine power production and also a farm. This thesis will investigate both cases. By looking at the power produced for three single wind turbines in an array, turbines in different formations, and Annual Energy Production (AEP) for three turbines in a farm. In the end, different distances between turbines will also be considered. There may also be an advantage of the wake deflected away from the downstream turbines in some cases, i.e., the wake effect is less prominent for those turbines.
The production losses from the tilt will be compared with untilted turbines, which will be called fixed turbines in this thesis. By using the software PyWake [18] developed by DTU, the power is calculated for single turbines with and without tilt. Further, an AEP will be calculated for three turbines, forming a farm, and a 10x10 turbine farm. In the second case with tilt, it will be used an fixed tilt. The third case will investigate the tilt loss at different distances.

1.4 Research questions

This section presents the research questions raised within the area of tilt losses. These questions will be discussed and answered later in this thesis.

- **RQ1:** What is the effect of tilt on FOWT?

  RQ1.1: How will the tilt of the turbines affect production of one turbine?
  RQ1.2: How will the tilt of the turbines affect production of multiple turbines?
  RQ1.3: How will the tilt of the turbines affect production for downwind turbines?
  RQ1.4: How will the tilt of the turbines affect AEP in a farm?
  RQ1.5: How will the tilt of the turbines affect production with different wake models?
  RQ1.6: How will the tilt of the turbines affect production with different distances?
  RQ1.7: Is there a loss or a gain when the turbines are tilted?

Chapter 2

Related Work

Within the problem stated, there are a few articles discussing the tilt loss of FOWT [19]. However, some articles are investigating the power gain by using tilt control with fixed tilt [20] [15] and active tilt control [21]. Other articles use similar methods for investigating yaw misalignment steering, [22] [23]. This literature review will present all mentioned above and use it later in the discussion.
NREL [20] deals with the advantages of wake steering and evaluated tilt for wind farms by evaluating the tilt for two or three turbines in an array. By tilting the turbines in a certain configuration, the authors demonstrate how a two-turbine array's power output can be increased. The total percentage of power gain increases when the number of turbines is increased, as is shown with the three-turbine array. For the two turbine cases, tilting the turbine 25°in the negative direction (wake steered downwards) experiences a power gain of 8.3 % while tilting the turbine in the positive direction (wake steered upwards) results in a 3.8 % power loss. Figure 2.1 shows the results of tilting turbines.

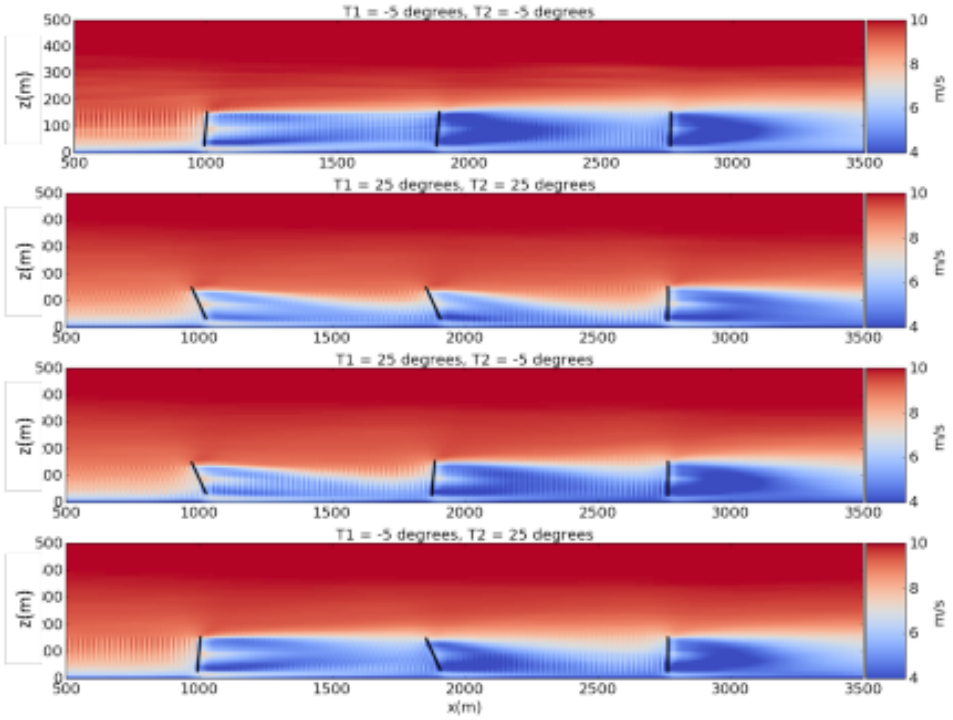

Figure 2.1: Results from NREL of wake steering [20].

Further, NREL has another paper investigating flow control leveraging downwind rotors for improved wind power plant operation [24]. Two elements of flow control are wake steering via yaw and tilt of a turbine. This work enhances the wake engineering model FLOw Redirection and Induction in Steady State (FLORIS) to include these curled wake effects due to tilt. As

said by NREL: "In order to develop, test, and tune wind power plant controllers efficiently, an accurate engineering model of the turbine wake dynamics is required".
In [15] vertical wake deflection for floating wind turbines by differential ballast control is investigated. The purpose is again to steer the wake, but by pitching the floater. There is executed an combined simulation-experimental study with wind tunnel testing and a CFD analysis of two turbines in a array, using large eddy simulation (LES) and actuator line method (ALM) implemented in FOAM-extend. Results obtained showed that a negative tilt (wake steered downwards) of 15°will give a power gain for 3% with a spacing of 10-12 diameters, while a power gain of 7% with a spacing of 6-8 diameters.

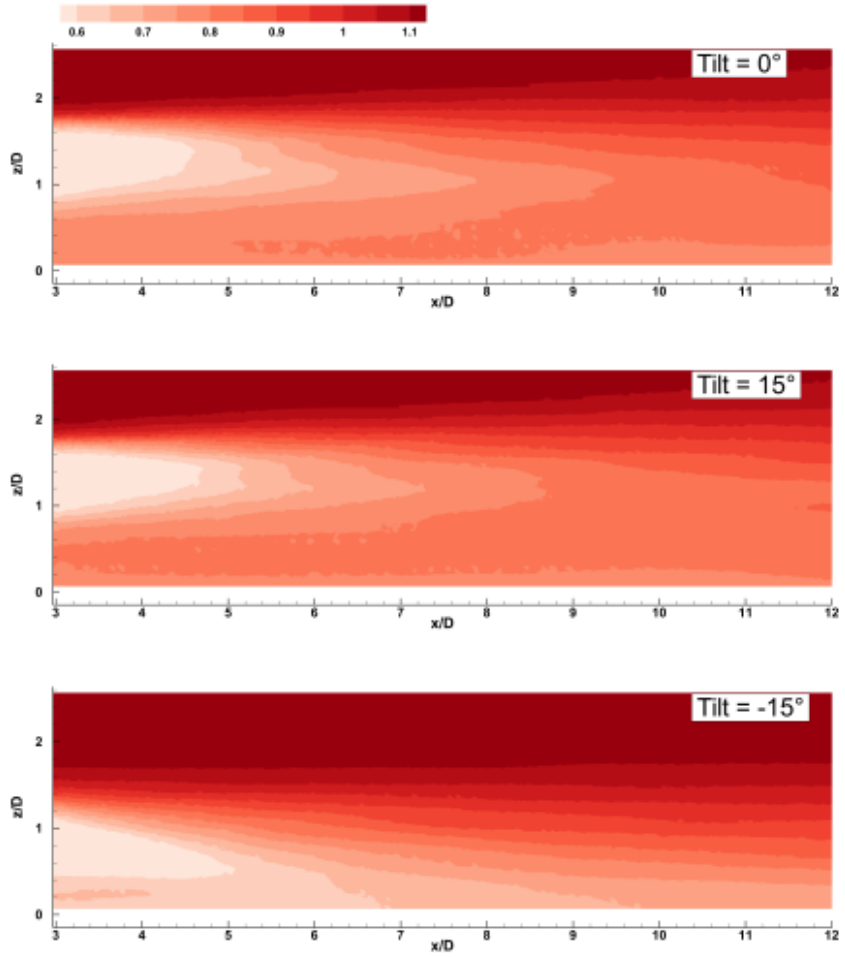

Figure 2.2: Results from EAWE of wake steering [15].

So far, wake-steering via yaw misalignment has drawn the most attention since it can be adapted to existing wind farms. Yet, several studies and recent experimental results have indicated that tilt-misalignment could allow for even larger gains. Tilt misalignment of a wind turbine deflects the wake vertically, such that a wake can be steered upwards into higher momentum flow or downwards into the ground.
In [21], the research explores tilt angle and active tilt control optimization for a full wind farm. Using an analytic wake model [25], researchers modeled an entire wind farm and analyzed the advantages of wake deflection from turbine tilt. They explored the possibility of optimizing a fixed tilt angle for each turbine, assuming the same angle for all wind directions, as well as active control of turbine tilt. However, implementing a tilt mechanism would be costly and complicated, increasing turbine capital costs. This study is a preliminary step in determining if the benefits of active tilt control outweigh the challenges of implementing it in actual wind farms. The modified Bastankhah model demonstrated that a tilt angle of around negative 20°to 25°(wake steered downwards) in the upstream turbine could increase

the total power production of a two-turbine array in line with the wind direction by about 6%, whereas a tilt angle of positive 25°(wake steered upwards) could lead to a 6% power loss. Optimizing the AEP of the Princess Amalia wind farm showed a 2.77% increase in AEP with fixed tilt angles of 5°at 6D distance, a 7.75% increase in AEP with active yaw control, and a 13.64% increase in AEP with active tilt control. The power gain of 2.77% with fixed tilt angles suggests that manufacturing turbines with a fixed tilt angle may not be as advantageous as other fixed methods, such as variable tower heights, which would be easier to manufacture. However, active tilt control offers significant benefits compared to yaw control.

The main focus of [26] was to optimize the power coefficient of floating offshore wind turbines (FOWTs) to preserve their wind power performance. This optimization aimed to address the issues arising from the tilt angle of the wind turbine platform, which can negatively impact the effective area for extracting wind turbine energy. To analyze and compare FOWTs with a variable-speed fixed-pitch control strategy, the researchers conducted experiments using a wind tunnel and a CFD analysis. The study considered wind speeds ranging from 2 to 5.5 m/s and tilt angles between 3.5-6.1°. The results demonstrated that, within tip speed ratios of 7.7 to 9.6, average rotational speed differences of 16.4% and optimal power coefficients of 0.35 to 0.36 were attainable during wind speeds of 3 to 5 m/s, with tilt angles of 3.9-5.8°. These findings provide insights into a new concept of power coefficient optimization using variable tilt angles for small to medium fixed pitch FOWTs, to reduce the cost of pitch control systems.

In [19], the study conducted a wind tunnel test and mathematical modeling to compare the impact of rotor tilt angle between a FOWT and a fixed tower turbine. Wind velocities ranging from 2 to 5.5 m/s were tested. The results showed that the rotational speeds of FOWTs were lower than those of fixed tower turbines. Additionally, at tilt angles ranging from 3.5°to 6.1°, performance was reduced, with losses varying between 22% and 32% at different wind speeds.

In [27], they investigate Characterizing tilt effects on wind plants. The tilt angle was varied in the third turbine row from 15° to 15° in chosen 5° increments. Numerical simulations predict losses in net efficiency for positive angles but diverge for negative tilt angles. The results demonstrate that the tilt angle influences wake magnitude, displacement, and recovery. Positive angles deflect wakes above the wind plant, while negative angles encourage entrainment into the wind plant and exhibit rapid recovery.

After reviewing the litterateur, it can be seen that most of the studies conducted in this area are focused on the wake steering capabilities of the tilt. However, with the increase in floating wind turbines, there is a challenge of power fluctuations due to the tilt experienced by the rotor due to the floating actions of the platform. This has not been particularly studied. In some of the mentioned studies, there is a pre-set angle for the tilt, and the relationship between the incoming flow and the resulting tilt is not properly explored. Tilt loss of FOWT is the area this thesis will contribute to and what this study is trying to discover more about.

Chapter 3

Theory

3.1 Wind Energy

A wind turbine transforms the kinetic energy in the wind into electrical power[28]. It starts with the rotor starting to rotate due to the aerodynamic forces lift, which arises when the wind flows over the airfoil shape of the blade. Since the rotor is extracting power, the velocity of the wind is slowed down and mixed up to a turbulence state behind the turbine, called wake. This is explained in the Blade Element and Momentum Theory. Thereafter, the theoretical limit of extracting power from the wind was discovered by Betz, called Betz limit. The electrical power of a turbine is expressed by a power curve to predict the production at different wind speeds of a chosen turbine. Further, a thrust curve is used to see the relationship between the thrust and the wind speed. These two curves depend on the theory mentioned above and will be necessary for the work of this thesis. The thrust curve is a measure of the aerodynamic performance of the turbine, and the power curve, on the other hand, is a measure of the turbine's overall performance, taking into account both the aerodynamics of the blades and the efficiency of the generator.

3.1.1 Power curve

The power curve is a graph that shows the relationship between the wind speed and the power output of a wind turbine [29], as seen in Figure 3.1. It is used to understand a wind turbine's performance and determine its optimal operating conditions. The power curve is divided into different regions, with a cut-in wind speed, which is the minimum wind speed at which the turbine begins to generate power. As the wind speed increases, the turbine's power output also increases until it reaches a peak output, known as the turbine's rated power. Beyond the rated power, the turbine reaches a point known as the cut-out wind speed, which is the maximum wind speed at which the turbine is designed to operate. The shape of the power curve can vary depending on the turbine type, design, and location. The turbine's control systems, such as the pitch, can also affect the power curve. For example, if the pitch control system is set to limit the rotor speed, the power curve will flatten out at high wind speeds, which can help to protect the turbine from damage. It is important to note that the power curve is not constant. It can change over time due to factors such as turbine aging, blade erosion, and dirt accumulation.

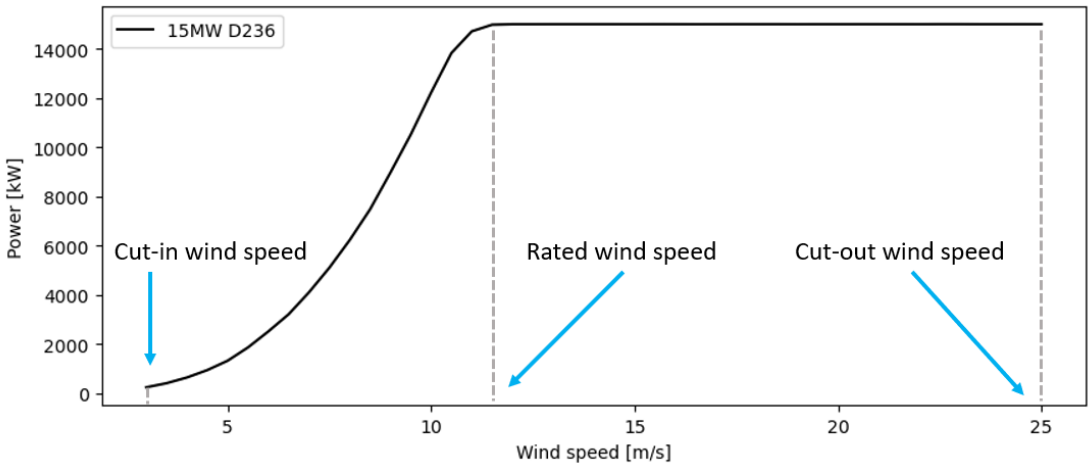

Figure 3.1: Power curve of a wind turbine.

The power P extracted by a wind turbine is given by [30] :

$$P = \frac{1}{2}\rho A v^3 C_p \tag{3.1}$$

where ρ is the density, A is the swept area of the blades, v is the wind velocity and C_p is the power coefficient. The power coefficient (C_p) of a wind turbine is a measure of its efficiency in converting wind energy into electrical energy, it is a non-dimensional factor [29][30]. The power coefficient can be determined by measuring the power output of the turbine and the wind speed some distance upstream of the rotor ("free" wind speed). The maximum value of C_p is defined by betz limit, which states that the turbine can not extract more than 59.3% of the power from the wind. The C_p can then be calculated using the following formula, Equation 3.2.

$$C_p = \frac{Pout}{0.5\rho A v^3} \tag{3.2}$$

where ρ is the density of air and A is the area swept by the rotor blades. The typical range of the power coefficient for HAWT is between 0.3 to 0.5.

3.1.2 Thrust curve

The thrust curve for a wind turbine generator shows the relationship between the wind speed and the amount of thrust produced by the turbine. The curve typically starts at zero thrust at low wind speeds, increases to a maximum at the turbine's rated wind speed, and then levels off or decreases at higher wind speeds. The equation for calculating the thrust of a turbine is:

$$F_T = \frac{1}{2}\rho A v^2 C_T \tag{3.3}$$

The power curve is generally steeper than the thrust curve, as the turbine's generator typically becomes more efficient as the wind speed increases. So, the power curve will reach its maximum sooner than the thrust curve.
The thrust coefficient is a dimensionless parameter that describes the efficiency of the turbine in converting the kinetic energy of the wind into mechanical energy. It is defined as the ratio of the thrust force generated by the turbine to the kinetic energy of the wind passing through the turbine rotor area. The mathematically expression for the thrust coefficient (C_T) is seen in Equation 3.4.

$$C_{\mathrm{T}} = \frac{F_T}{0.5\rho A v^2} \tag{3.4}$$

3.1.3 Wind turbine control

A wind turbine has several control systems to regulate the power to optimize production. The main physical mechanisms are pitch and yaw [31]. Pitch is controlling the angle of the blade towards the wind, called the angle of attack. The optimal angle of attack will vary with different airfoils and blade twist. The pitch control limits the amount of lift force created when the turbine reaches the capacity of the generator. Further, the pitch can also put the blade into the position of stall, which is a state where the fluid is no longer attached to the surface of the blade, and turbulence arises. This leads to the lift force no longer working, and the blades will stop rotating. The yaw mechanism is between the tower and nacelle and rotates the rotor and nacelle towards the wind direction. This is for the turbine to always face the wind. However, yaw can also be used to steer the wake to optimize downwind turbine production.

3.2 Tilt

The turbine will produce less power when tilted, due to the decreased area facing the inflow. The tilt angle of the rotor will influence the wake as a wake deflection. The wake deficit is caused by a reduction to the thrust force, which slows down the incoming velocity [18]. Figure 3.2 shows the decomposition of the forces where the force (f) is the thrust force (T).

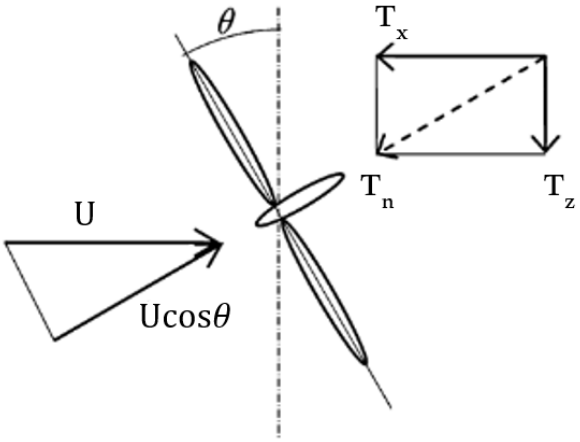

Figure 3.2: Body forces introduced by the rotor exposed to the tilt angle θ, acording to the actuator disk theory, figure modified from [32].

Thrust force normal to the rotor plane:

$$T_n = \frac{1}{2}\rho C_{\mathrm{T,n}} A (U cos\theta)^2 \tag{3.5}$$

In non-aligned inflow, the thrust force that slows down the flow, in the mean wind direction:

$$T_x = \frac{1}{2}\rho C_{\mathrm{T,x}} (A cos\theta) U^2 \tag{3.6}$$

From these two equations above, the relationship between the thrust coefficient in the rotor normal direction and the thrust coefficient in the down-wind direction can be found.

$$T_x = T_n cos\theta \tag{3.7}$$

$$\frac{1}{2}\rho C_{\mathrm{T,x}}(Acos\theta)U^2 = \frac{1}{2}\rho C_{\mathrm{T,n}}A(Ucos\theta)^2 cos\theta \tag{3.8}$$

$$C_{\mathrm{T,x}} = C_{\mathrm{T,x}} cos^2\theta \tag{3.9}$$

3.3 Annual Energy Production

Calculating the annual energy production for wind turbines is important because it helps determine the overall efficiency and economic feasibility of a wind energy project. By measuring the amount of energy produced by a wind turbine over the course of a year, developers and investors can estimate how much electricity the turbine will generate. This information is crucial for determining a project's feasibility and making decisions about optimizing the turbine's performance over time. Additionally, measuring the annual energy production can be used to compare the performance of different turbines. Since the wind speed over a year is used, a probability distribution function (pdf) of wind speed and wind direction frequency is used. The AEP is calculated by Eq. 3.10.

$$AEP = 8760 \int_0^\infty p(U)P(U)dU \tag{3.10}$$

where 8760 is number of hours in a year, p(U) is the pdf of the wind speed and P(U) is the power curve for the turbine [33].

3.3.1 Wind Speed Distribution Models

Wind power has randomness, volatility, and intermittent properties, causing wind farm production power to fluctuate significantly [34]. In wind farm analysis, planning, design, construction, and operation, several probability distribution models have been widely employed. There are several probability distributions commonly used in wind data analysis. Some common wind speed distributions models are listed below.

- **Weibull distribution:** often used to model wind speed data, as it can fit a wide range of shapes for the wind speed distribution.
- **Rayleigh distribution:** a special case of the Weibull distribution that is commonly used to model wind speeds in the absence of strong gusts or turbulent conditions.
- **Normal distribution:** can be used to model wind direction data, as wind direction is typically thought to be a random variable that is uniformly distributed around the compass.
- **Lognormal distribution:** also commonly used to model wind speed data, as it can capture the skewed distribution often seen in wind speeds.

It is important to note that the choice of distribution depends on the specific data set and its characteristics, and that is a good practice to validate the assumption of the chosen distribution by using fit tests. The Rayleigh distribution uses one parameter, which is the mean wind speed, while the Weibull distribution uses two parameters which are the scale and shape factor which can better represent a wider variety of wind regimes [29].

3.3.2 Weibull

The Weibull distribution is a probability distribution that is commonly used to model wind speeds at a specific location [29] [35] [36]. It is often used in the design and analysis of wind turbines, as it can accurately describe the variability of wind speeds over time. The Weibull distribution is characterized by two parameters: the scale parameter (k) and the shape parameter (c) [35]. These parameters can be estimated from measured wind speed data and can be used to predict the probability of different wind speeds occurring at a given location. This information is useful for determining the power output of a wind turbine, as well as its reliability and expected lifetime. It is not always a good representation, and therefore in some cases it can be be used different scale factors and shape factors for the different seasons [35].
The Weibull function can represent the wind speed distribution as a function f(U)

$$f(U) = e^{-(\frac{U}{c})^k} \tag{3.11}$$

where U is the wind speed and c is the scale factor

$$c = \frac{U_{\text{mean}}}{\gamma(1 + \frac{1}{k})} \tag{3.12}$$

with gamma being the gamma function and k the shape factor.

$$f(u) = k(\frac{U_{\text{mean}}}{c})^k u^{(k-1)} e^{-(\frac{U_{\text{mean}}}{c} u)^k} \tag{3.13}$$

With u = U/U_{mean}
The Weibull probability density function is given as

$$f(U) = 1 - e^{-\frac{U}{c}^k} \tag{3.14}$$

with the average velocity determined as followed

$$U_{\text{mean}} = c\gamma(1 + \frac{1}{k}) \tag{3.15}$$

where gamma function:

$$\gamma(x) = \int_0^\infty e^{-t} t^{x-1} dt \tag{3.16}$$

3.4 Wake

The wake of a wind turbine falls within the topic of advanced aerodynamics, according to [29]. It is characterized by a reduction in wind velocity and an increase in turbulence, which can affect the performance of downstream turbines. Wind turbine wakes are often divided into a near wake and a far wake. The difference between these two is a function of spatial distribution and intensity of turbulence, see Figure 3.3. Through fluid flow modeling and experiments, it is found that each blade generates a sheet of vortices on the trailing edge of the blades. Additionally, the hub also generates a vortex, and strong vortices are generated on the tip of the blades. All these are transported through the wake by the mean axial and rotational flow in the wake. This vortex and the mechanically generated turbulence are mixed in the near wake. Much of the periodic nature from the hub and tip vortex is lost in the near wake. However, the far wake still experiences high relative turbulence from the tip speed vortex surrounding the less turbulent core of the wake. The consequences of the wake consisting of turbulence and vorticity are increased loads and fatigue on downstream turbines. Further, the tip and hub vortices can reduce the turbine's energy production. As

mentioned, the main effect of wake is on the downstream turbines, therefore, to mitigate the effects of wake, spacing and layout are important parameters that requires modeling and control techniques to optimize the performance. Additionally, wake steering techniques can be used to redirect the wake to minimize its impact on downstream turbines. The wake steering will also influence the wake.

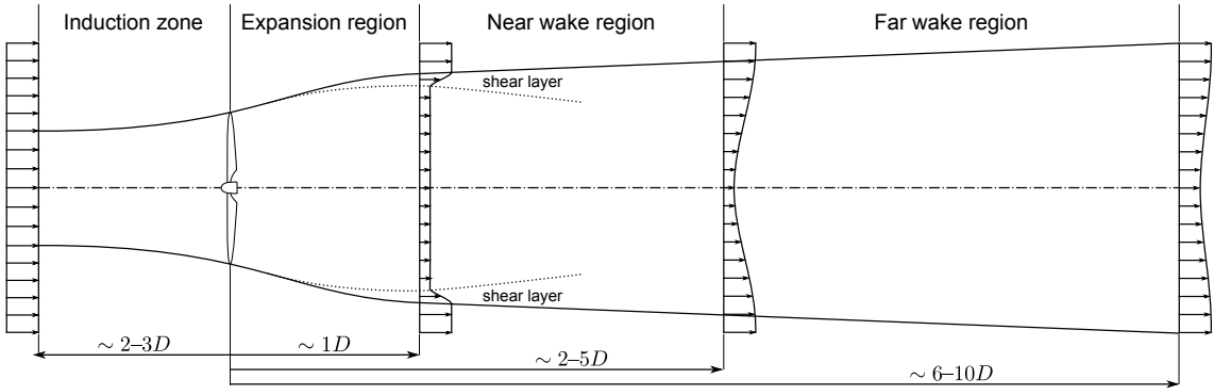

Figure 3.3: Flow regions around a wind turbine. Figure by Dries Allaerts.

3.4.1 Spacing

Spacing is about placing the turbines far away enough for the wake to recover as much as possible, while on the other side, the cost of cables and the potential area would recommend them as close as possible. So with these parameters, the optimal distance can be found. Usually, the turbines are placed in the far wake region, around 3-10 diameters are typical [37]. The turbine spacing is typically determined based on the wake width and wind speed. Generally, the wider the wake and the lower the wind speed, the greater the distance between the turbines should be.

3.4.2 Wake modelling

Wake modeling of wind farms involves simulating the wind turbine wakes's effects on the wind flow through a wind farm. This is important for understanding and predicting the power output of a wind farm and optimizing the placement of turbines within a wind farm to minimize the wake effects. Wake models can be divided into two main categories:

- Analytical models
- Computational Fluid Dynamics (CFD) models

Analytical models are based on simplified equations and assumptions, also called engineering models, while CFD models solve the Navier-Stokes equations using numerical methods. Both models have their advantages and limitations, and they are used in different situations depending on the level of accuracy and computational resources required. The engineering models are cheaper and faster, while CFD is more accurate or realistic.

NOJ

The Jensen model (NOJ) [38] wake model was published as early as 1983 and is a commonly used analytical method for predicting the velocity deficit caused by a wind turbine. It is based on the assumption that the wake expands linearly with downstream distance and that the velocity deficit decays exponentially with distance from the center of the wake. It is a simple wake model, where the near field behind the wind turbine, consisting of periodic

and deterministic swirling vortices, is neglected. Making it possible to treat the wake as a turbulence wake or negative jet.

A balance of momentum gives,

$$\pi r_0^2 v_0 + \pi(r^2 - r_0^2)u = \pi r^2 v \tag{3.17}$$

where v_0 is the velocity just behind the rotor, u is the ambient wind velocity, and v is the velocity in the wake at distance x from the rotor. Assuming a linear wake and setting the velocity right behind the rotor to $1/3u$, v can be solved as:

$$v = u1 - \frac{2}{3}(\frac{r_0}{r_0 + \alpha x})^2 \tag{3.18}$$

The NOJ model assumes a linear expansion of the wake with downstream distance, which is valid for relatively low turbulence intensity and weak atmospheric stability conditions. For higher turbulence intensity and stronger atmospheric stability, the wake expansion rate may deviate from linear, and the model may need to be modified or replaced with a more accurate model, such as the Bastankhah-Gaussian wake model.

Bastankhah-Gaussian

A new analytical model was proposed to predict the deficit of the streamwise velocity in the wake of a wind turbine by [25]. To this end, a Gaussian distribution is considered for the velocity deficit in the wake, and mass and momentum conservation are applied to evaluate the velocity profiles downwind of the turbine. The BastankhahGaussian wake model is derived by neglecting viscous and pressure terms in the momentum equation and applying mass and momentum conservation:

$$\rho \int U_W(U_\infty - U_W)dA = T, \tag{3.19}$$

T is the total force over the wind turbine and are expressed by:

$$T = \frac{1}{2}C_T \rho A_0 U_\infty^2 \tag{3.20}$$

The self-similarity in the wake describes the normalized velocity deficit as:

$$\frac{\Delta U}{U_\infty} = C(x)f(r/\sigma(x)) \tag{3.21}$$

where $C(x)$ represents the maximum normalized velocity deficit at each downwind location which occurs at the center of the wake, r is the redial distance from the center of the wake and $\sigma(x)$ is the characteristic wake width at each x. Since the velocity deficit in the turbine wake is assumed to have a Gaussian shape the equation can be written as:

$$\frac{\Delta U}{U_\infty} = C(x)e^{-\frac{r^2}{2\sigma^2}} \tag{3.22}$$

where σ is the standard deviation of the gaussian-like velocity deficit profile at x. Further, the wake velocity is given as:

$$U_W = U_\infty(1 - C(x)e^{-\frac{r^2}{2\sigma^2}}) \tag{3.23}$$

Now, Eq 3.20 and Eq. 3.23 are inserted into Eq. 3.19 and integrating from 0 to ∞ yield:

$$8(\frac{\sigma}{d_0})^2 C(x)^2 - 16(\frac{\sigma}{d_0})^2 C(x) + C_T = 0 \tag{3.24}$$

By solving Eq. 3.24 there are two solutions for $C(x)$, but only the one who predicts the smaller value for velocity deficit at large downwind distance is physically acceptable:

$$C(x) = 1 - \sqrt{1 - \frac{C_T}{8(\sigma/d_0)^2}} \tag{3.25}$$

An assumption of linear expansion for the wake is assumed, like Jensen [38], σ/d_0 can be written like:

$$\sigma/d_0 = k^* \frac{x}{d_0} + \epsilon \tag{3.26}$$

where $k^* = \delta\sigma/\delta x$ is the growth rate and ϵ is equivalent to the value of σ/d_0 as x approaches zero. Further, ϵ is determined by equating the total mass flow deficit rate at x = 0, concluding that $\epsilon = 0.25\sqrt{\beta}$. Simplified to $\epsilon = 0.2\sqrt{\beta}$. Where β is a function off C_T:

$$\beta = \frac{1}{2}\frac{1 + \sqrt{1 - C_T}}{\sqrt{1 - C_T}} \tag{3.27}$$

Inserting Eq. 3.25 and Eq. 3.26 into 3.22, giving:

$$\frac{\Delta U}{U_\infty} = \left(1 - \sqrt{1 - \frac{C_T}{8(k^* x/d_0 + 0.2\sqrt{\beta})^2}}\right) * exp\left(-\frac{1}{8(k^* x/d_0 + 0.2\sqrt{\beta})^2}\{(\frac{z_h}{d_0})^2 + (\frac{y}{d_0})^2\}\right), \tag{3.28}$$

where y and z are spanwise and vertical coordinates, respectively, and z_h is the hub height. Eq. 3.28 gives the normalized velocity deficit in the wake as a function of normalized coordinates (x/d_0, y/d_0 and z/d_0), C_T and k^*.

3.4.3 Deflection of wake

Deflection of wake caused by a yaw or tilt misalignment has been calculated by [39]. The authors carried out a Large Eddy Simulation (LES) to characterize the turbulence behind a wind turbine given the wake deflection created by different yaw angle and thrust coefficient settings, which will be used for tilt angle deflection in this case. The Jimenez wake deflection model describes how the wake deflects downstream as it interacts with the incoming wind. It assumes that the wake expands linearly with downstream distance, and the amount of wake deflection depends on the initial wake radius, ambient turbulence intensity, and the wind turbine's thrust coefficient. The model also takes into account the effect of the wind direction on the wake deflection angle. Figure 3.4 shows the schematic of the deflection model used by Jimenez.

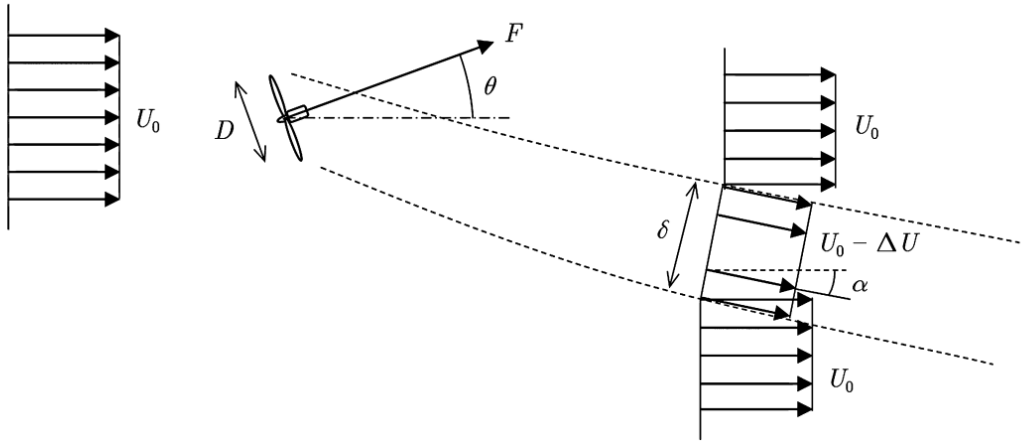

Figure 3.4: Schematic of deflection model, [39] .

In Equation 3.29 and 3.30 is the relationship between the obtained force exerted by the turbine on the flow. Equation 3.29 is the projection in the incident wind direction and in Equation 3.30 is the projection for the other horizontal direction perpendicular to the first equation.

$$f_x = -\rho U_0 \Delta U \frac{\pi \delta^2}{4} \tag{3.29}$$

ΔU is the velocity deficit in the wake.

$$f_z = -\rho U_0^2 \frac{\pi \delta^2}{4} \alpha \tag{3.30}$$

The value of α can be obtained as a function of δ and are shown in Equation 3.31.

$$\alpha \approx \left(\frac{D}{\delta}\right)^2 cos^2\theta sin\theta \frac{C_T}{2} \tag{3.31}$$

For the deflection angle right behind the turbine, also called initial skew angle of the wake it is assumed that $\delta \approx$D, this give the equation:

$$\alpha_{x=0} \approx cos^2\theta sin\theta \frac{C_T}{2} \tag{3.32}$$

If, however, the wake cross-section is assumed to rise linearly with downstream distance x, and $\delta = D + \beta x$, the expression results in:

$$\alpha \approx \frac{cos^2\theta sin\theta \frac{C_T}{2}}{\left(1 + \beta \frac{x}{D}\right)^2} \tag{3.33}$$

This is the background for the wake deflection model used later.

Chapter 4

Methodology: Simulation setup

This chapter explains the method utilized for the simulations. All simulations are conducted in PyWake. Different setups are presented and given case names. There will be mainly three parts of simulations.

4.1 PyWake

PyWake is an open-source wind farm layout optimization tool based in Python. It is used for studying the interaction between turbines in a wind farm and its influence on the farm's flow field and power production. It also has a function to calculate the AEP. PyWake is a very fast tool and can handle many variables at once, even given its heavy vectorization and use of numerical libraries. The philosophy consists of a highly modular architecture allowing users to combine different AEP modeling blocks. Figure 4.1 shows PyWake architecture for the wind farm model (wfm) used in this thesis. The wfm is initialized with the *Site* and *WindTurbine* and will return a *SimulationResult* containing the effective wind speed, power production, and thrust coefficient of each individual turbine. Getting the AEP and a flow map for the farm is also possible.

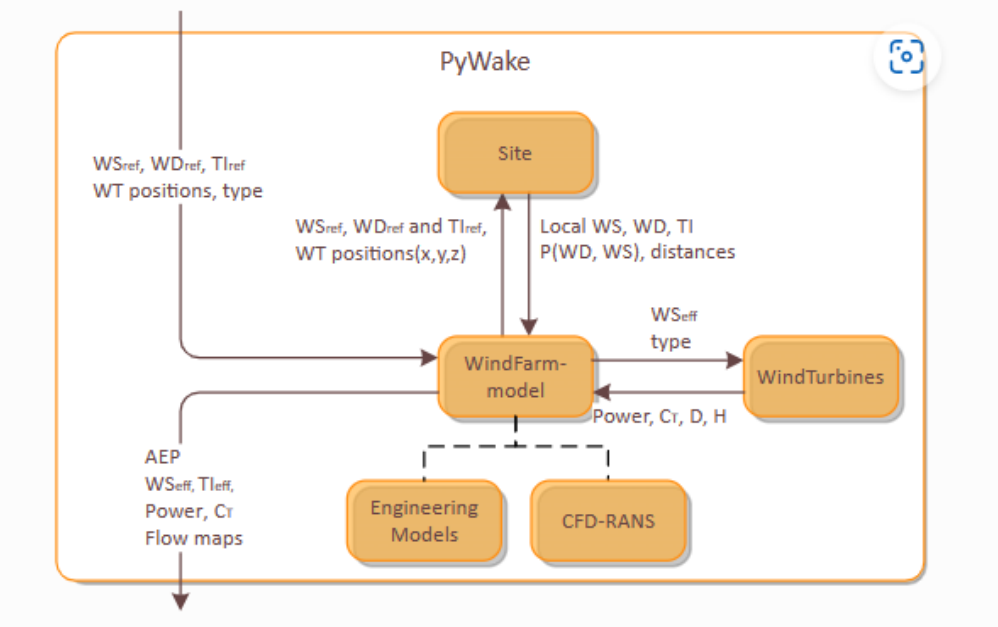

Figure 4.1: Architecture of PyWake, where WS_{ref} is the reference wind speed, WD_{ref} is the reference wind direction, TI_{ref} are the turbulence intensity and WT position and type are defined as inputs. P(WD, WS) is the probability of each wind speed and wind direction to occure. WS_{eff} is the effective wind speed at each turbine and TI_{eff} is the turbulence at each turbine, figure by [18].

4.1.1 Setup

The code used in this thesis is based on the deflection exercise example from PyWake. First, necessary modules are imported, such as deflection models and a wind farm model (wfm). The site and wind turbine objects are made and imported, and the placement of the turbines is decided with x and y coordinates. Further, a relationship between tilt angle and wind speed are imported from a csv file. This is used in a function for calculating the tilt to the corresponding wind speed. The function for calculating the flow field behind the turbines and the AEP is provided by PyWake, and modified to obtain the required results of the tilt. The turbines are named WT0, WT1, and WT2 in the program. The code for running the three-turbine array is provided in Appendix A.

WFM - propopgate downwind

The PropagateDownwind model for wind farms is known for its high speed due to its minimal number of deficit calculations. The model iterates through each turbine in downstream order and calculates the effective wind speed at each turbine by subtracting the sum of deficits from upstream sources from the free stream wind speed. Using this effective wind speed, the model then calculates the deficit caused by the current turbine on all downstream destinations. However, it's important to note that this procedure does not consider any upstream blockage effects, which occur when turbines are placed close together, and a suction effect arises, providing the turbine with higher wind velocity.

Wind turbine object

A user-defined wind turbine object is imported by specifying the inputs, wind speed, thrust coefficient, and power curve. Hub height and diameter are also specified. The chosen wind turbine is a 236D 15MW turbine. The thrust coefficient and power curve are given as turbine data and inserted directly.
Turbine specifications:

- Rotor diameter: 236 m
- Power rating: 15 MW
- Hub height: 144.0 m
- Tip speed: 104 m/s
- Specific power: 343 W/m^2

Site object

The Site object provides the local wind condition for a chosen site. Using wind speed (WS), wind direction (WD), turbulence intensity (TI), and the probability of each combination of wind direction and wind speed as input. The probability is found by using Weibull distribution and making scale, shape, and frequency factors as the inputs. Furthermore, the Site object is responsible for calculating the down-wind, cross-wind, and vertical distance between wind turbines. The Site objects use the XRSite from the program. Figure 4.2 shows the wind rose of the chosen site. As seen, the prominent wind direction is at x°, which will be important when the turbines are placed in a farm formation. Figure 4.3 shows the probability density for the site. The code for the site is provided in Appendix A.0.2.

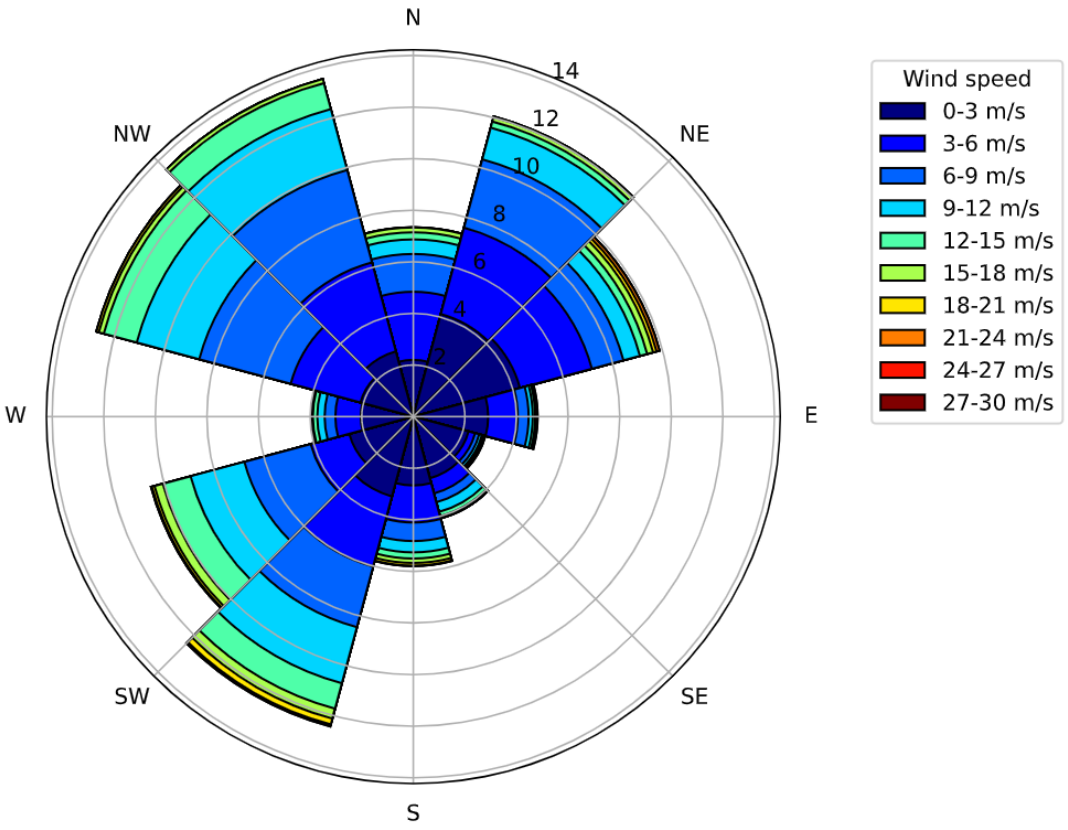

Figure 4.2: Wind rose from the chosen site, with prominent wind direction at 315°.

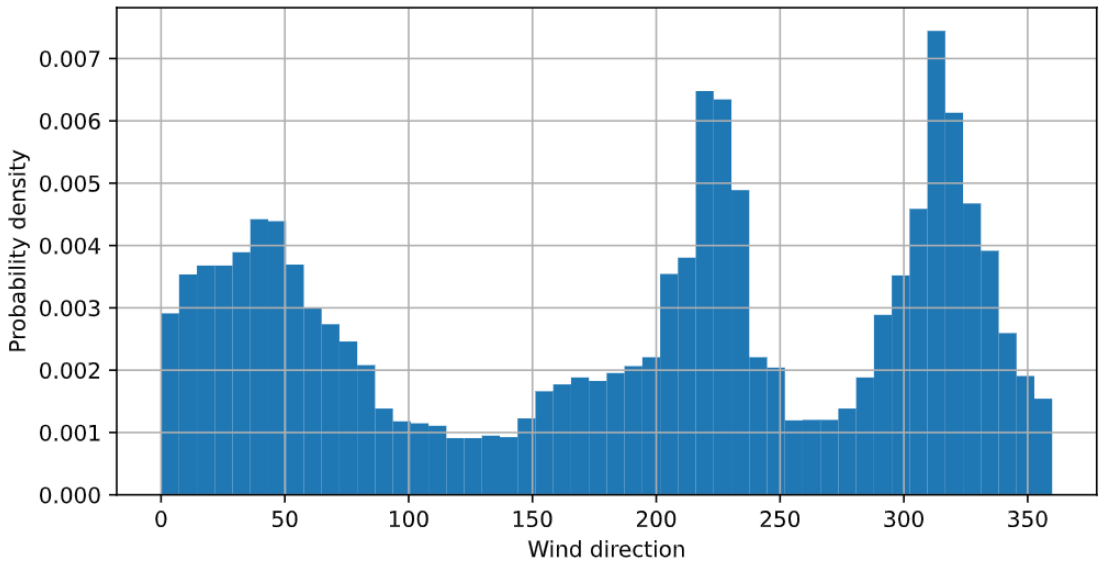

Figure 4.3: Probability density from the chosen site.

Wake model

The wake models used are provided by default in the program. The two wake models for this case are the BastankhahGaussian (BG) and Jensen (NOJ), which are both engineering wake models. The BG model assumes a Gaussian distribution for the velocity deficit in the wake and the NOJ model has been developed for the far wake and represents the wake as a simple top-hat wake and a linear wake expansion constant of k=0.1. Both models are valid only for the far wake [40].

Deflection model

To model the wake effect of tilting or yawing on turbines, the deflection formulation of Jiménez [39] is used. The deflection model uses the downwind and crosswind distances between the source wind turbine and the destination wind turbine as inputs and calculates a new set of deflected downwind and crosswind distances. This type of model is essential for simulations where the turbine experiences a change in angle between the incoming flow and the rotor, for example, in active yaw control, wake steering optimization, or FOWT.

Turbine distance

The distance between the turbines is usually 3-10 diameters (D) [37]. However, to be able to compare with other studies, 7D is used as the reference spacing, while for testing different distances, 3-12D is used. The distance or the layout is set by giving coordinates in x and y directions.

4.1.2 Tilt

The tilt for the turbines is used as a function of wind speed, as seen in Figure 4.4. This is an assumed behavior of the turbines static tilt and is done by scaling a thrust curve to be zero tilt at the cut in speed and 10 degrees tilt at max thrust, which similar has been done by others [41]. The simulations in PyWake do not account for any other force aspects than the forces on the rotor. Where a floating turbine will have 6 DOFs, this simulation only has 1 DOF, which is the tilt.

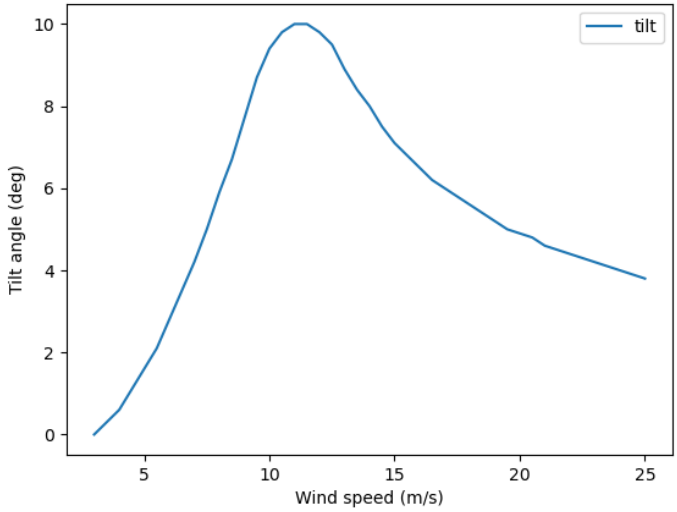

Figure 4.4: Tilt vs wind speed

To get the correct tilt for each turbine, a function **get_tilt** is defined. This function takes a single input parameter wind_speed which represents the wind speed, and returns the corresponding tilt angle. The tilt angle is obtained by using the **np.interp()** function from the NumPy library, which performs linear interpolation between the two columns in the **tiltvsws** DataFrame, 'ws' and 'tilt'. Since the turbine slows down the wind speed, the downwind turbine experiences another wind speed than the first turbine, which is the effective wind speed at the turbine. The code in Figures 4.5 and 4.6 show how the tilt is implemented in the program and updated due to the WS_{eff} at downwind turbines.
The tilt is initialized for all turbines based on all given wind speeds. Thereafter, the simulation is run using those tilts to get the corresponding simulation results, i.e., the turbines' effective wind speeds (WS_{eff}). Since the WS_{eff} for WT0 is the same as the incoming wind speed, the tilt for the first turbine is not updated with the WS_{eff}. While, for the second

and third turbines exposed to the wake deflection from the upstream turbine, the tilt must be decided from the WS_{eff}. It works as the first turbine gets a tilt from the incoming WS, which results in a WS_{eff} for WT1 used in the **get_tilt** definition for determining the tilt for WT1. The same procedure is repeated for WT2, where the new tilt for WT1 gives new wind conditions for WT2, and the WS_{eff} for WT2 is used to get the tilt. After computing/updating the tilts for all turbines using the effective wind speeds, the updated tilts are compared to the previous values. If they are within a 0.10 tolerance, the tilts are found. Otherwise, the iterative process continues using updated tilts.

```
# define function that gets the tilt angle as a function of wind speed
def get_tilt(wind_speed):
    return np.interp(wind_speed, tiltvsws[' ws '].values, tiltvsws[' tilt'].values)
```

Figure 4.5: Function for deciding the tilt angle for each turbine at different wind speeds.

```
tilt = np.array([get_tilt(ws), get_tilt(ws), get_tilt(ws)])
while True:
    sim_res = wfm(x, y, tilt=tilt , wd=270, ws=ws)
    tilt_old = tilt[1:]
    tilt[1] = get_tilt(sim_res.WS_eff[1])
    tilt[2] = get_tilt(sim_res.WS_eff[2])
    if np.max(np.abs(tilt[1:]-tilt_old))<0.1:
        break
```

Figure 4.6: The loop that uses the WS_{eff} at each wind turbine and iterates until the the tilt is as close as possible to the old tilt.

The tilt loss is calculated simply as Eq 4.1.

$$Tiltloss = (\frac{(FixedTurbines - TiltedTurbines)}{FixedTurbines}) * 100\% \tag{4.1}$$

4.2 Simulation scenarios

After describing the simulation setup, the simulation scenario is presented. The simulations in this thesis are divided into three main parts for investigating the tilt loss.

- Part 1: Power
- Part 2: AEP
- Part 3: Spacing

Within these parts, different setups of the turbines are used to test the tilt loss. For the power, there is considered a three-turbine array and three turbine farm layouts. The three-turbine array is a common way of testing wind turbine wake and can be found in other studies, [20] [15]. For AEP estimations, the three-turbine farm and an additional 10x10 wind farm with 100 turbines are used. In the last part, the three turbine array and the 10x10 are tested at different distances. The architecture for results is provided in Appendix B.

4.3 Part 1 - Power

Part 1 consists of three cases estimating the power of a three-turbine array and two wind farm configurations.

4.3.1 Case 1.1 Three turbine-array

In Case 1.1, a three-turbine array with 7D spacing is tested to see how the wake affects power production when turbines are directly exposed to the wake from the first-row turbine. In this case, the turbines are exposed to one fixed wind speed at a time and are ran for wind velocities from 3 to 25 m/s, which is cut-in and cut-out of the turbine. The inflow is also coming from only one direction. The flow map is shown from the side to visualize the wake deflection affected by the tilt, and the power loss/gain from the tilt is presented with a comparison with fixed turbines. As seen in Figure 4.8, the turbines are tilted only by the rotor, while the static tilt for a FOWT will be for the whole structure. This is a simplification used in the program, and it assumes there is no drag on the tower or nacelle.

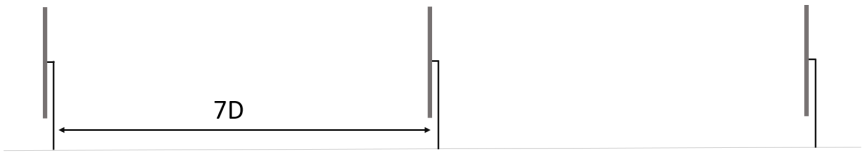

Figure 4.7: Setup with three turbine array with fixed turbines.

Figure 4.8: Setup with three turbine array with tilted turbines.

4.3.2 Case 1.2 One turbine in front, two behind

Figure 4.9 shows the setup for case 1.2. The turbines are placed with one turbine 7D in front of two turbines with 3D spacing. The same test was ran for this case, with the power of the individual turbines calculated for each wind speed.

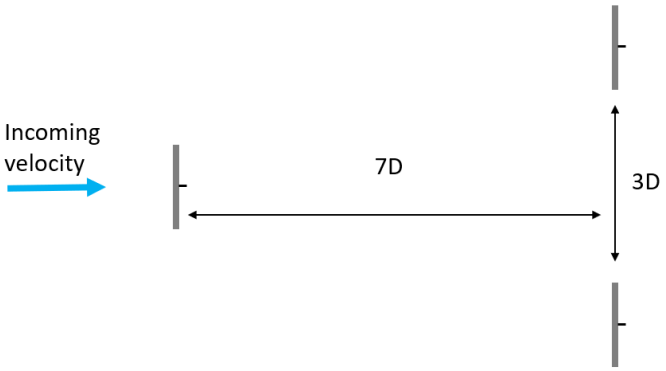

Figure 4.9: Setup with three turbines in a triangle.

4.3.3 Case 1.3 Two turbines in front, one in back

Figure 4.10 shows case 1.3, where the turbines are placed with a layout of two turbines in front with 3D spacing and a third turbine 7D behind.

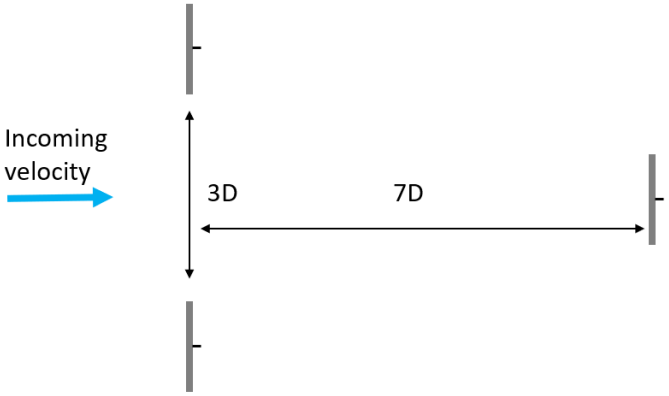

Figure 4.10: Setup with three turbines in a triangle.

The results for tilt loss and comparison of wake are obtained as seen in figure 4.11. Where the wind turbines will be tested with two different wake models, these produce results for fixed and tilted turbines. Further, the deviation gives the tilt loss. Then the wake models are compared with the result of the tilt loss.

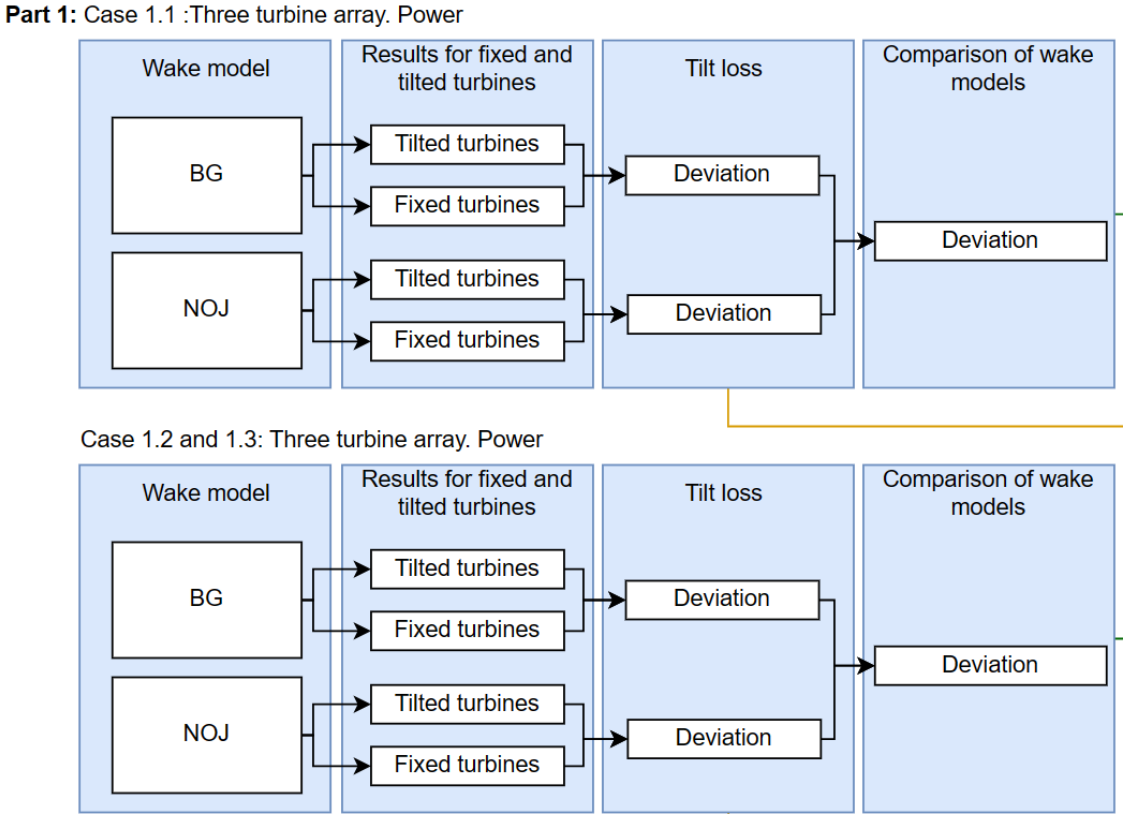

Figure 4.11: Archetecture of how results are obtained in Part 1

4.4 Part 2 - AEP

AEP calculation of a wind farm. In Part 2, the layout from Part 1 with the best results in power is considered for further investigation of AEP, Case 1.3. A 10x10 wind farm is also considered for the AEP estimation. The purpose is to simulate wind speed from all directions to calculate the AEP. Since the wind speed is Weibull distributed and the AEP is a sum of all wind speeds over a year, a mean tilt angle of the wind speed data is used. Also, the turbines are tested with a max tilt angle over a year.

4.4.1 Case 2.1: Three turbine wind farm.

The turbines are placed with the two turbines aligned in the prominent wind direction found when plotting the wind rose of the site. This is usually how the turbines are placed in a farm. Hence, there are more of them in a farm.

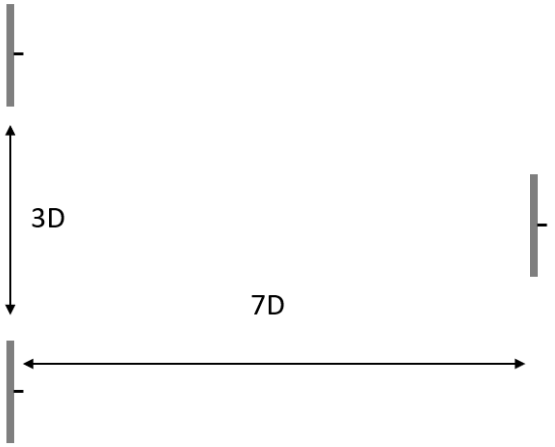

Figure 4.12: Setup with three turbine wind farm.

4.4.2 Case 2.2: 10x10 wind farm

With the engineering wake model used, it is easy to model in a large scale. Therefore, a 10x10 turbine wind farm is tested, with the same 15 MW turbine. The turbines are placed with 7D distance between all turbines, as seen in Figure 4.13. Case 2.2 is tested with both an average tilt and the max tilt.

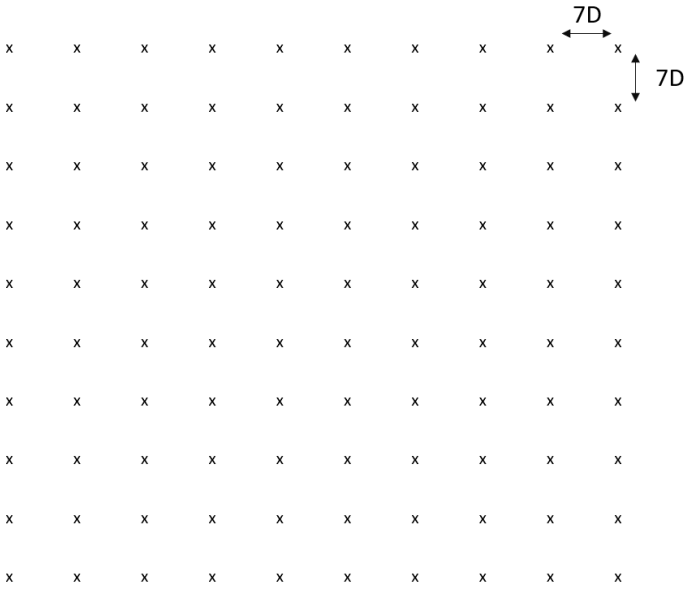

Figure 4.13: Setup with 10 x 10 wind farm.

Figure 4.14 shows the architecture of how results are obtained.

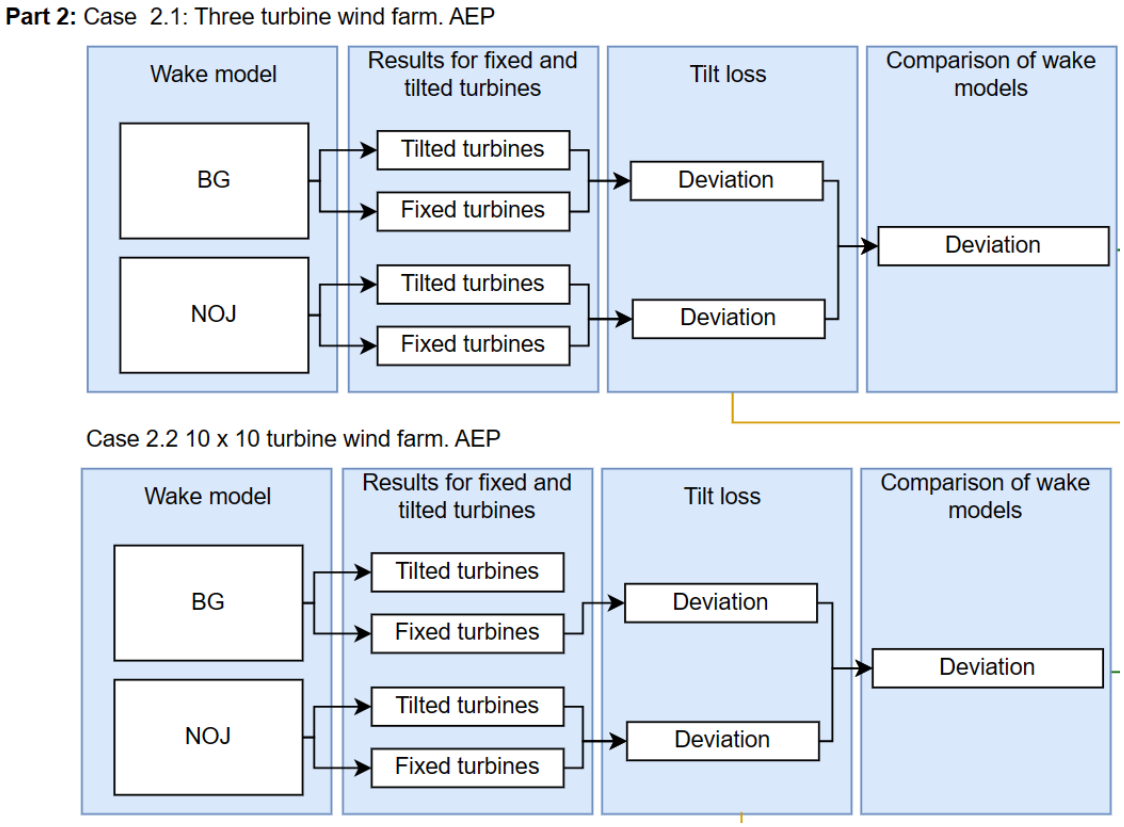

Figure 4.14: Architecture of how results are obtained in Part 1

4.5 Part 3 - Spacing

In Part 3, the power and AEP are investigated with different spacing between the turbines, from 3-13D.

4.5.1 Case 3.1: Three turbine-array with varying spacing

The different distances are tested on the three-turbine array where the wake is directly affecting the downwind turbines to see the effect of the power. The distances were implemented with a loop, running the program with a constant wind speed at different distances from 3 to 13 diameters.

4.5.2 Case 2.2: 10x10 wind farm

The 10 x 10 wind farm is also tested with different distances to see the effect of spacing on the AEP. In this case, the farm uses all wind speeds from all directions over a year at different distances from 3 to 12 diameters.

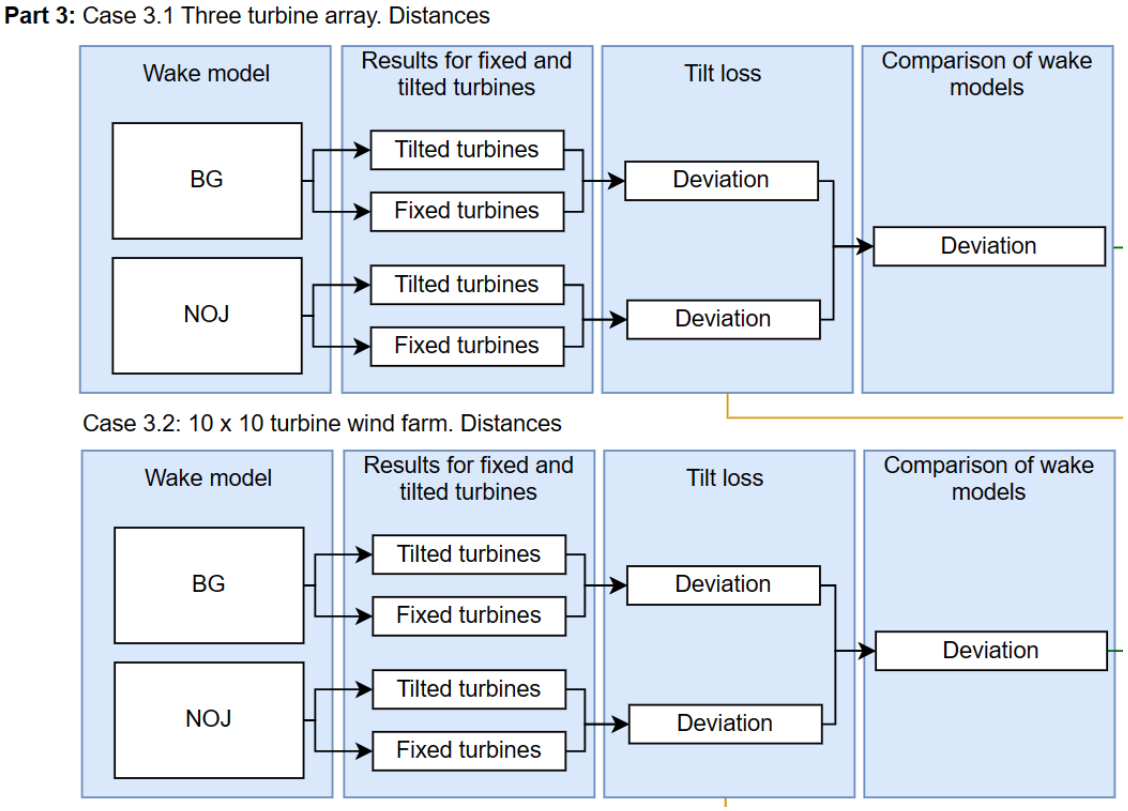

Figure 4.15: Archetecture of how results are obtained in Part 1

Chapter 5

Results and Discussion

This chapter presents and discusses the results of the analysis methods described in the previous chapter. The results are divided into three parts. The first part evaluates the power of tilted and fixed turbines with two different wake models. The second part calculates the AEP for a three-turbine wind farm and a 100-turbine wind farm, again with tilted and fixed and two wake models. The turbines are tested at different distances in the third and final part. The three-turbine array and the $10x10$ wind farm are used. All parts have different cases which describe the setup. The different cases are tested with the two wake models, Bastankhah Gaussian (BG) and Jensen (NOJ). Turbines are referred to as fixed when there is no tilt and tilted when the turbine is exposed to tilt.

5.1 Part 1 - Power losses due to rotor tilt

In the first part of these simulations, the power is evaluated for three cases with different setups. For each case, the power of each turbine will be presented at max tilt, and the total power from all turbines will then be used to compare the three different setups. The flow map of the wake is also shown to see the wake deflection of the tilted turbines.

5.1.1 Case 1: Three turbine array

The results from PyWake with three turbines in an array with 7D spacing are presented below. The case was simulated with wind speeds from 3 to 25 m/s. The turbines are named WT0, WT1, and WT2 in order of increasing streamwise distance.

Wake model BG

Figure 5.1 shows the flow field of the three fixed turbines. Figure 5.2 shows the three turbines with the corresponding tilt angle for the effective wind speed at each turbine. The wake in this case is deflected upwards as the turbine has a positive tilt angle. The wind speed with the largest corresponding tilt angle is used to visualize the wake deflection. The BG wake model has lower velocity in the center of the wake, which increases gradually further away from the center axis. Flow maps for different velocities are added in Appendix C.

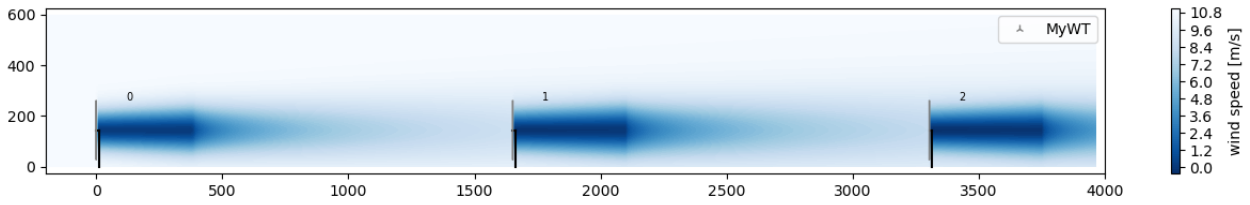

Figure 5.1: Flow field for three fixed turbines with BG wake model. Incoming wind speed = 11 m/s

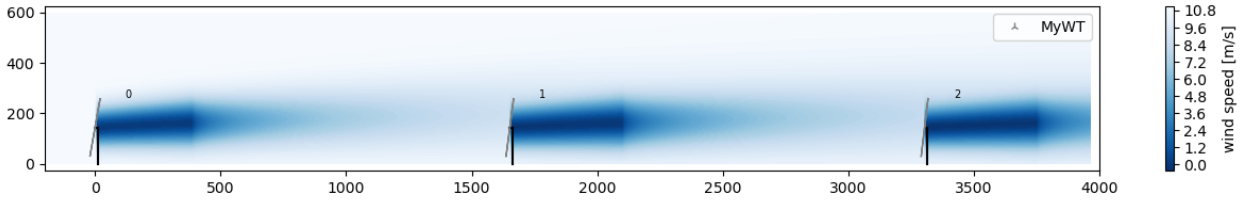

Figure 5.2: Flow field for three tilted turbines with BG wake model. Incoming wind speed = 11 m/s

Power BG

Figure 5.3 shows the power curve of all three turbines under both fixed and tilted conditions. As seen, the first turbine in both cases produces more power due to the second and third turbines being exposed to the wake from the first turbine. WT1 and WT2 are reaching rated power at higher wind speeds, and this is because the wind speed shown on the graph is the incoming velocity and not the effective wind speed working on the turbine. The effective wind speeds at turbines WT1 and WT2 are lower than the incoming velocity.
For further investigating of the tilt loss/gain, the differences in power with and without tilt for fixed and tilted turbines are also presented in Figure 5.3. + is power gain, and − is power loss. As seen from the figure, the first turbine WT0 suffers power loss due to tilt at all the wind velocities till it reaches the rated power. In contrast, WT1 gains power under tilted conditions except for wind speeds higher than 11.5 m/s. In the case of WT2, the rotor tilt appears to be favorable in power production at all wind speeds. Better performance of WT1 and WT2 under tilted conditions is due to the wake steering by the respective upwind turbines.

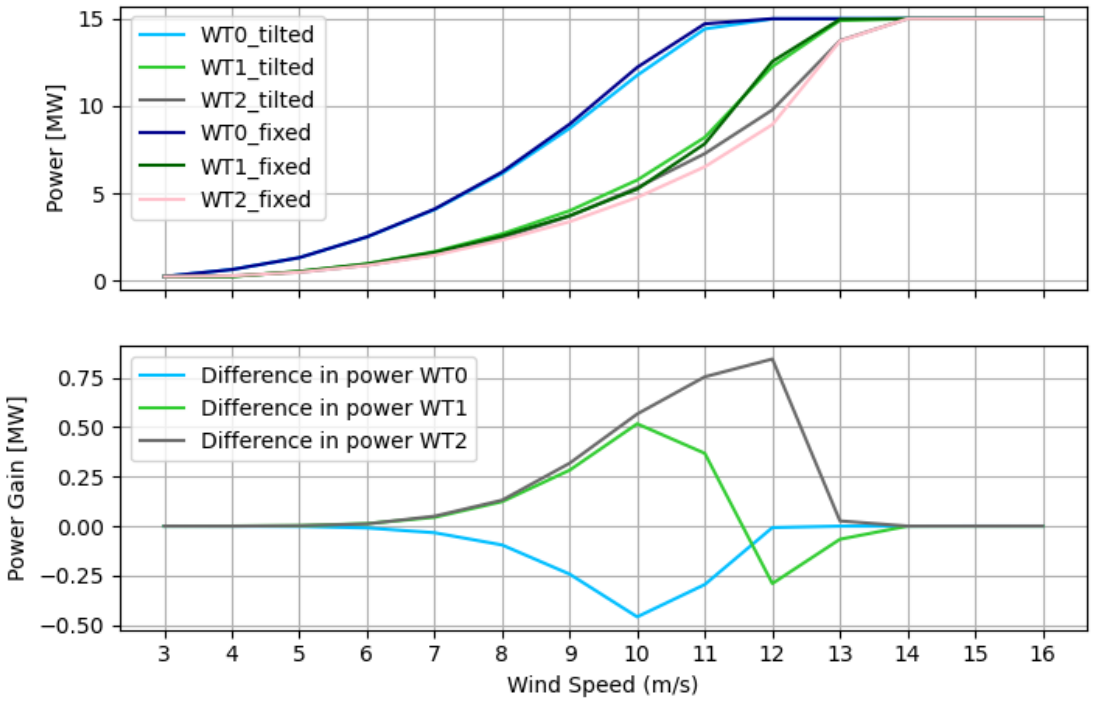

Figure 5.3: Top graph: Comparing power of fixed and tilted turbines with BG wake model. Bottom graph: Deviation (power gain) between power of the fixed and tilted turbines (Tilted - Fixed).

Wake model NOJ

The wake flow map for the three turbines in a row with the NOJ wake model is presented for the fixed turbines in Figure 5.4 and tilted turbines in Figure 5.5. As seen, the NOJ

wake model does not have lower wind speeds in the center of the wake, as the BG model has. The wake also expands linearly downstream and has a constant velocity deficit, unlike BG, which has a Gaussian-shaped expansion and a variable velocity deficit. Because of the assumption of linear wake expansion and exponential velocity deficit, this model seems to not affect downstream turbines with the effect of wake deflection, as the BG model does. However, as seen in the figure there is a visible deflection of the wake, hence not considerable for downwind turbines.

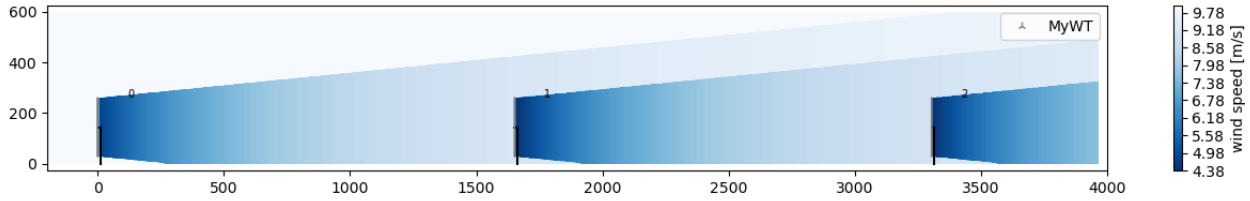

Figure 5.4: Flow field for fixed turbines. Wake model NOJ. Incoming wind speed = 11 m/s.

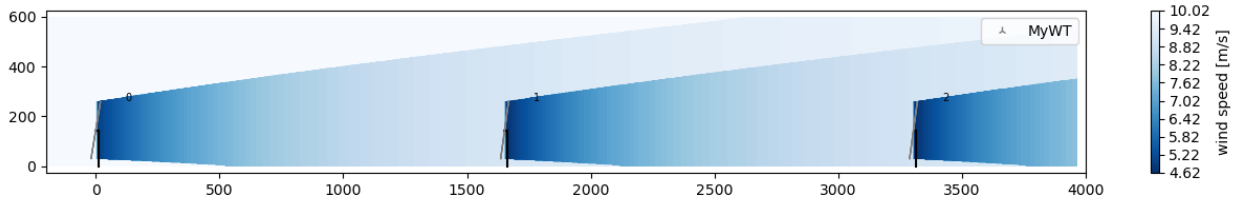

Figure 5.5: Flow field for tilted turbines. Wake model NOJ. Incoming wind speed = 11 m/s.

Power NOJ

To compare these two, Figure 5.15 shows the power curve and differences in power while the turbines are under tilted and fixed conditions. In this case, the difference between the three turbines is much smaller than for the BG wake model. This effect of the wake for the range of tilt angles investigated, the velocity is almost the same for the tilted and fixed turbines, i.e., the impact of wake deflection is negligible when using the NOJ model. Therefore, the wake deflection will not give better wind conditions for downwind turbines, but the tilted turbines will still produce less power since the projected area facing the wind is smaller due to the tilt. That is why the NOJ wake model only gives tilt losses, not a gain like BG.

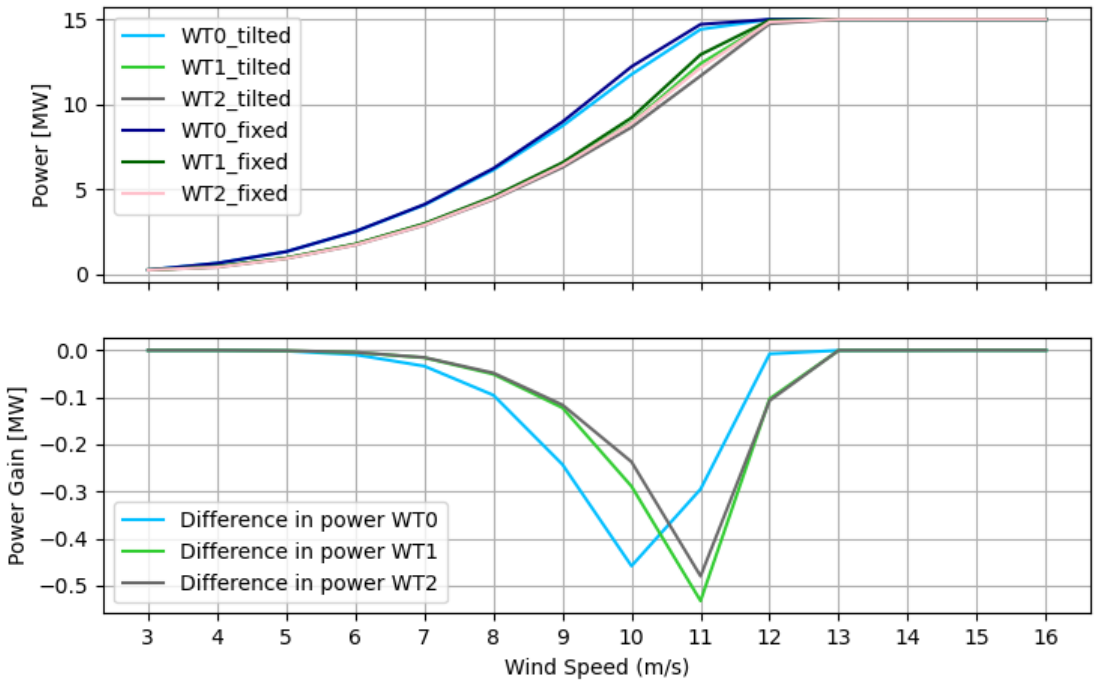

Figure 5.6: Top graph: Comparing the power of fixed and tilted turbines with NOJ wake model. Bottom graph: Deviation (power gain) between the power of the fixed and tilted turbines (Tilted - Fixed).

5.1.2 Comparison wake models BG vs. NOJ

The two different wake models presented above are compared in Figure 5.7. As seen for the first turbine, the power is the same, while for the second and third turbines, the NOJ wake model shows slightly higher power at lower wind speeds. Meaning the model provides better wind conditions for downwind turbines.

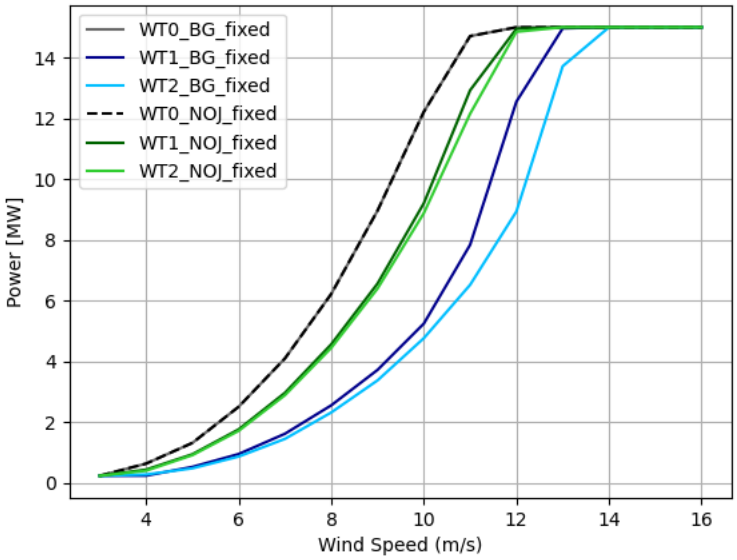

Figure 5.7: Power of fixed turbines with BG and NOJ wake models.

Table 5.1 shows the power for fixed and tilted turbines with the BG wake model at a wind speed of 11 m/s, where the tilt is at max. As seen, WT1 and WT2 for the tilted case produce more than the fixed turbines. The total power gain is 2.84%.

Table 5.1: Power for the BG wake model for fixed vs. tilted turbines, ws = 11 m/s, at highest tilt angle, θ.

BG	**Power fixed [MW]**	**Power tilted [MW]**	**Loss/gain**
WT0	14.709	14.414	-2.01%
WT1	7.839	8.207	4.69%
WT1	6.520	7.274	11.56%
Total	29.068	29.895	2.84%

Table 5.2 gives the power for the three turbines fixed versus tilted with the NOJ wake model. In this case, WT1 and WT2 are performing better in the fixed case, as stated earlier, due to the simple wake model. The loss is approximately -3.29%

Table 5.2: Power for the NOJ wake model for fixed vs. tilted turbines, ws = 11 m/s, at highest tilt angle, θ.

NOJ	**Power fixed [MW]**	**Power tilted [MW]**	**Loss/gain**
WT0	14.709	14.414	-2.01%
WT1	12.926	12.393	-4.12%
WT1	12.153	11.673	-3.95%
Total	39.788	38.480	-3.29%

Looking into the total power, there is a vast difference between the wake models. So, a good choice of wake model is very important. The tilt has an effect that can be either negative or positive depending on the wake model (particularly dependent on the wake expansion behavior). BG gives a gain (tilt increases the power estimated), while NOJ gives a loss.

The results showed that for the first turbine (WT0), the power of the fixed turbine was higher due to the first turbine being in free air and not exposed to any wake. So, the only difference is that the tilted turbine will have a smaller projected area towards the wind. With the BG wake model, WT1 experiences a gain of approximately 4.69%, and WT2 gains 11.56%. With the NOJ wake model, results showed WT1 lost approximately -4.12% in production, and the power production of WT2 decreased by approximately -3.95%. The loss for each turbine is shown in Table 5.3.

Table 5.3: Tilt loss/gain for single turbines in an array. Gains are positive, and losses are negative.

Case 1.1	**Loss/gain BG**	**Loss/gain NOJ**
WT0	-2.01%	-2.01%
WT1	+4.69%	-4.12%
WT2	+11.56%	-3.95%

5.1.3 Case 1.2: Three turbines in a triangle, one facing front

Figure 5.8 shows the flow map of the tilted turbines seen from above for case 1.2, with the BG model, and Figure 5.9 for the NOJ model. With one turbine in the prominent wind direction and two behind.

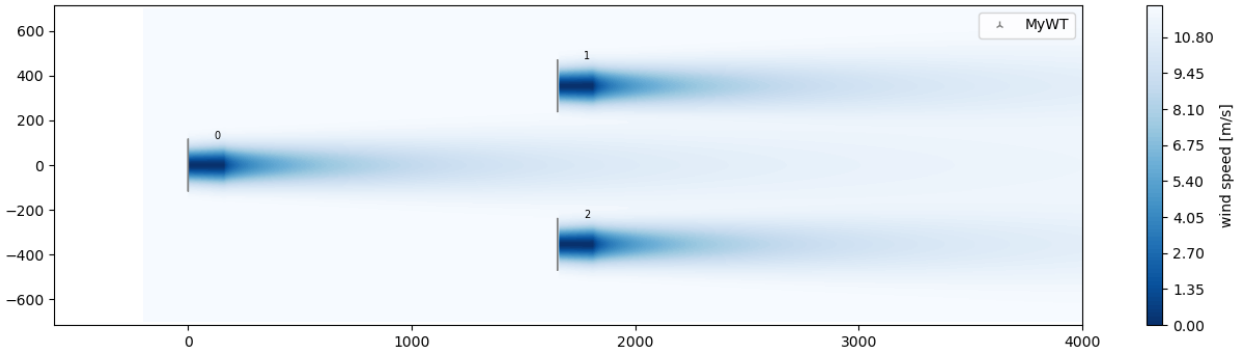

Figure 5.8: Flow field for tilted turbines in case 1.2. Wake model BG. Incoming wind speed = 11

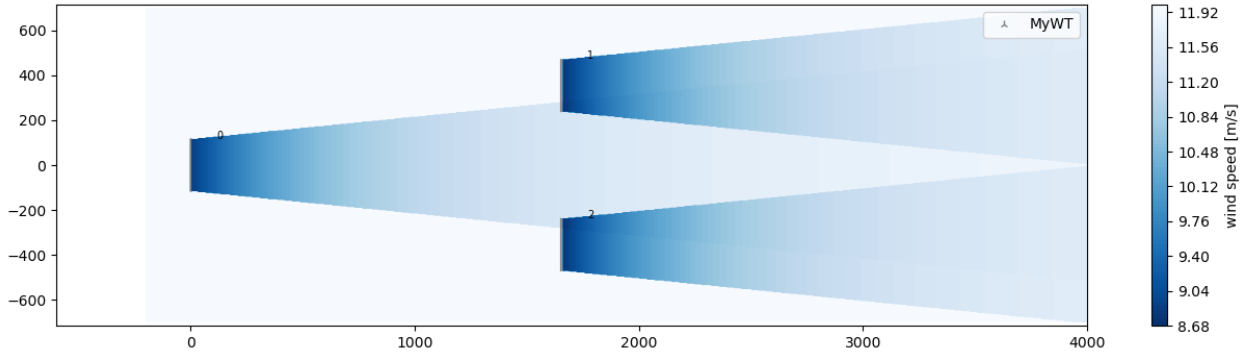

Figure 5.9: Flow field for tilted turbines in case 1.2. Wake model BG. Incoming wind speed = 11

BG

Further, Figure 5.10 presents the power curve and the difference in power (power gain). As seen, there is a minor difference between the turbines compared to the three turbine-array. As the bottom graph shows, all turbines experience a loss in this case.

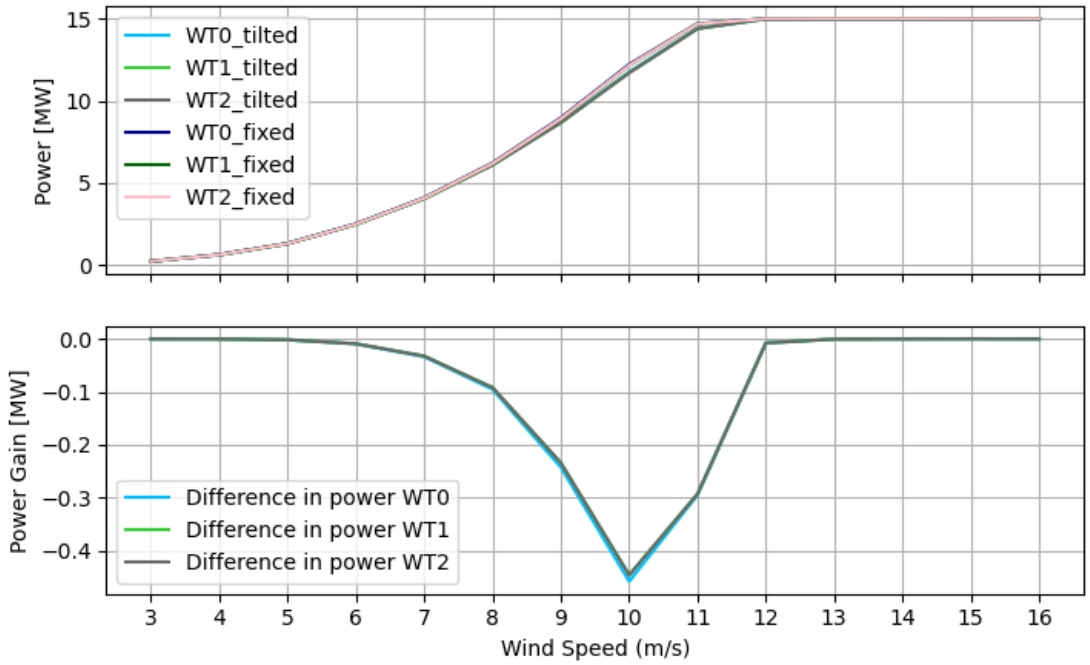

Figure 5.10: Top graph: Comparing the power of fixed and tilted turbines with BG wake model. Bottom graph: Deviation (power gain) between the power of the fixed and tilted turbines (Tilted - Fixed).

For further investigation, the power results are compared for the fixed and tilted turbines in Table 5.4. As seen, the difference between the fixed and tilted turbines is smaller than the three-turbine array due to the turbines not being aligned and the wake is not directly pointed at the second-row turbines. Like the NOJ wake model, the turbines probably experience the most significant loss by the decreased rotor area due to the tilt, but the wake from the front turbines may influence the second-row turbine, as seen in the table. The total loss is approximate -2.00% for the BG model.

Table 5.4: Power for the BG wake model for fixed vs. tilted turbines, case 1.2, ws = 11 m/s, at largest tilt.

BG	**Power fixed [MW]**	**Power tilted [MW]**	**Loss/gain**
WT0	14.709	14.414	-2.01%
WT1	14.689	14.396	-1.99%
WT2	14.689	14.396	-1.99%
Total	44.087	43.206	-2.00%

NOJ

The power curve and power gain are also presented for the NOJ wake model. From the power graph, there is a slight difference between the three turbines. However, in this case, WT0 experiences a larger tilt loss than the two downstream turbines, since the two downstream turbines has a total lower power.

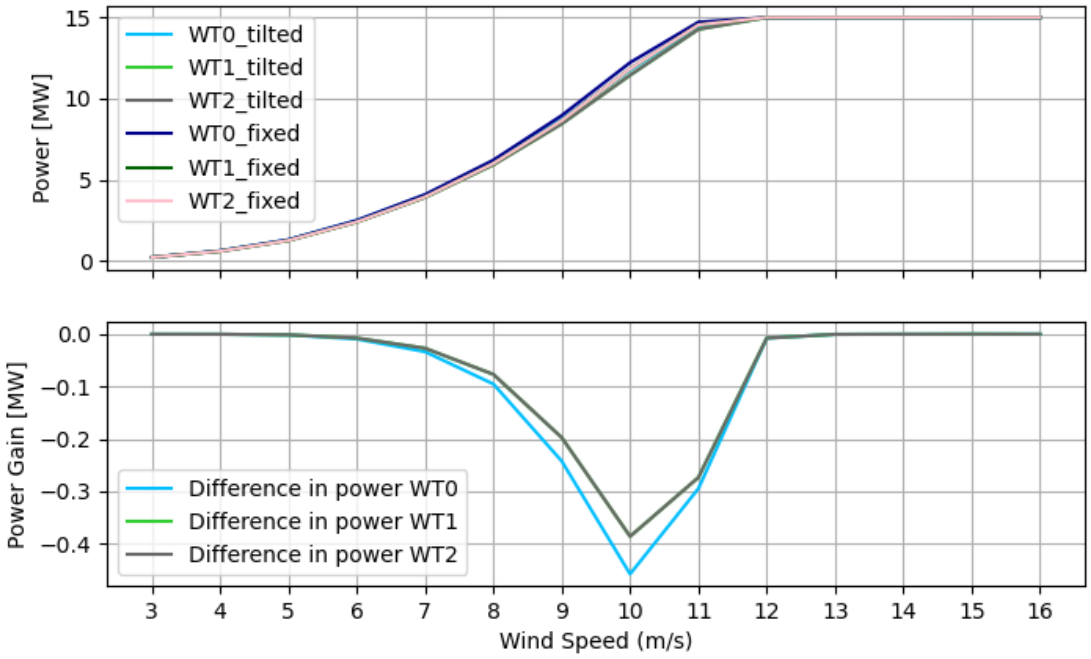

Figure 5.11: Top graph: Comparing the power of fixed and tilted turbines with NOJ wake model. Bottom graph: Deviation (power gain) between the power of the fixed and tilted turbines (Tilted - Fixed).

The power of the NOJ wake model is presented in 5.5. The total percentage loss due to tilt is -1.93% with the NOJ model. WT0 produces the same as BG, while WT1 and WT2 produce less and the deviation from WT0 is more significant.

Table 5.5: Power for the NOJ wake model for fixed vs. tilted turbines, case 1.2, ws = 11 m/s, at largest tilt.

NOJ	**Power fixed [MW]**	**Power tilted [MW]**	**Loss/gain**
WT0	14.709	14.414	-2.01%
WT1	14.540	14.266	-1.88%
WT2	14.540	14.266	-1.88%
Total	43.789	42.946	-1.93%

For comparison of single turbines with the two wake models in case 1.2 Table 5.6 is presented. It shows the loss for each turbine. As seen, the loss with the BG model is almost the same for all turbines, meaning the downstream turbines is only slightly be affected by the wake. For the NOJ model with the top-hat wake expansion, the downstream turbines may experience more significant wake effects from the upstream turbine and therefore experience a more extensive loss.

Table 5.6: Tilt loss/gain for single turbines in a farm. Gain is the positive value, and loss is the negative value.

Case 1.2	**Loss/gain BG**	**Loss/gain NOJ**
WT0	-2.01%	-2.01%
WT1	-1.99%	-1.88%
WT2	-1.99%	-1.88%
Total	-2.00%	-1.93%

5.1.4 Case 1.3: Three turbines in a triangle, two facing front

Figure 5.12 shows the flow map for case 1.3, with tilted turbines and the BG wake model, and Figure 5.13 for the NOJ model. In this case with two turbines in the prominent direction.

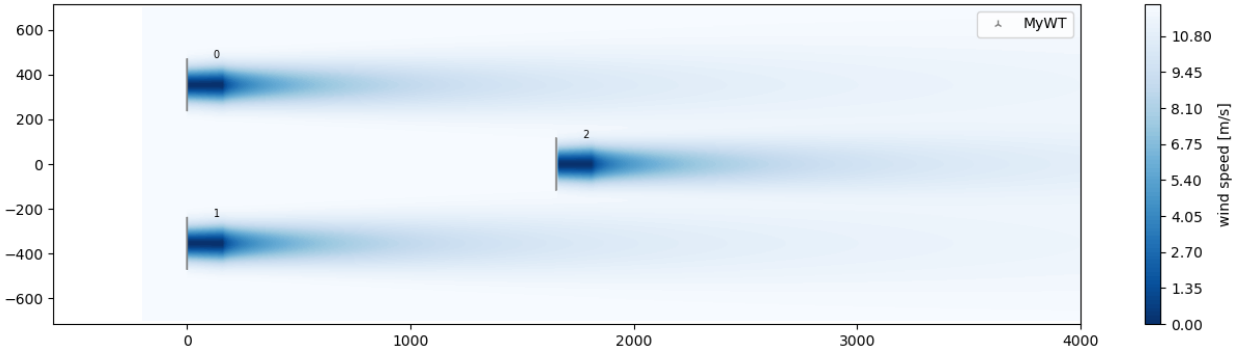

Figure 5.12: Flow field for tilted turbines in case 1.3. Wake model BG. Incoming wind speed = 11 m/s.

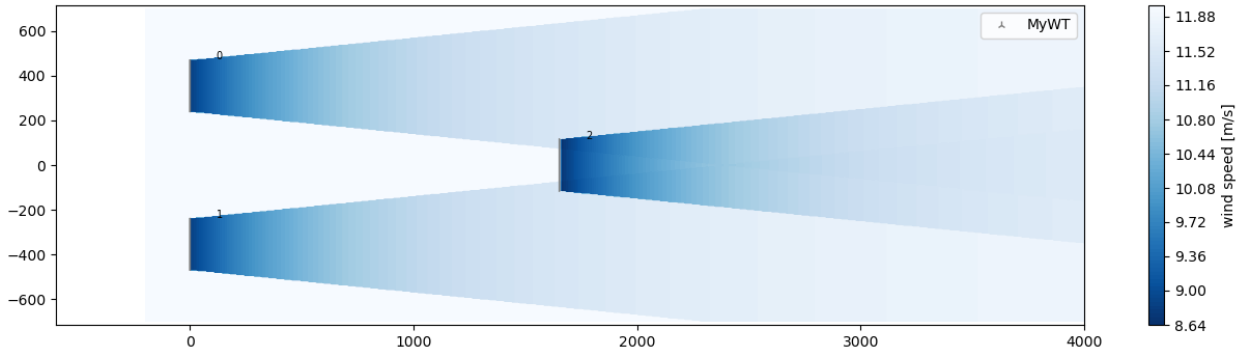

Figure 5.13: Flow field for tilted turbines in case 1.2. Wake model BG. Incoming wind speed = 11

BG

Figure 5.14 shows the power and power difference for case 1.3, with the BG wake model. Again the difference between turbines production is minor.

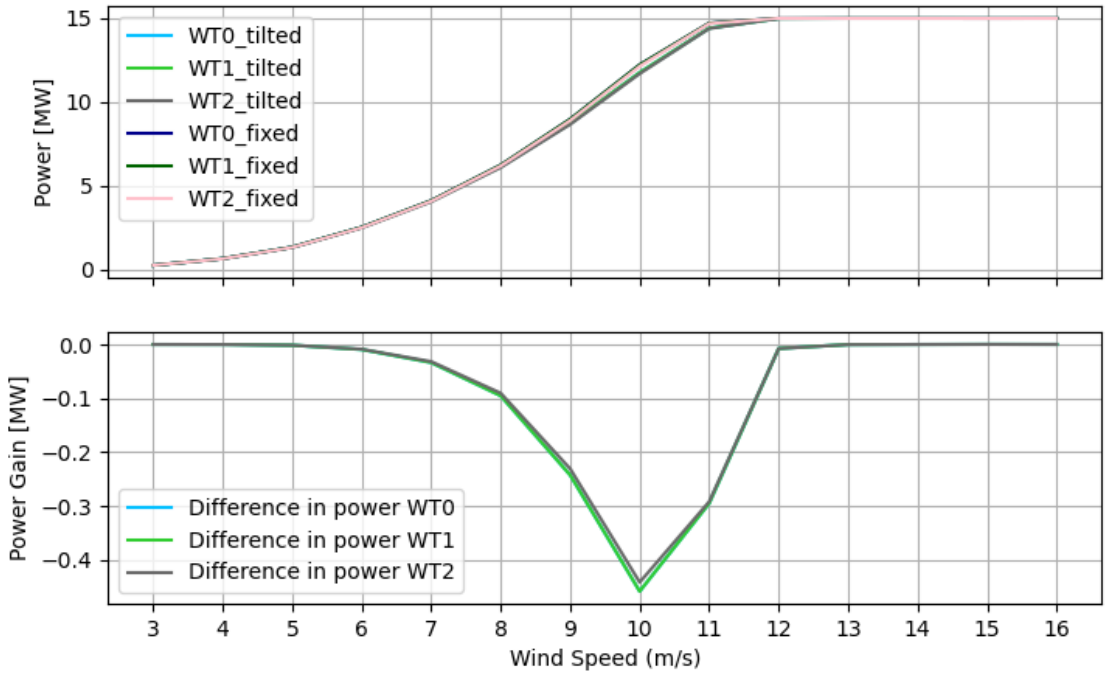

Figure 5.14: Top graph: Comparing the power of fixed and tilted turbines with BG wake model. Bottom graph: Deviation (power gain) between the power of the fixed and tilted turbines (Tilted - Fixed).

The results for power at the max tilt angle are obtained and shown in Table 5.7. As seen, the difference between the fixed and tilted turbines is still smaller than in case 1.1. However, this case with two turbines in front showed a slightly higher overall power, meaning the wake of turbines in front influences the downwind turbine. In these cases, however, the second-row tilted turbines are not gaining any power compared to the fixed turbines. The total loss is approximately -2.00%.

Table 5.7: Power for the BG wake model for fixed vs. tilted turbines, ws = 11 m/s, at largest tilt.

BG	**Power fixed [MW]**	**Power tilted [MW]**	**Loss/gain**
WT0	14.709	14.414	-2.01%
WT1	14.709	14.414	-2.01%
WT2	14.680	14.388	-1.99%
Total	44.098	43.216	-2.00%

Figure 5.15 shows the power and power difference but with the NOJ wake model this time. In this case, there is a more significant difference between the front and the downstream turbines compared to the BG model.

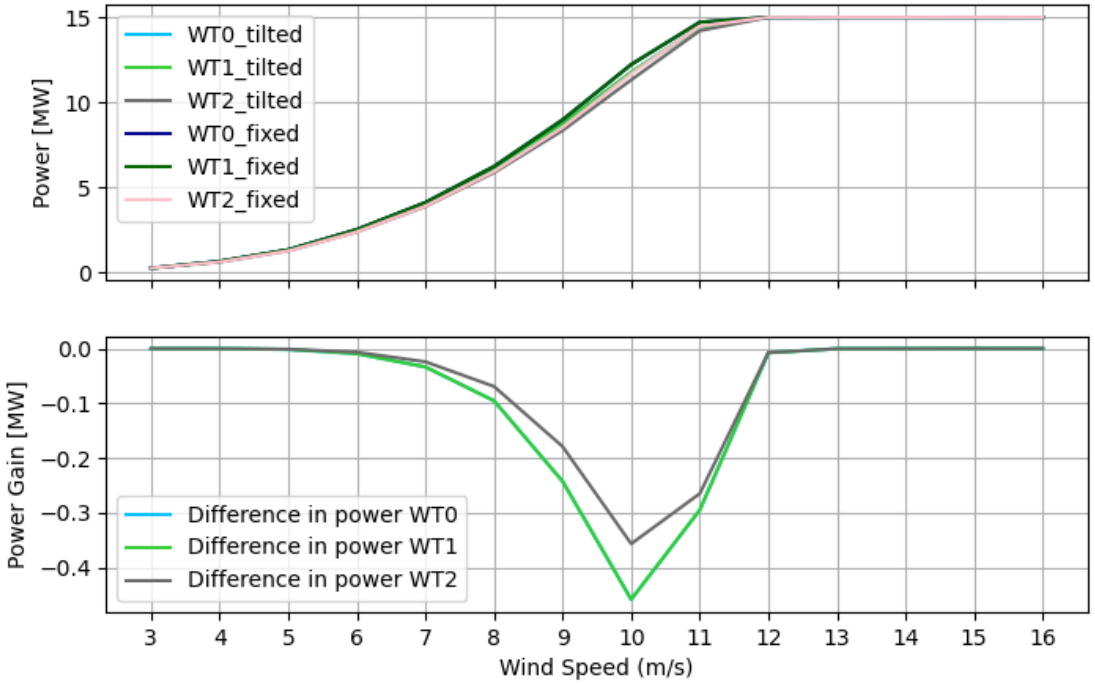

Figure 5.15: Top graph: Comparing the power of fixed and tilted turbines with NOJ wake model. Bottom graph: Deviation (power gain) between the power of the fixed and tilted turbines (Tilted - Fixed).

The total percentage loss due to tilt is -1.95% with the NOJ wake model, presented in 5.8.

Table 5.8: Power for the NOJ wake model for fixed vs tilted turbines, case 1.3, ws = 11 m/s, at largest tilt.

NOJ	**Power fixed [MW]**	**Power tilted [MW]**	**Loss/gain**
WT0	14.709	14.414	-2.01%
WT1	14.709	14.414	-2.01%
WT2	14.470	14.205	-1.83%
Total	43.888	43.033	-1.95%

Table 5.9 presents the loss for every single turbine for the two wake models. The BG model predicts a smaller difference between the power production of the three turbines, while the NOJ model seems to have a wake that affects the downstream turbines in a larger degree.

Table 5.9: Tilt loss/gain for single turbines in a farm. Gain is the positive values, and loss is the negative value.

Case 1.3	**Loss/gain BG**	**Loss/gain NOJ**
WT0	-1.99%	-2.04%
WT1	-1.99%	-2.04%
WT1	-1.99%	- 1.83%
Total	-2.00%	-1.95%

5.1.5 Comparison

For Case 1.1, the total power loss/gain from the tilt for three turbines in a row was +2.85 % and -3.29 % for the two different models. The BG wake model gives a total gain in power for the three turbine-array. Further, in case 1.2, the three turbines experienced a loss of -2.00% for BG and -1.93% for NOJ, and in case 1.3, a loss of -2.00% for BG and -1.95% for NOJ. However, even if the tilt loss is slightly higher for case 1.3, this case is producing more power, and will be used further for AEP estimations.

Tilt influence

Figure 5.16 shows a comparison between the power of WT0 vs. wind speed and tilt angle vs. wind speed. The graph shows that the tilt reaches its maximum at 11 m/s and decreases after. The fixed WT0 is not affected by the tilt graph, as it is in free air. However, the tilted WT0 is affected by the tilt, and the deviation between the fixed and tilted turbine increases with the increased tilt angle.

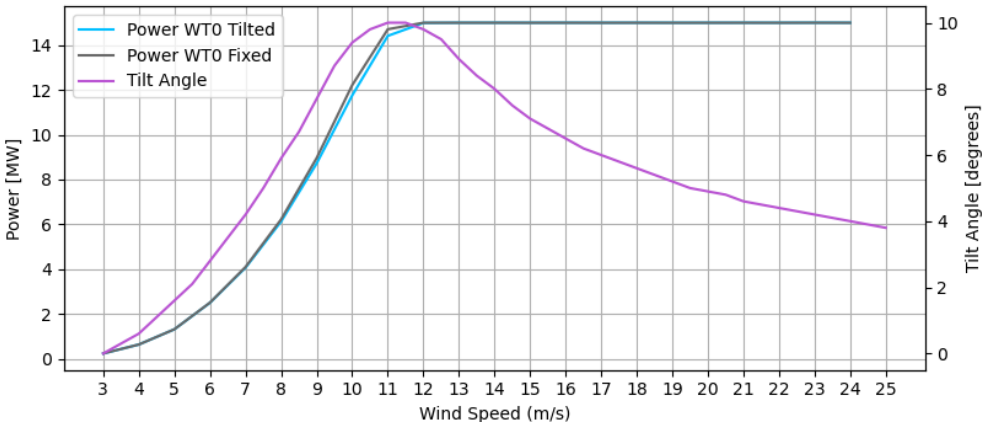

Figure 5.16: Comparison of power for WT0 and tilt angle.

One justification for this relationship between the velocity and tilt is that when the velocity increases from cut-in to rated, the rotor will have increasing forces. Further, when the velocity reaches the rated wind speed, the blade starts to pitch. So, pitching reduces lift as it makes the blades away from the optimal angle of attack. This is how power is reduced to keep the rated power, which will also influence the forces on the rotor. When the thrust force decreases, so does the tilt of the turbine. This leads to the tilt decreasing after the peak at 11 m/s. Figure 5.17 is included to see the difference between the fixed and tilted turbine versus the tilt angle.

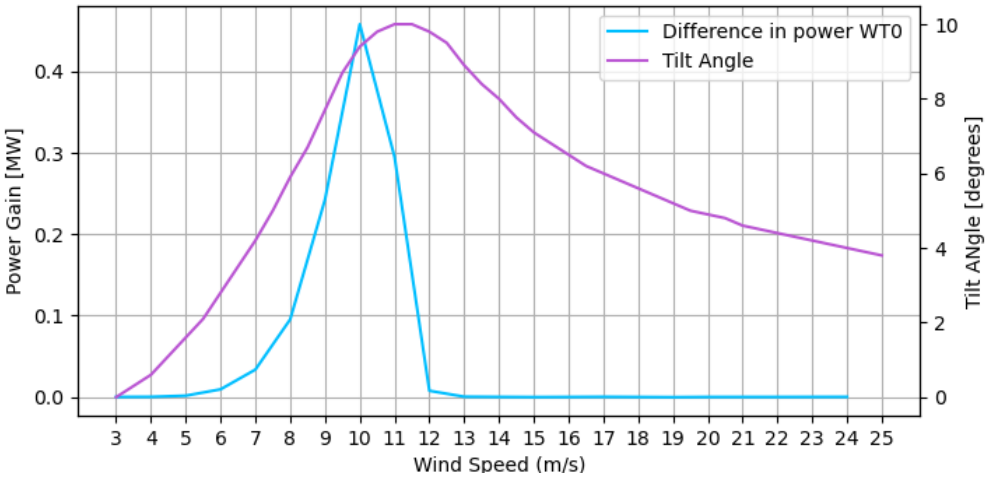

Figure 5.17: Comparison of the difference in power for fixed and tilted turbine for WT0 and tilt angle.

BG vs NOJ

There was also a deviation in the results from the two different wake models used in part 1. The graph showed that for the first turbine (WT0), the power was the same as expected because the first turbine (WT0) is in free air and is not exposed to any wake. While for WT1 and WT2, the wake deflection effect from the BG wake model seems to influence to a much larger degree than what the NOJ wake model does. As seen in Figure 5.18, the grey and the green lines are for the NOJ model, which are leading on the red and the blue lines, which are for the BG model. For the first turbine, the BG is producing more.
Respectively for BG and NOJ, the total power loss/gain due to tilt for a three-turbine array is 2.84% (BG) and -3.29 % (NOJ). Giving the BG model a gain because the model assumes that the wake is steered. While for the NOJ, there is a loss.

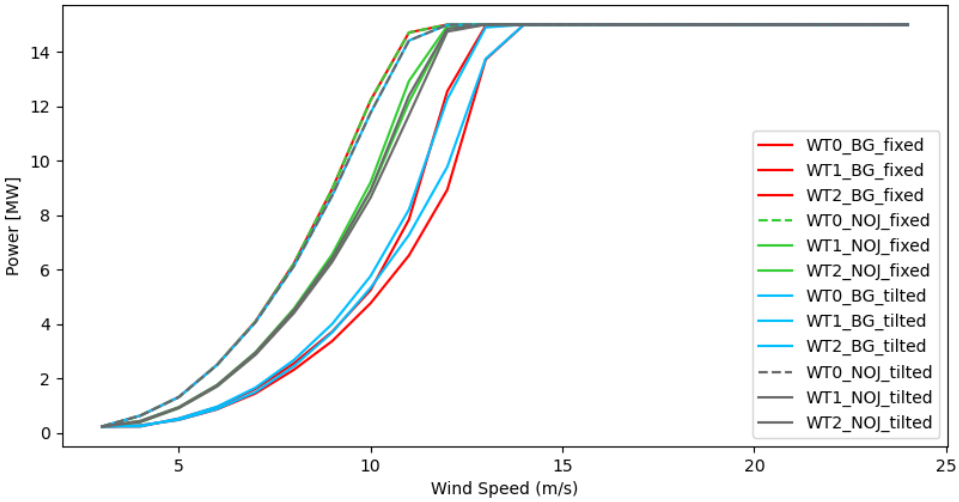

Figure 5.18: Comparison of power for fixed and tilted turbine for the three-turbine array (Case 1.1).

5.2 Part 2 - AEP

Results from Part 2 consist of AEP estimation of Case 2.1, a three-turbine farm, and Case 2.2, a 10x10 turbine farm. The results are presented for both wake models. The AEP estimation uses a wind speed distribution and wind direction over a year.

5.2.1 AEP of wind farm with three turbines.

The results for case 2.1 are the AEP for each turbine and a total for the farm consisting of three turbines. The AEP is simulated using the site with all wind speeds and directions, distributed over a year. The site is presented by a wind rose in the Chapter 4. In Table 5.10, the results of the AEP with fixed and tilted turbines are presented, for the BG wake model, with a fixed tilt of 10 deg, which is the max tilt, to see the max loss or gain. This was also the same tilt used in the previous part. The results gave a total tilt loss of -1.78% for the AEP with the BG model.

Table 5.10: AEP for the BG wake model for fixed and tilted turbines.

BG	**AEP fixed [GWh]**	**AEP with tilt [GWh]**	**Loss/gain**
WT0	63.52	62.36	-1.83%
WT1	62.45	61.39	-1.70%
WT2	63.97	62.81	1.81%
Total	189.94	186.56	-1.78%

Table 5.11 represents the AEP for the turbines with the NOJ wake model, with a fixed tilt of 10 deg. Comparing the two tables, there is a difference in AEP from the fixed to the tilted turbine. Meaning the park will produce less power when its influenced by the tilt. The results gave a total tilt loss of -2.41% for the AEP.

Table 5.11: AEP for the NOJ wake model for fixed and tilted turbines.

NOJ	**AEP Fixed [GWh]**	**AEP Tilt [GWh]**	**Loss/gain**
WT0	63.83	62.61	-1.91%
WT1	63.98	61.82	-3.38%
WT2	64.19	62.95	-1.93%
Total	192.00	187.38	-2.41%

Figure 5.19a and 5.19b show the flow map for the three turbines. As seen in the wake of the BG model, the two front turbines seem to influence the third turbine less than the NOJ model, where visually, it looks like a larger overlap.

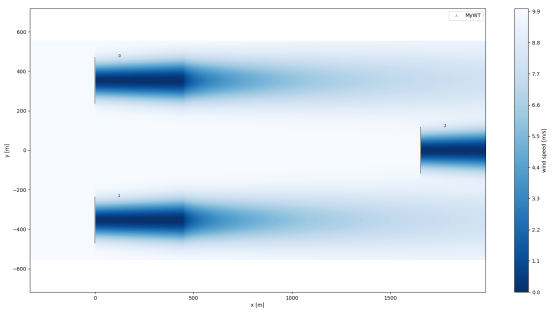

(a) Wake of fixed turbines with BG in a farm.

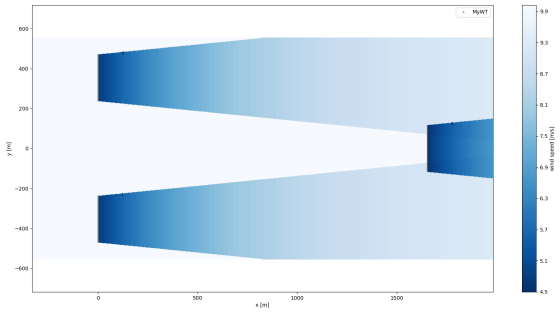

(b) Wake of fixed turbines with NOJ in a farm.

For the AEP simulation, the total AEP for the three turbines throughout the year gave a tilt loss of 3.38 GWh corresponding to the annual energy demand of 131 households[42], for the BG model. For the NOJ wake model, the deviation was slightly higher of 4.62 GWh corresponding to 179 households. -1.78% and -2.41% was the percentage tilt loss of energy for the two models. This is probably due to the fact that when the wind is coming from all directions, the NOJ model has a larger influence due to the linear expansion, or the fact that the BG model steers the wake.

5.2.2 AEP with a 10 x 10 wind farm

This section consists of AEP calculations for a 10 x 10 wind farm of 100 turbines. The turbines are tested with a fixed tilt for all wind turbines. First, a tilt of 5.7°, calculated from the average wind speed over a year, and then a tilt angle of 10°, the max tilt. The max tilt is used to compare with previous cases.

BG

Figure 5.20 shows the flow map for the 100 turbines with wind speed from the prominent wind direction of the site.

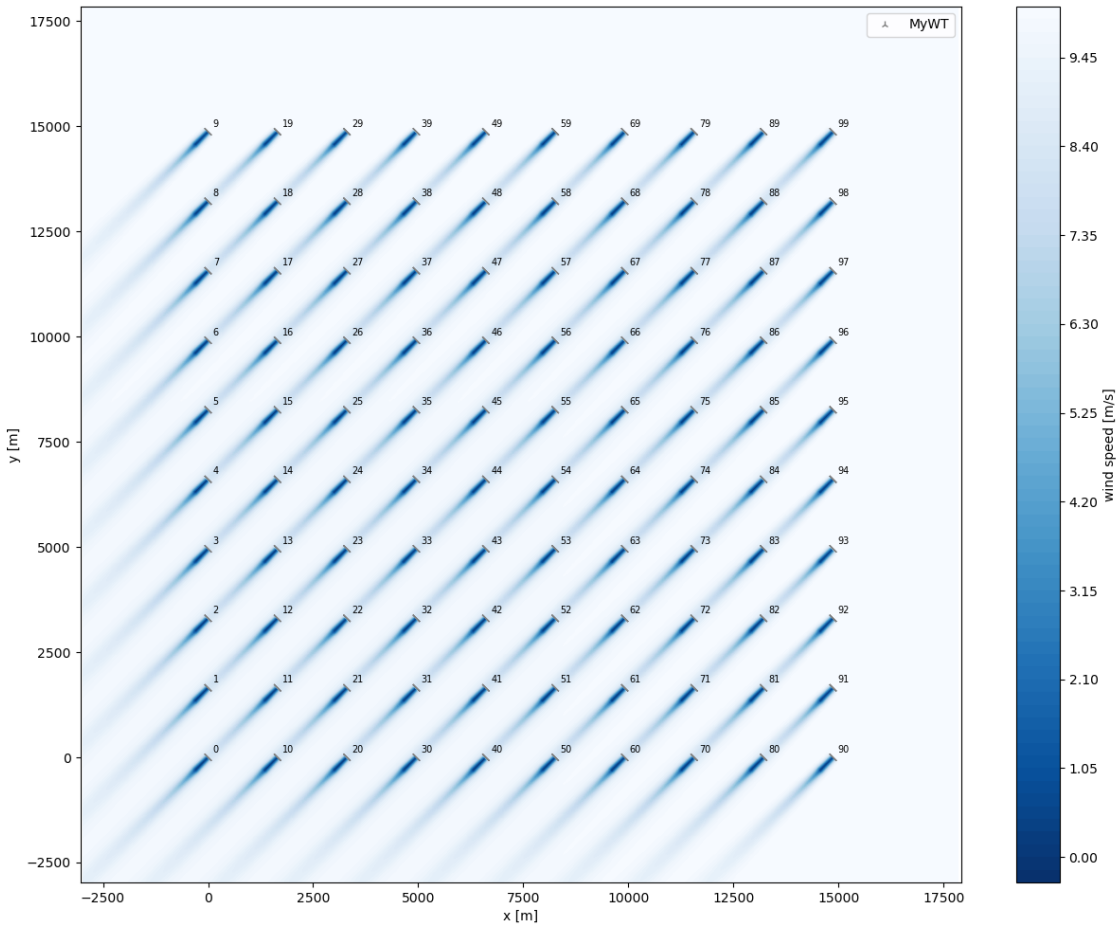

Figure 5.20: Flow map for the $10x10$ wind farm, wind direction 45°, which is the prominent wind direction for the site, with BG wake model.

The results of the tilt loss are presented as a deviation in Table 5.12. As seen a tilt cause a loss of -0.27% for the average tilt, and -0.98% for the max tilt.

Table 5.12: AEP for the BG wake model and deviation for fixed and tilted turbines.

BG	**AEP fixed [GWh]**	**AEP tilted [GWh]**	**Loss/gain**
$\theta = 5.7°$	6020.230	6003.947	-0.27%
$\theta = 10°$	6020.230	5960.954	-0.98%

NOJ

Figure 5.21 presents the flow map for the same farm with the NOJ wake model.

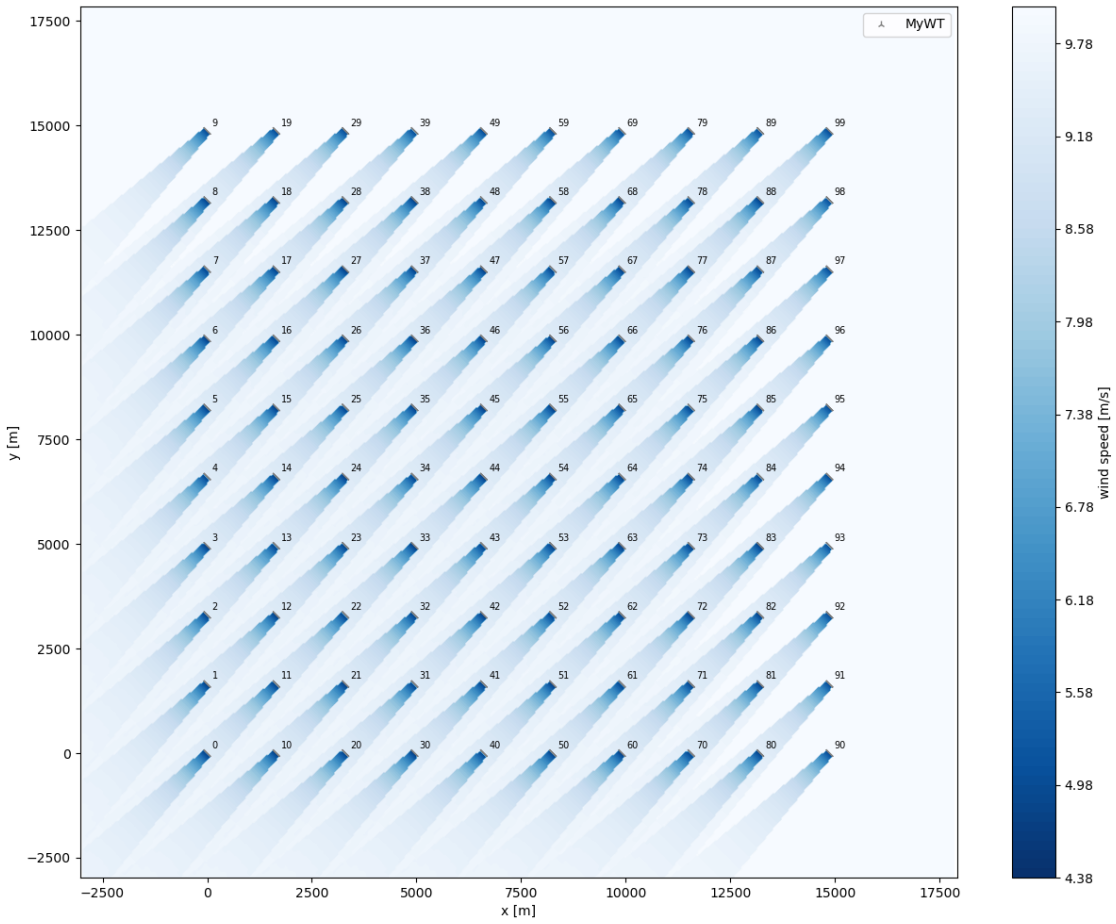

Figure 5.21: Flowmap for a 10 x 10 wind farm, with the NOJ wake model.

Table 5.13 provides the result of the AEP with the tilt loss presented as the deviation between the fixed and tilted turbines.

Table 5.13: AEP for the NOJ wake model and deviation for fixed vs. tilted turbines.

Tilt	**AEP fixed [GWh]**	**AEP tilted [MWh]**	**Loss/gain**
$\theta = 5.7°$	6167.432	6133.164	-0.55%
$\theta = 10°$	6167.432	6060.470	-1.73%

The results for 100 turbines in a 10 x 10 turbine farm are summarized in Table 5.14.

Table 5.14: Tilt loss/gain in AEP for 10x10 wind farm.

Case 10x10	**Tilt loss/gain** $\theta = 5.7°$	**Tilt loss/gain** $\theta = 10°$
BG	-0.27%	-0.98%
NOJ	-0.55%	-1.73%

To set the results in context, the BG model with a tilt angle of 5.7°show a deviation of 16.283 GWh, corresponding to around 630 households' annual energy demand, the BG model with 10°show a deviation of 59.276 GWh around 2300 homes. For the NOJ wake model, results show with a tilt angle of 5.7°, a deviation of 34.268 GWh, corresponding to 1330 households, and the 10°gave a deviation of 106.962 GWh, reaching 4150 households.

5.3 Part 3

The results for Part 3 present some earlier cases with different distances to see the effect of the tilt at different distances. Since 7D is used for earlier simulations, it is interesting to see if it is the optimum distance or if other distances could be used when the turbine is exposed to tilt. The first setup with a three-turbine array is tested with distances from 3D to 13D, which considers the power. For the AEP case, a 10x10 wind farm is considered.

5.3.1 Case 1.1 Three-turbine array with different distances

The three-turbine array is tested with different distances, and the power is evaluated for fixed and tilted turbines. The tilt is calculated by the program and updated as in Part 1. All numbers are added in Appendix D.0.1.

BG

Figure 5.22a shows the power vs. distance for both fixed and tilted turbines. As seen on the graph, the two top graphs represent WT0 for fixed and tilted cases, followed up for the same with WT1 and WT2. For WT0, the fixed turbine produces more power, while for WT1, the tilted turbine produces more up til around 10D, where they are equal, and after 12D, the fixed turbine produces more. For WT2, the tilted turbine will produce more than the fixed for all distances tested, but it looks like the same happens beyond the graph. Figure 5.22b shows the difference between the power produced by the fixed and tilted turbines. For WT0 the fixed turbine will produce more than the tilted one. While for WT1 and WT2, the tilted turbines produce more power than the fixed due to the deflection of the wake giving better wind conditions for the second and third turbines. The graph shows that the largest deviation is for WT2 at a 5D distance. WT2 is exposed to the lowest wind speed and has the smallest tilt angle, so the deviation is due to the wake steering from upwind turbines.

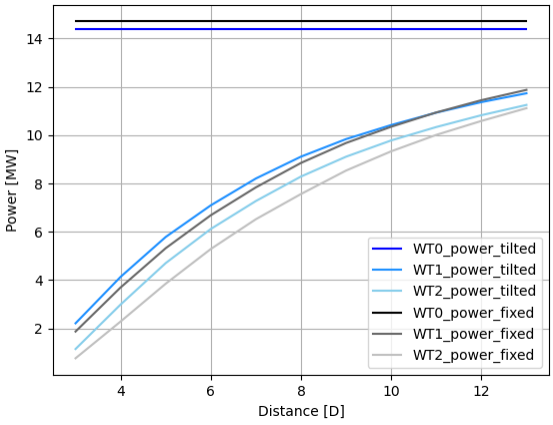

(a) Power vs. distances between the turbines for tilted and fixed in case 1.1. Wake model BG. Incoming wind speed = 11 m/s.

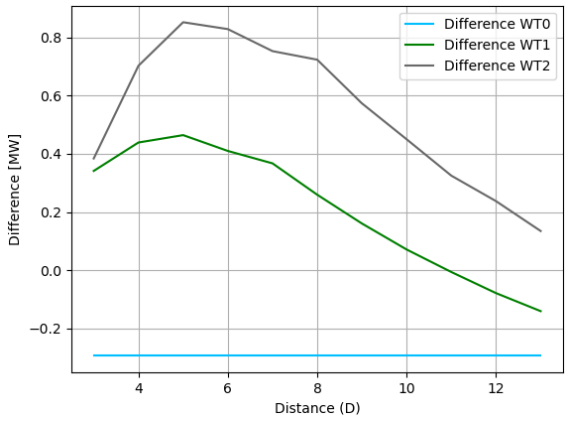

(b) The power difference between the fixed and the tilted turbines. Incoming wind speed = 11 m/s.

Table 5.15 shows the deviation between the tilted and fixed turbines at different distances. As seen, the deviation is calculated by taking the tilted minus the fixed turbine. Giving the positive deviation a gain and the negative a loss. The results show that the tilted turbines will have a gain in power up to 11D, where it will have a loss thereafter. The max gain in power due to the tilt is at 5D.

Table 5.15: Wind turbine power output at different distances for three turbine array (Case 1.1), with deviation in total power between fixed and tilted turbines.

Distance (D)	WS (m/s)	P_{Total} Fixed (MW)	P_{Total} Tilted (MW)	Loss/gain
3	11	17.341	17.770	2.47%
4	11	20.689	21.537	4.09%
5	11	23.880	24.903	4.28%
6	11	26.681	27.625	3.54%
7	11	29.069	29.895	2.84%
8	11	31.124	31.812	2.21%
9	11	32.922	33.361	1.33%
10	11	34.390	34.616	0.66%
11	11	35.662	35.685	0.06%
12	11	36.746	36.610	-0.37%
13	11	37.702	37.401	-0.80%

NOJ

Figure 5.23a presents the power for the three turbine array for distances 3D-13D. As seen, the fixed turbines perform better than the tilted turbines for all distances. For the tilted turbines, the power increase with the increased distance but does have a lower total power compared to the fixed turbines. The most significant increase is before 6D. Figure 5.23b shows the difference in power of the fixed and tilted turbines with the NOJ wake model. As seen, the difference is most considerable for the second turbine, in comparison to the BG model where the third turbine had the largest deviation.

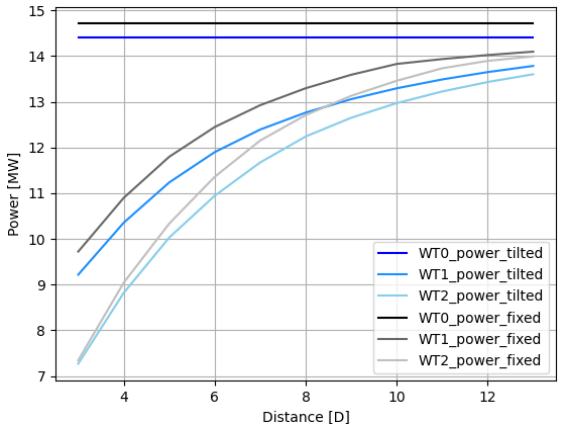

(a) Power vs distances between the turbines for tilted and fixed in case 1.1. Wake model NOJ. Incoming wind speed = 11 m/s

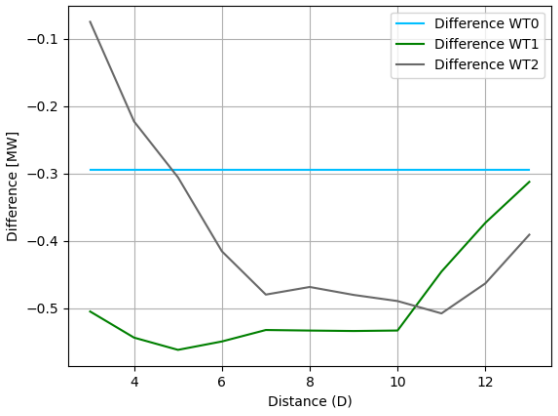

(b) The power difference between the fixed and the tilted turbines. Wake model NOJ Incoming wind speed = 11 m/s.

Table 5.16 shows the tilt loss/gain for the NOJ model. As seen the deviation is not varying as much as for the BG model. It is stable around a variation of -3%, except for 3D, 12D and 11D where the deviation is slightly lower.

Table 5.16: Wind turbine power output at different distances for the three-turbine array, with deviation in total power between fixed and tilted turbines NOJ.

Distance (D)	WS (m/s)	P_{Total} Fixed (MW)	P_{Total} Tilted (MW)	Loss/gain
3	11	31.778	30.902	-2.76%
4	11	34.649	33.588	-3.06%
5	11	36.841	35.679	-3.15%
6	11	38.518	37.257	-3.27%
7	11	39.788	38.481	-3.28%
8	11	40.716	39.419	-3.19%
9	11	41.432	40.123	-3.16%
10	11	41.997	40.681	-3.13%
11	11	42.442	41.129	-3.09%
12	11	42.628	41.497	-2.65%
13	11	42.801	41.802	-2.33%

5.3.2 10 x 10 farm with different distance

The wind farm with 10 x 10 turbines is also tested with different distances for both wake models. The AEP is presented below for fixed and tilted turbines with $\theta = 5.7°$ and $\theta = 10°$. Here all wind speed and directions are used.

BG

Figure 5.24 shows the AEP for the farm with different distances and different tilt angles. As seen, the tilted turbines produce more at small distances, which is the near wake region. After around 5D, the difference between the tilted and fixed turbine increase, with the fixed turbine producing the most. With $\theta = 10°$, the farm experience a gain of 1.81% at a distance of 3D and a loss of -1.87% at a distance of 12D. While for $\theta = 5.7°$, there is a gain of 0.74% at 3D and a loss of -0.53% at 12D. Where the difference decreases after 12D for both tilt angles. All numbers are added in Appendix D.0.2.

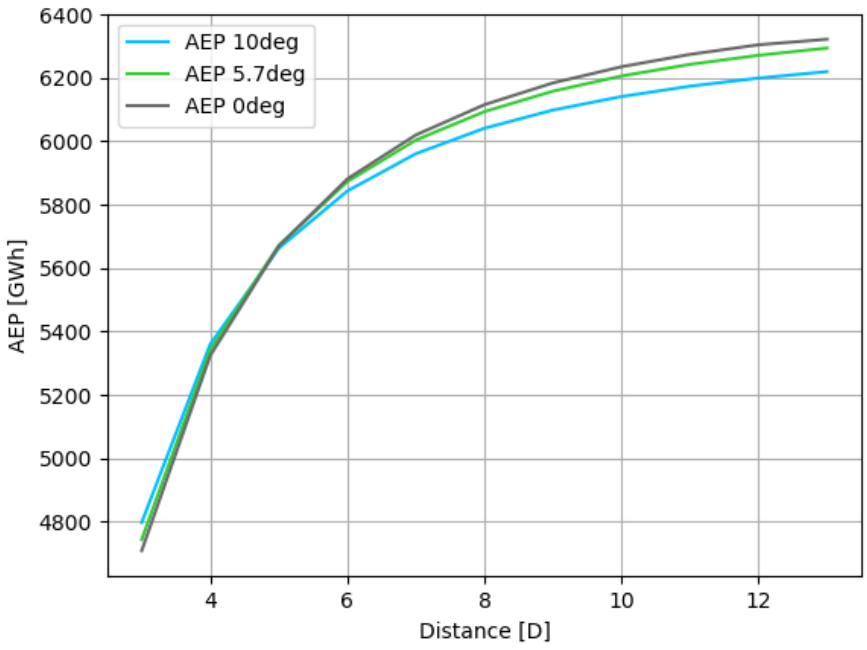

Figure 5.24: AEP at different distances for the 10x10 wind farm with the BG wake model.

NOJ

Figure 5.25 presents the AEP at different distances, again for fixed turbines, tilt angle 5.7°and 10°, for the NOJ model. As seen in this case, the tilted turbines will never produce more than the fixed turbines. And the difference increases with the higher distance. The largest deviation for $\theta = 10°$ is at 13D with a loss of -1.9%, and $\theta = 5.7°$ -0.61%. A table with the deviation of tilted and fixed turbines for tilt angle 5.7°and 10°with the NOJ model is added in Appendix D.0.2.

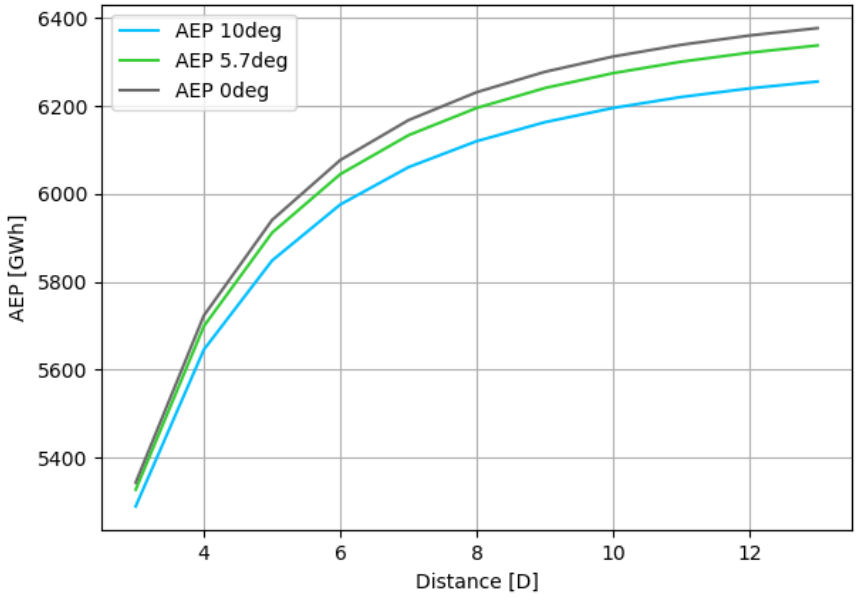

Figure 5.25: AEP at different distances for the 10x10 wind farm with the NOJ wake model.

In part 3, the discussion is up to how different spacing between turbines affects the tilt loss. From the result, the power increase with the increased distance. The results showed that for a three-turbine array, the turbines would gain power with tilted turbines from 3 to 11D, while after 12D, the fixed turbines would produce more. This is because the distance is large enough for the wake to recover, so the deflected wake will no longer be an advantage. Hence the tilt will give a loss due to the decrease in the area of the rotor. For the near wake and up to 5D, the downwind turbines experience low wind speeds and will have a small tilt angle and produce little. The deviation between the first and second turbines is relatively high at small distances. This is also the part where the wake models are not valid due to PyWake [18]. Further, from 6D, the deviation between the second and third turbines slows down.
The most significant deviation for the three turbine array is a gain of 4.11 % at 5D with the BG model and a loss of -3.39 % for the NOJ model at 6D. The power will increase with the larger distance for both fixed and tilted until, after 12D, the BG model experiences a loss in power between the fixed and tilted turbines. In contrast, this does not occur with the NOJ model, where there is a loss for all distances. Compared with the 10x10 wind farm, the corresponding deviation is at -0.65% for 6D with the BG model and -1.56% for 5D with the NOJ model.
The results of the 10x10 wind farm showed that with the BG model, the turbines would experience a tilt gain with distances from 3-5D, meaning that the turbines benefit from the tilt. However, after 5D they experience a loss due to the tilt. This is most impacted by the tilt of 10°, and by the average tilt angle of 5.7°, the tilt loss is minor.
If results from the BG model were to agree with reality, the results suggest that the spacing of offshore wind turbines exposed to tilt should be placed at a distance of 3-4D to experience a gain. However, the turbines will still produce poorly when the spacing is small. Further, since the wake model is stated to not be valid in the near wake, this needs further investigation.

5.4 Comparison

This section will compare and discuss findings from all parts and cases above. The tilt loss and wake models of all parts will be compared and discussed. Further, a comparison with other studies from the related work chapter will also be presented. Lastly, the limitations of engineering wake models will be discussed.

5.4.1 Tilt loss comparison

This part only considers results from the BG wake model to compare the tilt loss for all parts. In case 1.1, which involved three turbines in an array, the case with tilted turbines showed a 2.85% increase in power output compared to the fixed turbines. This suggests that, in some cases, a slight tilt angle can improve power production for downwind turbines directly exposed to the wake. However, in cases 1.2 and 1.3, which involved three turbines in a farm, the tilted turbines showed a decrease in power output of -2.00% for both. This suggests that in a wind farm, the interactions between the turbines and the wake effects may be more minor, and the principal loss is due to the impact of the single tilted rotor loss on the performance of the tilted turbines. Regarding AEP, the results show that tilted turbines in case 2.1 (three turbines in a farm) had a decrease in AEP of -1.78% compared to the fixed turbines. Similarly, in the wind farm with 100 turbines (AEP Wind Farm 10x10), the tilted turbines had a decrease in AEP of -0.98%. When looking at the effect of distance between turbines in an array (power distance Case 3.1), the results show a range of -0.80% to +4.00% for the tilted turbines compared to the fixed turbines. This indicates that the impact of tilt on power output can vary depending on the spacing between turbines. In the case of AEP for different distances (AEP Distances Wind Farm 10x10), the tilted turbines showed a range of -1.76% to +1.81% compared to the fixed turbines. The tilt loss/gain of all parts and cases are gathered in Table 5.17.

Table 5.17: Comparison of tilt loss/gain of all models with the BG model

Tilt angle	Case	Tilt loss/gain [%]
$\theta = 10°$	Power Case 1.1	+ 2.85
$\theta = 10°$	Power Case 1.2	-2.00
$\theta = 10°$	Power Case 1.3	-1.99
$\theta = 10°$	AEP Case 2.1	-1.78
$\theta = 10°$	AEP Wind Farm 10x10	-0.98
$\theta = 10°$	Power Distances Case 3.1	4.11 - (-0.80)
$\theta = 10°$	AEP Distances Wind Farm 10x10	1.81 - (-1.76)

5.4.2 Wake model comparison

For the two engineering wake models, results are obtained and presented in Table 5.18 for comparison. The most significant deviation of the wake models is in the first case, where a three-turbine array is distanced with 7D. This deviation shows that it is essential to carefully choose a wake model, considering testing wind turbines wake interaction, especially when there are few turbines. The reason may be that the NOJ has a top-hat distribution shape, which makes the wake wider. While for the BG, the Gaussian distribution shape makes the wake more narrow far downstream. Meaning that the NOJ wake deflection will not influence the downwind turbines with such small tilt angles due to the downstream turbines are still affected by the wake. It may, however, be otherwise with larger tilt angles, over 10°. For the case with AEP estimation, the deviation is much smaller. But here, the turbines are not exposed to wake directly like the array setup.

Table 5.18: Comparing the two wake models BG and NOJ by the tilt loss/gain results from all parts.

Tilt angle	Case	Tilt loss/gain BG [%]	Tilt loss/gain NOJ [%]	deviation [%]
$\theta = 10°$	Power Case 1.1	2.84	-3.29	6.40
$\theta = 10°$	Power Case 1.2	-2.00	-1.93	0.07
$\theta = 10°$	Power Case 1.3	-2.00	-1.95	0.05
$\theta = 10°$	AEP Case 2.1	-1.78	-2.41	0.63
$\theta = 10°$	AEP Wind Farm 10x10	-0.98	-1.73	0.75
$\theta = 10°$	Power distances Case 1.1	2.47 - (-0.80)	-2.76 - (-3.33)	
$\theta = 10°$	AEP Distances 10x10	1.81 - (-1.76)	-1.01 - (-1.90)	

The difference between the two wake models stems from their assumptions. The NOJ wake model assumes a constant expansion rate of the wake behind a turbine, along with a constant velocity deficit within the wake. This model is based on the conservation of momentum principle, whereby the momentum lost by the wind passing through the turbine is transferred to the wake. Although, the NOJ wake model does not consider the complex turbulence present within the wake, making it less accurate in highly turbulent conditions. On the other hand, the BG wake model operates under different assumptions. It considers that the velocity deficit within the wake decreases as the distance from the turbine increases and the wake expands in a Gaussian shape. This model is rooted in the principles of turbulence and the Gaussian distribution of turbulence intensity. By considering turbulence, the BG model can provide greater accuracy than the NOJ model in highly turbulent conditions. However, it also requires more input parameters compared to the NOJ model. In summary, while the NOJ and BG wake models estimate wake effects, they are based on different fluid mechanical principles and assumptions.
The BG wake model is based on the following assumptions:

- Gaussian wake expansion: The model assumes that the wake expands in a Gaussian shape with distance from the turbine. The wake expansion rate is characterized by the wake spread parameter, which is assumed to be a function of the downstream distance and the ambient turbulence intensity.

- No meandering: The model assumes that the wake centerline follows a straight path downstream, with no lateral meandering.

The NOJ wake model is based on the following assumptions:

- Incompressible flow: The NOJ wake model assumes that the wind flow is incompressible, which means that the air density is constant and does not change with wind speed.

- Linear momentum theory: The NOJ wake model is based on the linear momentum theory, which assumes that the wind flow interacts with the turbine rotor in a linear way, without any nonlinear effects.

- Constant thrust coefficient: The model assumes that the turbine operates at a constant thrust coefficient, which relates the power output of the turbine to the wind speed and the rotor diameter.

- No ambient turbulence: The NOJ wake model assumes that there is no ambient turbulence in the wind farm, and that any turbulence is only generated by the turbine wakes.

5.4.3 Comparison with other studies

From the literature review, there were others investigating similar cases. Table 5.19 shows the results obtained by others in comparison with results from this thesis. In [20], [15], and [21], the focus for all was to gain power by steering the wake with tilt. Thus, these results used a negative tilt angle (wake steered downwards) and are not interesting to compare with, they also gathered some results with a positive tilt. For most cases, the CFD analysis in SOWFA and FOAM-extend gave a loss of tilted turbines. However, some results showed by only tilting the front row turbines, the farm will have increased production. The table shows that the model from [20] gave a loss when the turbines were set with a positive tilt angle of 25°with a three-turbine array. The same was obtained by [21]. Even if the tilt angle in this study were slightly lower, the fact that this thesis found a gain while others found a loss raises questions to wake modeling techniques. However, for the AEP estimation, this thesis found a loss with a tilt angle, while [21] found a gain with a slightly lower tilt angle.

Table 5.19: AEP for the NOJ wake model for fixed vs tilted turbines, ws = 10 m/s.

	Model	Tilt Angle	**Tilt loss/gain Array**	Tilt Angle	**Tilt loss/gain AEP**
This thesis	BG wake model	$\theta = 10°$	+2.84%	fixed $\theta = 10°$	-1.78%
[20]	SOWFA	$\theta = 25°$	-3.8% (7D)	-	-
[15]	CFD	$\theta = -15°$	+7% (6-8D)	-	-
[21]	BG wake model	$\theta = 25°$	-6%	fixed $\theta = 5°$	+2.77% (6D)

5.4.4 Limitation

The purpose of using the engineering wake models is to for example estimate the annual energy production of larger wind farms by computing the overall power efficiency of such larger farms in a short time. However, the accuracy and accordance with reality are not as accurate as a wind tunnel test or a CFD analysis. The last two mentioned are expensive and time-consuming compared to the engineering model, hence a more precise description of a flow behind a wind turbine. Another fact is that the wake models used in this thesis are only valid in the far-wake regions. There are some limitations to engineering wake models:

- Simplified assumptions: Engineering wake models are based on simplified assumptions about the flow physics within the wake, such as assuming axisymmetric wake expansion, meaning the wake behind the turbine is assumed to be symmetric with respect to the centerline of the turbine rotor. This means that the wake expands uniformly in all directions behind the turbine. Which in reality is not right when turbines are tilted. The models also assumes that the wind turbine operates at a steady-state condition, with a constant rotor speed, constant wind speed, and constant wind direction. These assumptions may not accurately capture the complex flow physics in highly turbulent conditions or complex terrain.

- Homogeneous turbulence: Engineering wake models assume that the turbulence intensity in the wake is proportional to the ambient turbulence intensity. However, in reality, the turbulence within the wake can be highly non-uniform and may not follow a Gaussian distribution.

- Turbine interactions: Engineering wake models typically assume that the wakes from upstream turbines do not interact with each other. In reality, there can be complex interactions between wakes from multiple turbines in a wind farm, which can lead to non-linear effects and unpredictability.

Chapter 6

Conclusions

To conclude this thesis, the research questions will be answered.

- **RQ1.1:** How will the tilt of the turbines affect the production of one turbine?

  For a single turbine standing in the free wind as WT0 in cases 1.1, 1.2, and 1.3, there will be a loss of 2 % due to the tilt at a wind speed of 11 m/s, with the max tilt angle of 10°. This accounts for both wake models. So a single turbine will always experience a loss for all tilt angles.

- **RQ1.2:** How will the tilt of the turbines affect the power production of multiple turbines?

  There were three different setups for testing the power production of multiple turbines. In all cases, three turbines were considered. For case 1.1 with a three-turbine array, findings showed a total loss of -2.85% for the BG wake model and 3.28% for the NOJ wake model. Giving the turbines in case 1.1 with the BG wake model an advantage when the turbines are tilted and the wake is steered away from downwind turbines. In case 1.2, three turbines were placed in a triangular shape set from above, with one turbine in the prominent wind direction and two behind. Results obtained with the BG wake model, 7D spacing from the front to the back row, and 3D row distance showed a total loss of -1.99% with the BG model, and -1.92% for the NOJ model. For case 1.3, the setup is flipped around with two turbines in front in the prominent direction and one behind. Results gave a loss of -1.99% with BG model and 1.95% for the NOJ model. In conclusion, the loss or gain is most affected when turbines are exposed directly to the wake from other turbines. Further, for cases with turbines in a farm, the loss will not see a significant difference for the two different setups in cases 1.2 and 1.3 for the BG model. Thus, the NOJ model

- **RQ1.3:** How will the tilt of the turbines affect production for downwind turbines?

  The downwind turbines in case 1.1 is the one most affected due to direct exposition to the wake from the front turbine. With the BG wake model, WT1 had a gain of approximately 4.70%, and WT2 gained 11.53%. With the NOJ wake model, results showed WT1 loss of approximately 4.12%, and WT2 decreased the power production by approximately 3.95%. For case 1.2, the second-row turbines, approximately 1.99% loss in power is experienced. While for case 1.3, the loss was approximately 1.99%.

- **RQ1.4:** How will the tilt of the turbines affect AEP in a farm?

  The results showed a tilt loss for both cases with AEP simulations. With a three-turbine farm, the loss was -1.78% for the BG wake model. For the 10x10 farm, the results showed a loss of -0.98% with a tilt angle of 10°, corresponding to around 2300 households' annual energy demand. With an average tilt angle of 5.7°, the 10x10 wind farm experienced a loss of -0.27%, corresponding to 630 households, again with the BG wake model.

- **RQ1.5:** How will the tilt of the turbines affect production with different wake models?

  The results from the wake model comparison showed the most significant deviation for the case where the turbines were directly exposed to wake from upstream turbines, with a deviation of 6.40%. For other parts, the deviation was between 0 and 1%. As mentioned earlier, the BG wake model is more complex than the NOJ and more realistic to a real case scenario because the BG model is based on the principle of turbulence, where the wake expands with a Gaussian shape and a variable velocity deficit. In contrast, the NOJ takes assumptions like linear wake expansion and a constant velocity deficit. However, the accuracy of these wake models is to be tested with the data from real wind farms, which is beyond the scope of this thesis.

- **RQ1.6:** How will the tilt of the turbines affect production with different distances?

  The power will increase with the larger distance, as expected. The results obtained showed that for a three-turbine array, the turbines would gain power with tilted turbines from 3 to 11D, while after 12D, the fixed turbines would produce more. The largest deviation in tilt loss is a gain of 4.11% at 5D with the BG model and a loss of -3.39% for the NOJ model at 6D. For the 10x10 wind farm the loss in AEP increased with the larger distance.

- **RQ1.7:** Is there a loss or a gain when the turbines are tilted?

  The results obtained showed both gain and loss in the different cases and parts. However, the major part resulted in a loss. These results are not reliable by themselves and need further investigation, which will be discussed in the next section, further work.

6.1 Further Work

Validation through CFD Analysis: Compare the results of the simple wake models used in this thesis with more advanced computational fluid dynamics (CFD) simulations. This was supposed to be a part of this thesis, but because there was not enough time, it was not completed. Conduct a detailed CFD analysis considering the tilted turbine configuration and assess the accuracy of the simple wake models in capturing the complex flow phenomena. Compare the load predictions and wake characteristics obtained from the simple models with those from the CFD simulations to validate the models' reliability.
The realism of Wake Deflection: Evaluate the realism of assuming uniform flow in the wake deflection scenario. Investigate the wind speeds "made available" to downstream turbines when the wake is deflected upwards. Analyze the impact of the wake deflection on the wind resource and assess its feasibility in a real-world wind farm setting. Consider the spatial and temporal variations in wind speed and direction and their influence on the wake behavior and turbine performance.
Reliability of Simple Wake Models: Assess the reliability and limitations of the simple wake models used in this thesis. Evaluate their ability to predict the wake characteristics, load distribution, and power output accurately in the presence of turbine tilt. Analyze the discrepancies between the simple models and the CFD simulations to determine the range of applicability and the potential areas for improvement.
Dynamic Effects of Tilt: Investigate the dynamic contributions of turbine tilt to power production and wake behavior. Analyze how the changes in turbine orientation over time influence the power output and the characteristics of the deflected wake. Consider transient wake behavior, changes in wind conditions, and the interaction between turbine dynamics and wake dynamics. Evaluate the significance of these dynamic effects on turbine performance.

Appendix A

Datasheet A

A.0.1 PyWake function for calculating power and AEP

```
# setup site, wind turbines and wind farm model with the corresponding ...
    wake models
import numpy as np
from ipywidgets import interact
from ipywidgets import IntSlider
import matplotlib.pyplot as plt
import pandas as pd
import matplotlib.pyplot as plt
from py_wake.flow_map import HorizontalGrid
from py_wake import XZGrid
from py_wake.examples.data.iea37._iea37 import IEA37Site, IEA37_WindTurbines
from py_wake.deficit_models.gaussian import BastankhahGaussian
from py_wake.deflection_models.jimenez import JimenezWakeDeflection
from py_wake import NOJ
from wt_site_guide import my_wt, my_site

# Importing tilt angle as a function of wind speed
tiltvsws = pd.read_csv(r'C:/Users/Camilla ...
    Leikvoll/Desktop/windmaster/tilt.csv')

# Importing turbine, site and wfm
site = my_site
x, y = [0, 1652, 3304], [0, 0, 0]
windTurbines = my_wt
wfm = BastankhahGaussian(site, windTurbines, ...
    deflectionModel=JimenezWakeDeflection())


# define function that gets the tilt angle as a function of wind speed
def get_tilt(wind_speed):
    return np.interp(wind_speed, tiltvsws[' ws '].values, tiltvsws[' ...
        tilt'].values)

# define function that plots the flow field and AEP history of 3 wind turbines
def plot_flow_field_and_aep(ws, plot=True):
    # ws = 10
    if plot:
        ax1 = plt.figure(figsize=(16,2)).gca()
        ax2 = plt.figure(figsize=(10,3)).gca()
    tilt = np.array([get_tilt(ws), get_tilt(ws), get_tilt(ws)])
    # tilt = np.array([get_tilt(ws + WT0), get_tilt(ws + WT1), get_tilt(ws ...
        + WT2)])
    while True:
        sim_res = wfm(x, y, tilt=tilt , wd=270, ws=ws)
```

```
        # sim_res = wfm(x, y, tilt=np.reshape([WT0,WT1,WT2],(3,1,1)), ...
            wd=270) # what is the wind speed? average? using weibull
        tilt_old = tilt[1:]
        tilt[1] = get_tilt(sim_res.WS_eff[1])
        tilt[2] = get_tilt(sim_res.WS_eff[2])
        if np.max(np.abs(tilt[1:]-tilt_old))<0.1: #differanse mellom ...
            forrige tilt vinkel og den nye
            break
    if plot:
        sim_res.flow_map(grid=XZGrid(y=0, z=np.arange(0, 600, 2)), ...
            wd=[270]).plot_wake_map(ax=ax1)
        ax1.set_xlim([-200,4000])
        # center_line = min(sim_res.WS_eff)
        # ax1.plot(center_line.x/ax1, center_line/ax1,'--k')
        aep.append(sim_res.aep().sum(dim='ws').values)
        aep_arr = np.array(aep)
        for i in range(3):
            ax2.plot(aep_arr[:,i], '.-', label='WT%d, %.2f'%(i,aep_arr[-1,i]))
        ax2.plot(aep_arr.sum(1), '.-', label='Total, %.2f'%aep_arr[-1].sum())
        ax2.axhline(aep_arr[0].sum(),ls='--',c='r')
        ax2.set_ylabel('AEP [MWh]')
        ax2.set_xlabel('Iteration')
        ax2.legend(loc='upper left')
    return sim_res

aep = []
ws_eff = []
results_df = pd.DataFrame(columns=['ws', 'WT0_tilt', 'WT1_tilt', ...
    'WT2_tilt', 'WT0_power', 'WT1_power', 'WT2_power' , 'WT0_WS_eff', ...
    'WT1_WS_eff', 'WT2_WS_eff'])
for ws in range(10,11):
    sim_res = plot_flow_field_and_aep(ws, plot = True)
    # ws_eff.append(sim_res.ws_eff.values)
    results_df = results_df.append({'ws': ws, 'WT0_tilt': ...
        sim_res.tilt.values[0], 'WT1_tilt': sim_res.tilt.values[1], ...
        'WT2_tilt': sim_res.tilt.values[2],
                                    'WT0_WS_eff': ...
                                        sim_res.WS_eff.values[0], ...
                                        'WT1_WS_eff': ...
                                        sim_res.WS_eff.values[1], ...
                                        'WT2_WS_eff': ...
                                        sim_res.WS_eff.values[2],
                                   'WT0_power': sim_res.Power.values[0], ...
                                      'WT1_power': ...
                                      sim_res.Power.values[1], ...
                                      'WT2_power': ...
                                      sim_res.Power.values[2]}, ...
                                      ignore_index=True)
```

A.0.2 Site and Wind Turbine object

Inline python code: `variabel = max(input)`

PyWake code in section:

```
@author: Camilla Leikvoll
"""

import numpy as np
import xarray as xr
```

```
import matplotlib.pyplot as plt
from py_wake.wind_turbines import WindTurbine
import py_wake
from py_wake.wind_turbines.power_ct_functions import PowerCtTabular, ...
    SimpleYawModel
from py_wake.site import XRSite


# Turbine data
u = [3, 3.5, 4, 4.5, 5, 5.5, 6, 6.5, 7, 7.5, 8, 8.5, 9, 9.5, 10, 10.5, 11, ...
    11.5, 12,
      12.5, 13, 13.5, 14, 14.5, 15, 15.5, 16, 16.5, 17, 17.5, 18, 18.5, 19, ...
         19.5, 20,
      20.5, 21, 21.5, 22, 22.5, 23, 23.5, 24, 24.5, 25]

ct = [0.97, 0.91, 0.85, 0.82, 0.81, 0.81, 0.81, 0.8, 0.8, 0.8, 0.8, 0.8, ...
    0.8, 0.8,
       0.78, 0.73, 0.65, 0.55, 0.46, 0.39, 0.34, 0.3, 0.27, 0.24, 0.21, ...
          0.19, 0.17,
       0.16, 0.14, 0.13, 0.12, 0.11, 0.1,  0.09, 0.09, 0.08, 0.08, 0.07, ...
          0.07, 0.06,
       0.06, 0.05, 0.05, 0.05, 0.05]

power = [234.56, 402.22, 634.28, 934.78, 1316.01, 1856.39, 2506.38, ...
    3206.09, 4098.54,
          5097.77, 6221.65, 7469.81, 8964.12, 10510.9, 12217.4, 13826.89, ...
             14709.39,
          14978.4, 14999.89, 15000.08, 15000.94, 15000.96, 15000.99, ...
             15000.73, 14999.85,
          15001.12, 15000.73, 14998.98, 14999.56, 15001.05, 15000.43, ...
             15000.99, 14999.01,
          15000.28, 14999.79, 15000.79, 15000.39, 15000.1, 14999.61, ...
             15001.9, 15001.8,
          14999.46, 14999.86, 15000.65, 14999.51]

my_wt = WindTurbine(
    name='MyWT',
    diameter=236,
    hub_height=144,
    powerCtFunction=PowerCtTabular(
        u, power, 'kW', ct, additional_models=[SimpleYawModel()]))


# Site with Weibull shape, scale and frequency factors.
f = [0.07337514, 0.12041049, 0.09880274, 0.0481756 , 0.02890536,
       0.04082098, 0.05792474, 0.12434436, 0.10524515, 0.03933865,
       0.12719498, 0.1354618 ]
A = [ 9.09608115,  9.03693285,  8.70865267,  6.9893408 ,  6.16278353,
        7.50624882,  8.63867235, 11.08530575, 11.4464287 ,  7.51157958,
       11.36076425, 10.6134112 ]
k = [2.12071594, 2.23204458, 1.77743311, 1.72145024, 1.29647691,
       1.38817186, 1.53828289, 2.03135986, 2.22851829, 1.68913119,
       2.60100154, 2.60102019]
ti = 0.06
wd = np.arange(0, 360, 30)
my_site = XRSite(ds=xr.Dataset(data_vars={'Sector_frequency': ('wd', f),
                                          'Weibull_A': ('wd', A),
                                          'Weibull_k': ('wd', k),
                                          'TI': ti},
                               coords={'wd': wd}))
```

Appendix B

Datasheet B

B.1 Results architecture

This is the architecture of how result are obtained.

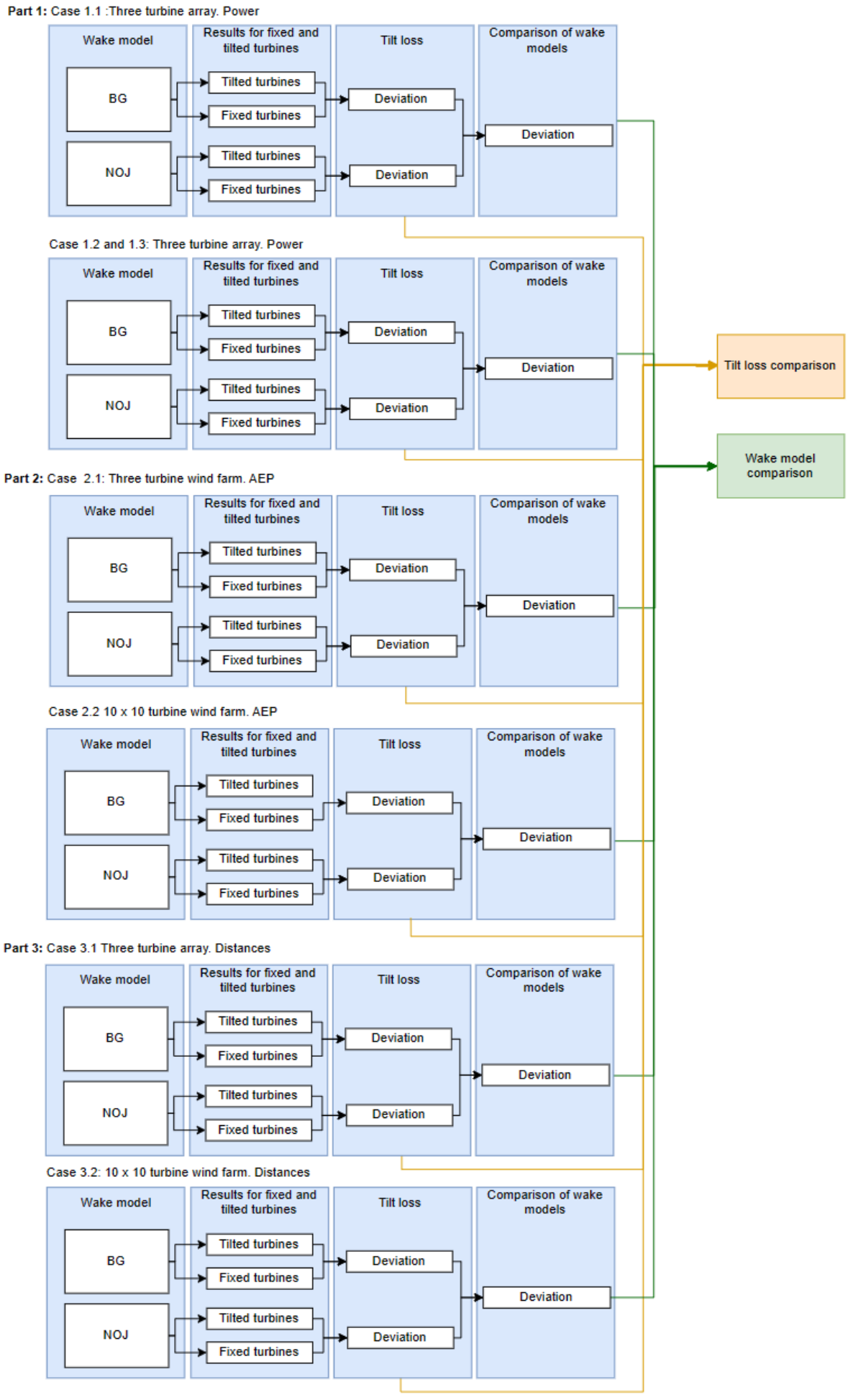

Figure B.1: Architecture for obtaining results for comparison.

Appendix C

Datasheet C

C.1 Case1.1

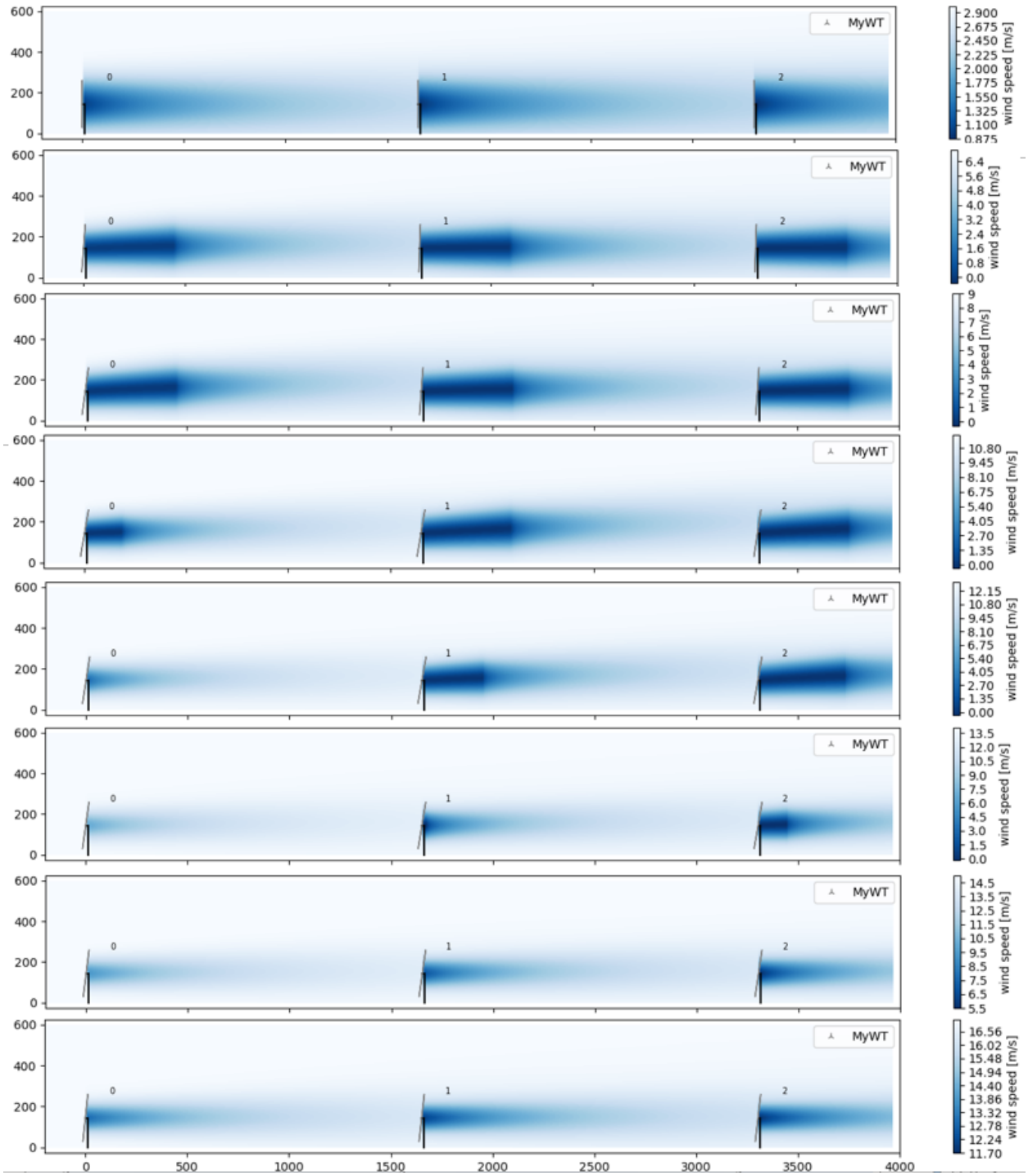

Figure C.1: Flow map of BastankhahGaussian wake model at different wind speeds between 3 and 17 m/s.

Appendix D

Datasheet D

D.0.1 Distances, case 3.1.

BG

Table **??** shows the simulation results for the fixed turbines. The tilt is expressed with θ for each turbine and P is the power. As seen the total power increase with the larger distance.

Distance	WS	θ_{WT0}	θ_{WT1}	θ_{WT2}	P_{WT0}	P_{WT1}	P_{WT2}	P_{Total}
(D)	(m/s)	(deg)	(deg)	(deg)	(MW)	(MW)	(MW)	(MW)
3	11	0	0	0	14.709	1.869	0.762	17.341
4	11	0	0	0	14.709	3.695	2.285	20.689
5	11	0	0	0	14.709	5.320	3.850	23.880
6	11	0	0	0	14.709	6.685	5.287	26.681
7	11	0	0	0	14.709	7.839	6.520	29.069
8	11	0	0	0	14.709	8.851	7.563	31.124
9	11	0	0	0	14.709	9.677	8.535	32.922
10	11	0	0	0	14.709	10.349	9.332	34.390
11	11	0	0	0	14.709	10.941	10.012	35.662
12	11	0	0	0	14.709	11.448	10.589	36.746
13	11	0	0	0	14.709	11.875	11.173	37.702

Table D.1: Wind turbine power output at different distances, with the BG wake model, and fixed turbines.

Table D.2 shows the simulation results for the setup of case 1.1 for tilted turbines. As seen the total power increase with the larger distance.

Distance	WS	θ_{WT0}	θ_{WT1}	θ_{WT2}	P_{WT0}	P_{WT1}	P_{WT2}	P_{Total}
(D)	(m/s)	(deg)	(deg)	(deg)	(MW)	(MW)	(MW)	(MW)
3	11	10.0	2.605	1.450	14.414	2.210	1.146	17.770
4	11	10.0	4.402	3.419	14.414	4.134	2.988	21.537
5	11	10.0	5.767	4.864	14.414	5.785	4.703	24.903
6	11	10.0	6.666	6.021	14.414	7.095	6.116	27.625
7	11	10.0	7.463	6.803	14.414	8.207	7.274	29.895
8	11	10.0	8.074	7.518	14.414	9.111	8.287	31.812
9	11	10.0	8.551	8.073	14.414	9.838	9.109	33.361
10	11	10.0	8.863	8.515	14.414	10.420	9.782	34.616
11	11	10.0	9.082	8.825	14.414	10.934	10.337	35.685
12	11	10.0	9.263	9.037	14.414	11.369	10.826	36.610
13	11	10.0	9.408	9.214	14.414	11.734	11.252	37.401

Table D.2: Wind turbine power output at different distances, with the BG wake model, and tilted turbines.

NOJ

Table D.3 shows the results for the three turbine array with different distanced for the NOJ wake model. As seen the power increase with the larger distance.

Distance	WS	θ_{WT0}	θ_{WT1}	θ_{WT2}	P_{WT0}	P_{WT1}	P_{WT2}	P_{Total}
(D)	(m/s)	(deg)	(deg)	(deg)	(MW)	(MW)	(MW)	(MW)
3	11	0.0	0.0	0.0	14.709	9.723	7.345	31.778
4	11	0.0	0.0	0.0	14.709	10.898	9.042	34.649
5	11	0.0	0.0	0.0	14.709	11.797	10.335	36.841
6	11	0.0	0.0	0.0	14.709	12.449	11.360	38.518
7	11	0.0	0.0	0.0	14.709	12.926	12.153	39.788
8	11	0.0	0.0	0.0	14.709	13.297	12.710	40.716
9	11	0.0	0.0	0.0	14.709	13.592	13.131	41.432
10	11	0.0	0.0	0.0	14.709	13.828	13.460	41.997
11	11	0.0	0.0	0.0	14.709	13.935	13.734	42.378
12	11	0.0	0.0	0.0	14.709	14.023	13.896	42.628
13	11	0.0	0.0	0.0	14.709	14.098	13.994	42.801

Table D.3: Wind turbine power output at different distances, with the NOJ wake model, and fixed turbines.

Table D.4 is showing the results for fixed turbines. For the tilted turbines, the power increase with the increased distance, but does have a lower total power compared to the fixed turbines. The largest increase is before 6D.

Distance	WS	θ_{WT0}	θ_{WT1}	θ_{WT2}	P_{WT0}	P_{WT1}	P_{WT2}	P_{Total}
(D)	(m/s)	(deg)	(deg)	(deg)	(MW)	(MW)	(MW)	(MW)
3	11	10.0	8.144	6.799	14.414	9.218	7.270	30.902
4	11	10.0	8.833	7.879	14.414	10.355	8.819	33.588
5	11	10.0	9.207	8.677	14.414	11.236	10.029	35.679
6	11	10.0	9.448	9.086	14.414	11.899	10.944	37.257
7	11	10.0	9.568	9.389	14.414	12.394	11.673	38.481
8	11	10.0	9.661	9.529	14.414	12.764	12.241	39.419
9	11	10.0	9.736	9.633	14.414	13.058	12.651	40.123
10	11	10.0	9.795	9.714	14.414	13.295	12.971	40.681
11	11	10.0	9.822	9.778	14.414	13.489	13.226	41.129
12	11	10.0	9.843	9.815	14.414	13.650	13.433	41.497
13	11	10.0	9.860	9.837	14.414	13.785	13.603	41.802

Table D.4: Wind turbine power output at different distances, with the NOJ wake model, and tilted turbines.

D.0.2 Distances, 10x10 wind farm case 3.2.

BG

The wind farm with 10 x 10 turbines are also tested with different distances. The AEP is presented below for fixed turbines, and tilted turbines for $\theta = 5.7°$ and $\theta = 10°$. The deviation or tilt loss is also added.

Table D.5: Annual energy production (AEP) at different distances from a wind farm 10 x 10, with different tilts for BG wake model.

Distance (D)	AEP [GWh] ($\theta = 0°$)	AEP [GWh] ($\theta = 5.7°$)	Deviation (0°vs 5.7°)	AEP [GWh] ($\theta = 10°$)	Deviation (0°vs 10°)
3	4708.119	4743.134	0.74%	4797.287	1.81%
4	5323.832	5341.380	0.33%	5360.012	0.57%
5	5669.473	5671.865	0.04%	5662.512	-0.12%
6	5881.425	5872.874	-0.15%	5843.315	-0.65%
7	6020.230	6003.947	-0.27%	5960.954	-0.99%
8	6115.647	6093.754	-0.36%	6041.337	-1.02%
9	6184.441	6158.337	-0.42%	6098.728	-1.38%
10	6235.470	6206.281	-0.47%	6141.362	-1.52%
11	6274.466	6242.985	-0.50%	6174.123	-1.69%
12	6304.844	6271.585	-0.53%	6199.710	-1.87%
13	6322.237	6294.390	-0.44%	6220.154	-1.76%

NOJ

Table D.6 shows the deviation of tilted and fixed turbines for tilt angle 5.7°adn 10°with the NOJ model.

Table D.6: Annual energy production (AEP) at different distances from a wind farm 10 x 10, with different tilts for NOJ wake model.

Distance (D)	AEP [GWh] ($\theta = 0°$)	AEP [GWh] ($\theta = 5.7°$)	Deviation (0°vs 5.7°)	AEP [GWh] ($\theta = 10°$)	Deviation (0°vs 10°)
3.0	5343.171	5326.982	-0.30%	5289.048	-1.01%
4.0	5723.082	5698.876	-0.42%	5645.555	-1.35%
5.0	5940.315	5911.354	-0.49%	5848.042	-1.56%
6.0	6076.676	6044.534	-0.53%	5975.530	-1.67%
7.0	6167.432	6133.164	-0.56%	6060.471	-1.75%
8.0	6230.981	6195.135	-0.58%	6119.649	-1.80%
9.0	6277.373	6240.506	-0.59%	6162.783	-1.83%
10.0	6312.116	6274.319	-0.60%	6195.186	-1.85%
11.0	6338.871	6300.420	-0.61%	6220.135	-1.87%
12.0	6359.984	6320.968	-0.61%	6239.692	-1.89%
13.0	6376.760	6337.425	-0.61%	6255.354	-1.90%

D.0.3 distances, other results

Figure D.1 shows the power for different distances at ws 7m/s.

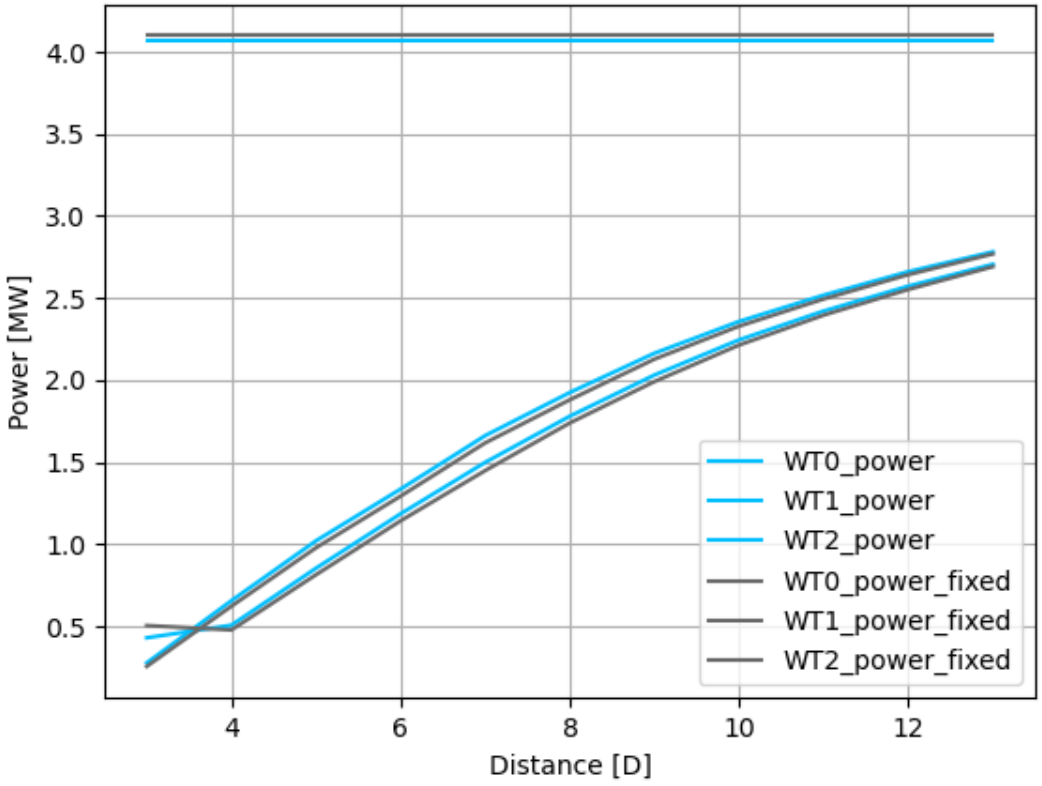

Figure D.1: Power for different distances

Table D.7: Wind turbine power output at different distances, with the BG wake model, and tilted turbines, ws = 7 m/s.

Distance (m)	WS (m/s)	θ_{WT0} (deg)	θ_{WT1} (deg)	θ_{WT2} (deg)	P_{WT0} (MW)	P_{WT1} (MW)	P_{WT2} (MW)	P_{Total} (MW)
3	7	4.2	0.082	0.343	4.065	0.278	0.431	4.774
4	7	4.2	0.648	0.442	4.065	0.657	0.507	5.229
5	7	4.2	1.226	0.978	4.065	1.021	0.854	5.941
6	7	4.2	1.633	1.443	4.065	1.337	1.186	6.588
7	7	4.2	1.935	1.784	4.065	1.663	1.499	7.227
8	7	4.2	2.195	2.044	4.065	1.925	1.781	7.770
9	7	4.2	2.453	2.310	4.065	2.164	2.031	8.260
10	7	4.2	2.662	2.541	4.065	2.358	2.245	8.668
11	7	4.2	2.834	2.730	4.065	2.518	2.421	9.004
12	7	4.2	2.978	2.889	4.065	2.661	2.573	9.299
13	7	4.2	3.099	3.023	4.065	2.782	2.706	9.553

Table D.8: Wind turbine power output at different distances, with the BG wake model, and tilted turbines, ws = 10 m/s.

Distance (D)	WS (m/s)	θ_{WT0} (deg)	θ_{WT1} (deg)	θ_{WT2} (deg)	P_{WT0} (MW)	P_{WT1} (MW)	P_{WT2} (MW)	P_{Total} (MW)
3	11	10.0	2.605	1.450	14.414	2.210	1.146	17.770
4	11	10.0	4.402	3.419	14.414	4.134	2.988	21.537
5	11	10.0	5.767	4.864	14.414	5.785	4.703	24.903
6	11	10.0	6.666	6.021	14.414	7.095	6.116	27.625
7	11	10.0	7.463	6.803	14.414	8.207	7.274	29.895
8	11	10.0	8.074	7.518	14.414	9.111	8.287	31.812
9	11	10.0	8.551	8.073	14.414	9.838	9.109	33.361
10	11	10.0	8.863	8.515	14.414	10.420	9.782	34.616
11	11	10.0	9.082	8.825	14.414	10.934	10.337	35.685
12	11	10.0	9.263	9.037	14.414	11.369	10.826	36.610
13	11	10.0	9.408	9.214	14.414	11.734	11.252	37.401

Table D.9: Wind turbine power output at different distances, with the BG wake model, and fixed turbines.

Distance (D)	WS (m/s)	θ_{WT0} (deg)	θ_{WT1} (deg)	θ_{WT2} (deg)	P_{WT0} (MW)	P_{WT1} (MW)	P_{WT2} (MW)	P_{Total} (MW)
3	11.000	0.000	0.000	0.000	14.709	1.869	0.762	17.341
4	11.000	0.000	0.000	0.000	14.709	3.695	2.285	20.689
5	11.000	0.000	0.000	0.000	14.709	5.320	3.850	23.880
6	11.000	0.000	0.000	0.000	14.709	6.685	5.287	26.681
7	11.000	0.000	0.000	0.000	14.709	7.839	6.520	29.069
8	11.000	0.000	0.000	0.000	14.709	8.851	7.563	31.124
9	11.000	0.000	0.000	0.000	14.709	9.677	8.535	32.922
10	11.000	0.000	0.000	0.000	14.709	10.349	9.332	34.390
11	11.000	0.000	0.000	0.000	14.709	10.941	10.012	35.662
12	11.000	0.000	0.000	0.000	14.709	11.448	10.589	36.746
13	11.000	0.000	0.000	0.000	14.709	11.875	11.173	37.702

Bibliography

[1] IEA. *Wind Electricity*. URL: https://www.iea.org/reports/wind-electricity. (accessed: 10.05.2023).

[2] UN. *Take Action for the Sustainable Development Goals*. URL: https://www.un.org/sustainabledevelopment/sustainable-development-goals/. (accessed: 10.05.2023).

[3] GWEC. *Global Wind Report 2022*. URL: https://gwec.net/global-wind-report-2022/. (accessed: 10.05.2023).

[4] Xuan Mei and Min Xiong. "Effects of Second-Order Hydrodynamics on the Dynamic Responses and Fatigue Damage of a 15 MW Floating Offshore Wind Turbine." In: *Journal of Marine Science and Engineering* 9.11 (2021). ISSN: 2077-1312. DOI: 10.3390/jmse9111232. URL: https://www.mdpi.com/2077-1312/9/11/1232.

[5] Thomas Mazarakos and Spyridon Mavrakos. "Experimental investigation on mooring loads and motions of a Spar Buoy floating wind turbine." In: July 2016.

[6] Thomas Mazarakos et al. "Analytical Investigation of Tension Loads Acting on a TLP Floating Wind Turbine." In: *Journal of Marine Science and Engineering* 10 (Feb. 2022), p. 318. DOI: 10.3390/jmse10030318.

[7] Equinor. *Hywind Scotland*. URL: https://www.equinor.com/energy/hywind-scotland. (accessed: 20.04.2023).

[8] Equinor. *Hywind Tampen*. URL: https://www.equinor.com/no/energi/hywind-tampen. (accessed: 20.04.2023).

[9] Principle Power. *Kincardine Offshore wind farm*. URL: https://www.principlepower.com/projects/kincardine-offshore-wind-farm. (accessed: 20.04.2023).

[10] Principle Power. *Windfloat Atlantic*. URL: https://www.principlepower.com/projects/windfloat-atlantic. (accessed: 20.04.2023).

[11] Principle Power. *Les Éoliennes Flottantes du Golfe de Lion (EFGL)*. URL: https://www.principlepower.com/projects/les-eoliennes-flottantes-du-golfe-du-lion. (accessed: 20.04.2023).

[12] Principle Power. *Erebus*. URL: https://www.principlepower.com/projects/erebus. (accessed: 20.04.2023).

[13] BW IDEOL. *A PRE-COMMERCIAL PROJECT OF 3 UNITS EOLMED PROJECT*. URL: https://www.bw-ideol.com/en/eolmed-project. (accessed: 20.04.2023).

[14] Principle Power. *WindFloat®*. URL: https://www.principlepower.com/. (accessed: 20.04.2023).

[15] Emmanouil Nanos et al. "Vertical wake deflection for floating wind turbines by differential ballast control." In: (Aug. 2021). DOI: 10.5194/wes-2021-79.

[16] O. Apata and D.T.O. Oyedokun. "An overview of control techniques for wind turbine systems." In: *Scientific African* 10 (2020), e00566. ISSN: 2468-2276. DOI: https://doi.org/10.1016/j.sciaf.2020.e00566. URL: https://www.sciencedirect.com/science/article/pii/S2468227620303045.

[17] Yaoyu Li and Zhongyou Wu. "Stabilization of floating offshore wind turbines by artificial muscle based active mooring line force control." In: *2016 American Control Conference (ACC)*. 2016, pp. 2277–2282. DOI: 10.1109/ACC.2016.7525257.

[18] Alexander Meyer Forsting Mads M. Pedersen. *PyWake 2.5.0: An open-source wind farm simulation tool*. Feb. 2023. URL: https://gitlab.windenergy.dtu.dk/TOPFARM/PyWake.

[19] Decha Intholo Wongsakorn Wisatesajja Wirachai Roynarin. "Comparing the Effect of Rotor Tilt Angle on Performance of Floating Offshore and Fixed Tower Wind Turbines." In: *Journal of Sustainable Development* 12 (Sept. 2019). DOI: 10.5539/jsd.v12n5p84.

[20] Jennifer Annoni et al. "Evaluating Tilt for Wind Farms Preprint Evaluating Tilt for Wind Plants." In: (). URL: http:/www.osti.gov/scitech.

[21] James Cutler et al. "Optimization of Turbine Tilt in a Wind Farm." In: (2021), p. 4550. DOI: 10.2514/6.2021-1180. URL: https://scholarsarchive.byu.edu/facpubhttps://scholarsarchive.byu.edu/facpub/4550.

[22] Fernando Porte-Agel Majid Bastankhan. *Experimental and theoretical study of wind turbine wakes in yawed conditions*. Tech. rep. Lausanne, Switzerland, 1016.

[23] N. J. Gaukroger. "Analytical solution for the icumulative wake of yawed wind turbines." In: (2022).

[24] Christopher Bay et al. "Flow Control Leveraging Downwind Rotors for Improved Wind Power Plant Operation." In: July 2019, pp. 2843–2848. DOI: 10.23919/ACC.2019.8815277.

[25] Majid Bastankhah and Fernando Porté-Agel. "A new analytical model for wind-turbine wakes." In: *Renewable Energy* 70 (2014). Special issue on aerodynamics of offshore wind energy systems and wakes, pp. 116–123. ISSN: 0960-1481. DOI: https://doi.org/10.1016/j.renene.2014.01.002. URL: https://www.sciencedirect.com/science/article/pii/S0960148114000317.

[26] Wongsakorn Wisatesajja and Decha Intholo. "Analysis of Influence of Tilt Angle on Variable-Speed Fixed-Pitch Floating Offshore Wind Turbines for Optimizing Power Coefficient Using Experimental and CFD Models." In: *International Journal of Renewable Energy Development* 10 (May 2021), pp. 201–212. DOI: 10.14710/ijred.2021.33195.

[27] Ryan Scott, Juliaan Bossuyt, and Raúl Bayoán Cal. "Characterizing tilt effects on wind plants." In: *Journal of Renewable and Sustainable Energy* 12 (July 2020), p. 043302. DOI: 10.1063/5.0009853.

[28] Huanyu Shi et al. "Wind Speed Distributions Used in Wind Energy Assessment: A Review." In: *Frontiers in Energy Research* 9 (2021). ISSN: 2296-598X. DOI: 10.3389/fenrg.2021.769920. URL: https://www.frontiersin.org/articles/10.3389/fenrg.2021.769920.

[29] J.F Manwell. *Wind energy explained : theory, design and application*. eng. Chichester, 2009.

[30] Martin Hansen. *Aerodynamics of Wind Turbines*. 3rd. Accessed on 14 Oct. 2022. Taylor and Francis, 2015. URL: https://www.taylorfrancis.com/books/9781315686894.

[31] O. Apata and D.T.O. Oyedokun. "An overview of control techniques for wind turbine systems." In: *Scientific African* 10 (2020), e00566. ISSN: 2468-2276. DOI: https://doi.org/10.1016/j.sciaf.2020.e00566. URL: https://www.sciencedirect.com/science/article/pii/S2468227620303045.

[32] Angel Jimenez, Antonio Crespo, and Emilio Migoya. "Application of a LES technique to characterize the wake deflection of a wind turbine in yaw." In: *Wind Energy* 13 (Sept. 2009), pp. 559–572. DOI: 10.1002/we.380.

[33] Dian Wang et al. "Modelling Analysis of Methods for Wind Turbine Annual Energy Production." In: Jan. 2016. DOI: 10.2991/icseee-15.2016.101.

[34] Huanyu Shi et al. "Wind Speed Distributions Used in Wind Energy Assessment: A Review." In: *Frontiers in Energy Research* 9 (2021). DOI: 10.3389/fenrg.2021.769920. URL: https://www.frontiersin.org/articles/10.3389/fenrg.2021.769920.

[35] *Wind energy handbook*. eng. 2nd ed. Chichester: Wiley, 2011. ISBN: 9780470699751.

[36] Trevor Letcher. *Wind energy engineering : a handbook for onshore and offshore wind turbines*. eng. London, England, 2017.

[37] Sina Shamsoddin Fernando Porté-Agel Majid Bastankhah. "Wind-Turbine and Wind-Farm Flows: A Review." In: *Boundary-Layer Meteorology* 174 (Sept. 2020). DOI: 10.1007/s10546-019-00473-0.

[38] "A note on wind generator interaction." In: (1983).

[39] Angel Jimenez, Antonio Crespo, and Emilio Migoya. "Application of a LES technique to characterize the wake deflection of a wind turbine in yaw." In: *Wind Energy* 13 (Sept. 2009), pp. 559–572. DOI: 10.1002/we.380.

[40] Jana Fischereit et al. "Comparing and validating intra-farm and farm-to-farm wakes across different mesoscale and high-resolution wake models." In: *Wind Energy Science* 7 (May 2022), pp. 1069–1091. DOI: 10.5194/wes-7-1069-2022.

[41] Thanh Dam Pham and Hyunkyoung Shin. "A New Conceptual Design and Dynamic Analysis of a Spar-Type Offshore Wind Turbine Combined with a Moonpool." In: *Energies* 12.19 (2019). ISSN: 1996-1073. DOI: 10.3390/en12193737. URL: https://www.mdpi.com/1996-1073/12/19/3737.

[42] Elvia. *Normalt strømforbruk*. URL: https://www.elvia.no/smart-forbruk/forbruk-og-sparing/normalt-stromforbruk/. (accessed: 20.05.2023).